

# **The combined effects of arsenic, cadmium and mercury on hepatocarcinoma and neuroblastoma cells *in vitro***

by

Muhammad Yousaf

A dissertation submitted in fulfillment of the requirements for the degree

**Magister Scientiae**

in

**Pharmacology**

in the

Faculty of Health Sciences

at the

University of Pretoria

**Supervisor**

Prof V Steenkamp

**Co-supervisor**

Dr W Cordier

July 2018

**Faculty of Health Sciences  
University of Pretoria**

## Acknowledgements

---

I would like to thank to all people who have helped and inspired me during my MSc study. In the first place, I would like to thank ALLAH, The Almighty. He blessed me and my family with resources, courage, and patience to complete this study.

My utmost gratitude goes to my supervisor Prof. Dr. Vanessa Steenkamp, for her motivation, encouragement, valuable suggestions and kind attitude during my research work. I pay special thanks to Dr. Werner Cordier for providing research facilities and technical guidance. I also wish to extend my thanks to cell culture lab in charge, Ms Margo Nell, for her support, expertise and patience throughout my training. I am also thankful to other colleague, Ms Keagile Lepule.

My deepest gratitude goes to my wife Dr. Mamoonah Chaudhry for her motivation and support throughout; this dissertation is simply impossible without her. I pay special thanks to my mother for her constant motivation.

I wish to thank my best friend Dr M Ataul for helping me get through the difficult times.

*Muhammad Yousaf*

# Declaration

---

**University of Pretoria**

**Faculty of Health Sciences**

**Department of Pharmacology**

I, Muhammad Yousaf,

**Student number:** 16136022

**Subject of the work:** The combined effects of arsenic, cadmium and mercury on hepatocarcinoma and neuroblastoma cells *in vitro*

## Declaration

1. I understand what plagiarism entails and am aware of the University's policy in this regard.
2. I declare that this project (e.g. essay, report, project, assignment, dissertation, thesis etc.) is my own, original work. Where someone else's work was used (whether from a printed source, the internet or any other source) due acknowledgement was given and reference was made according to departmental requirements.
3. I did not make use of another student's previous work and submitted it as my own.
4. I did not allow and will not allow anyone to copy my work with the intention of presenting it as his or her own work.

Signature Muhammad Yousaf

## Abstract

---

Among several heavy metallic elements, arsenic, cadmium and mercury are most toxic in the environment. These metals are acquired by humans through food and water, which result in severe health related issues. One of the most toxic metals is arsenic and it is derived from the natural environment. The main source of arsenic toxicity is due to contamination of drinking water from natural geological sources rather than from mining, smelting, or agricultural sources. Another naturally occurring highly toxic heavy metal is cadmium and possesses considerable toxicity with destructive impact on most organ systems. To date cadmium has no physiological function in the human body. Mercury is another important toxic metal found in nature and noted for inducing public health disasters. The current study has been considered to investigate individual and combined toxic effects in HepG2 hepatocarcinoma and SH-SY5Y neuroblastoma cell lines as a measure of hepatotoxicity and neurotoxicity, respectively. The aim was achieved through investigation of individual metals and their combinations on cell density, mitochondrial membrane potential, adenosine triphosphate levels, reactive oxygen species generation, glutathione levels and caspase-3/7 activity.

Arsenic displayed gradual, dose-dependent cytotoxicity in both cell lines. In the HepG2 cells,  $IC_{50}$  of arsenic was determined as 6.71 mg/L and in the SH-SY5Y cells,  $IC_{50}$  of 1.19 mg/L. Arsenic had minimal effects on HepG2 mitochondrial membrane potential at  $IC_{50}$  (~12%). A gradual, tapered reduction (25% to 62%) was observed in the SH-SY5Y cell line from 0.94 mg/L to 2.78 mg/L. This decline parallels the reduction in cell density in the SH-SY5Y cell line. Arsenic profoundly decreased adenosine triphosphate levels at  $IC_{75}$  (9.61 mg/L for HepG2 and 2.78 mg/L for SH-SY5Y cells) for both cells indicating mitochondrial toxicity. A decline in reactive oxygen species level was noted for both cells after 24 h incubation with arsenic. The glutathione was reduced by 35%, 64% and 94% in HepG2 cells and 47%, 67% and 96% in SH-SY5Y cells which paralleled the results obtained for cell density, adenosine triphosphate levels and mitochondrial membrane potential. Mitochondrial toxicity lead to an increase in caspase-3/7 in both cell lines.

Greater cytotoxicity was displayed in the HepG2 cells after cadmium exposure ( $IC_{50} = 0.43$  mg/L) than the SH-SY5Y cells ( $IC_{50} = 1.47$  mg/L). The dose dependent mitochondrial depolarization leads to mitochondrial toxicity and there is a direct correlation to the reduction in cell density. Cadmium decreased adenosine triphosphate levels when exposed to the  $IC_{25}$  (0.22 mg/L) by 39%, by 62% at  $IC_{50}$  (0.43 mg/L) and by 88% at  $IC_{75}$  (1.11 mg/L). The trend was similar to that detected for arsenic, albeit being less toxic. In SH-SY5Y cells, there was complete reduction in adenosine triphosphate levels as was found by arsenic. A gradual decrease in reactive oxygen species was noted in both cells after exposure to cadmium. The reduction in glutathione levels related to cell density as well as mitochondrial membrane potential reduction. The increase in caspase 3/7 activity in SH-SY5Y cells was nearly double that observed in HepG2 cells at the same concentrations tested indicating apoptosis.

Mercury was more cytotoxic towards SH-SY5Y cells ( $IC_{50} = 11.99$  mg/L) than HepG2 cells ( $IC_{50} = 26.23$  mg/L). Mercury was found to be the least toxic among all three metals tested. Mercury decreased mitochondrial membrane potential and reactive oxygen species in both cells in a dose dependent manner. The adenosine triphosphate concentration was almost completely inhibited in HepG2 cells while a more gradual decrease in the SH-SY5Y cells of 30%, 77% and 99% when exposed to  $IC_{25}$  (8.45 mg/L),  $IC_{50}$  (11.99 mg/L) and  $IC_{75}$  (14.36 mg/L) concentrations of mercury, was noted.

The glutathione reduction in both cell lines was dose dependent, with virtually total inhibition (99%) of glutathione when treated with the  $IC_{75}$  concentration of mercury. This reduction in glutathione levels correlates with the reduction in cell density, reduction in adenosine triphosphate level as well as the loss in mitochondrial membrane potential. Mercury decreased caspase-3/7 in HepG2 cells from basal level at all concentrations tested. In contrast caspase-3/7 activity was increased by 320%, 181% and 327% in SH-SY5Y cells when exposed to  $IC_{25}$  (8.45 mg/L),  $IC_{50}$  (11.99 mg/L) and  $IC_{75}$  (14.36 mg/L) concentrations of mercury.

After exposure to the IC and EPA mixtures, the reduction in cell density was far greater than that observed for any of the single metals alone in HepG2 cells, which may imply additive or synergistic activity. Combinations of metal mixtures displayed greater mitochondrial toxicity than

the metals alone. This was most prominent in the HepG2 cell line. The combination mixtures in both the cell lines almost completely inhibited adenosine triphosphate levels indicating cell death from apoptotic to necrotic pathways.

Reactive oxygen species was reduced in a dose dependent manner in both cell lines. The IC combinations abolished glutathione levels completely in hepatoma and neuronal cells. All the EPA combinations reduced glutathione levels in a dose dependent manner which paralleled what was noted for cell density, mitochondrial membrane potential and adenosine triphosphate levels. An increase in caspase 3/7 activity was noted when the cells were exposed to 4mg/L EPA mixture concentration with respect to arsenic (505%) indicating additive or synergistic effect.

Understanding how metal mixtures affect health is critical to decide on treatment strategies. The results indicate the potential mechanistic routes of cytotoxicity incurred by the heavy metals and their combinations. Cytotoxicity of metal mixtures was more pronounced than when cells were exposed to individual metals.

# Table of Contents

---

<b>Contents</b>	<b>Page number</b>
<b>1. Literature review</b>	<b>1</b>
1.1. Arsenic	1
1.1.1. Background and exposure sources	1
1.1.2. Toxicokinetics and toxicodynamics	2
1.1.3. Health risks and treatment options	3
1.2. Cadmium	4
1.2.1. Background and exposure sources	4
1.2.2. Toxicokinetics and toxicodynamics	5
1.2.3. Health risks and treatment options	5
1.3. Mercury	6
1.3.1. Background and exposure sources	6
1.3.2. Toxicokinetics and toxicodynamics	7
1.3.3. Health risks and treatment options	7
1.4. Organ toxicity of heavy metals	9
1.4.1. Hepatotoxicity	9
1.4.2. Neurotoxicity	10
1.5. Metal mixtures	11
1.6. Common mechanisms leading to cytotoxicity	12
1.6.1. Cytotoxicity	12
1.6.2. Mitochondrial membrane potential	13
1.6.3. Adenine di- and triphosphate levels	15

1.6.4. Reactive oxygen species	16
1.6.5. Reduced glutathione levels	17
1.6.6. Cell death and caspase activity	17
1.7. Aim of the study	19
1.8. Objectives of the study	20
1.9. Project overview	20
<b>2. Materials and methods</b>	<b>21</b>
2.1. Heavy metals	21
2.2. Cell culture and maintenance	21
2.3. Seeding and exposure of cell lines	22
2.4. Cytotoxicity	22
2.5. Mitochondrial membrane potential	23
2.6. Intracellular adenosine triphosphate levels	23
2.7. Reactive oxygen species generation	24
2.8. Intracellular reduced glutathione concentrations	24
2.9. Caspase-3/7 activity	25
2.10. Statistical analysis	25
<b>3. Results and Discussion</b>	<b>27</b>
3.1. Arsenic	27
3.1.1. Cell density	27
3.1.2. Mitochondrial membrane potential	30
3.1.3. Intracellular ATP levels	31
3.1.4. Reactive oxygen species generation	34
3.1.5. Reduced glutathione levels	35



3.1.6. Caspase 3/7 activity	37
3.2. Cadmium	40
3.2.1. Cell density	40
3.2.2. Mitochondrial membrane potential	41
3.2.3. Intracellular ATP levels	43
3.2.4. Reactive oxygen species	44
3.2.5. Reduced glutathione levels	45
3.2.6. Caspase 3/7 activity	46
3.3. Mercury	48
3.3.1. Cell density	48
3.3.2. Mitochondrial membrane potential	50
3.3.3. Intracellular ATP levels	51
3.3.4. Reactive oxygen species	52
3.3.5. Reduced glutathione levels	53
3.3.6. Caspase 3/7 activity	54
3.4. Heavy metal combinations	54
3.4.1. Cell density	54
3.4.2. Mitochondrial membrane potential	56
3.4.3. Intracellular ATP levels	58
3.4.4. Reactive oxygen species	59
3.4.5. Reduced glutathione levels	60
3.4.6. Caspase 3/7 activity	61
<b>4. General discussion</b>	<b>63</b>
<b>5. Conclusions</b>	<b>68</b>
<b>6. Limitations of study and recommendations</b>	<b>69</b>

<b>7. References</b>	<b>71</b>
<b>Appendix I: Ethics approval certificate</b>	<b>85</b>
<b>Appendix II: Reagents and preparation</b>	<b>86</b>

## List of Figures

---

Contents	Page number
<b>Figure 1:</b> Biotransformation of inorganic arsenic in mammalian systems.	2
<b>Figure 2:</b> Dysfunction of Ca <sup>2+</sup> buffering, protein import, loss of mitochondrial membrane potential, mitochondrial respiration and ATP production. The final result is the loss of the mitochondrial membrane potential, causing the induction of mitophagy and/or the release of proapoptotic factors from the organelle	15
<b>Figure 3:</b> Flow diagrammatic representation of the project	20
<b>Figure 4:</b> Cell density in (A) HepG2 and (B) SH-SY5Y cells after 24 h exposure to negative (untreated), vehicle (deionized water/medium mixture 1:4) and positive (saponin 1%) controls. Comparison to the negative control. *** $p < 0.001$	27
<b>Figure 5:</b> Dose-dependent reduction of cell density in (A) HepG2 and (B) SH-SY5Y cells after exposure to As for 24 h. Comparison to the negative control. *** $p < 0.001$ , ** $p < 0.01$	28
<b>Figure 6:</b> Cell density in (A) HepG2 and (B) SH-SY5Y cells after exposure to the IC <sub>25</sub> , IC <sub>50</sub> and IC <sub>75</sub> of As for 24 h. Comparison to the negative control. *** $p < 0.001$	28
<b>Figure 7:</b> Mitochondrial membrane potential in (A) HepG2 and (B) SH-SY5Y cells after 24 h exposure to the negative (untreated), vehicle (deionized water/medium mixture 1:4) and positive (Rotenone 200 nM) controls Comparison to the negative control. *** $p < 0.001$ , ** $p < 0.01$	30
<b>Figure 8:</b> Mitochondrial membrane potential in (A) HepG2 and (B) SH-SY5Y cells after 24 h exposure the IC <sub>25</sub> , IC <sub>50</sub> and IC <sub>75</sub> of As. Comparison to the negative control. *** $p < 0.001$ , ** $p < 0.01$ , * $p < 0.05$	31
<b>Figure 9:</b> Intracellular ATP levels in (A) HepG2 and (B) SH-SY5Y cells after 24 h exposure to the negative (untreated), vehicle (deionized water/medium mixture 1:4) and positive (Camptothecin; 20 $\mu$ M and 40 $\mu$ M, Saponin 1%) controls. Comparison to the negative control. *** $p < 0.001$ , ** $p < 0.01$ , * $p < 0.05$	32
<b>Figure 10:</b> Intracellular ATP levels in (A) HepG2 and (B) SH-SY5Y cells after 24 h exposure the IC <sub>25</sub> , IC <sub>50</sub> and IC <sub>75</sub> of As. Comparison to the negative control. *** $p < 0.001$ , * $p < 0.05$	33
<b>Figure 11:</b> Reactive oxygen species levels in (A) HepG2 and (B) SH-SY5Y cells after 24 h exposure to the negative, vehicle (deionized water/medium mixture 1:4) and positive (AAPH, 1 mM) controls. Comparison to the negative control: *** $p < 0.001$	34

<b>Figure 12:</b> Reactive oxygen species levels in (A) HepG2 and (B) SH-SY5Y cells after 24 h exposure to the IC <sub>25</sub> , IC <sub>50</sub> and IC <sub>75</sub> of As. Comparison to the negative control. *** $p < 0.001$	35
<b>Figure 13:</b> Glutathione concentration in (A) HepG2 and (B) SH-SY5Y cells after 24 h exposure to negative (medium), vehicle (deionized water/medium mixture 1:4) and positive control (n-Ethylmaleimide, 25 $\mu$ M). Comparison to the negative control: *** $p < 0.001$	36
<b>Figure 14:</b> Glutathione concentration in (A) HepG2 and (B) SH-SY5Y cells after 24 h exposure to the IC <sub>25</sub> , IC <sub>50</sub> and IC <sub>75</sub> of As. Comparison to the negative control. *** $p < 0.001$ , ** $p < 0.01$ , * $p < 0.05$	37
<b>Figure 15:</b> Caspase-3/7 activity in (A) HepG2 and (B) SH-SY5Y cells after treatment with negative (medium), vehicle (deionized water/medium mixture 1:4) and positive control (Camptothecin 40 $\mu$ M) for 24 h. Comparison to the negative control: *** $p < 0.001$	38
<b>Figure 16:</b> Caspase-3/7 activity in (A) HepG2 and (B) SH-SY5Y cells after treatment after 24 h exposure to the IC <sub>25</sub> , IC <sub>50</sub> and IC <sub>75</sub> of As. Comparison to the negative control. ** $p < 0.01$ , * $p < 0.05$	38
<b>Figure 17:</b> Dose-dependent reduction in cell density in (A) HepG2 and (B) SH-SY5Y cells after exposure to Cd for 24 h. Comparison to the negative control. *** $p < 0.001$ , * $p < 0.05$	40
<b>Figure 18:</b> Cell density in (A) HepG2 and (B) SH-SY5Y cells after 24 h exposure to the IC <sub>25</sub> , IC <sub>50</sub> and IC <sub>75</sub> of Cd. Comparison to the negative control. *** $p < 0.001$	41
<b>Figure 19:</b> Mitochondrial membrane potential in (A) HepG2 and (B) SH-SY5Y cells after 24 h exposure the IC <sub>25</sub> , IC <sub>50</sub> and IC <sub>75</sub> of Cd. Comparison to the negative control. *** $p < 0.001$ , ** $p < 0.01$ , * $p < 0.05$	42
<b>Figure 20:</b> Intracellular ATP levels in (A) HepG2 and (B) SH-SY5Y cells after 24 h exposure the IC <sub>25</sub> , IC <sub>50</sub> and IC <sub>75</sub> of Cd. Comparison to the negative control. ** $p < 0.01$	43
<b>Figure 21:</b> Reactive oxygen species Concentrations in (A) HepG2 and (B) SH-SY5Y cells after 24 h exposure to the IC <sub>25</sub> , IC <sub>50</sub> and IC <sub>75</sub> of Cd. Comparison to the negative control. *** $p < 0.001$ , ** $p < 0.01$	44
<b>Figure 22:</b> Glutathione levels in (A) HepG2 and (B) SH-SY5Y GSH after 24 h treatment with to the IC <sub>25</sub> , IC <sub>50</sub> and IC <sub>75</sub> of Cd. Comparison to the negative control. *** $p < 0.001$ , ** $p < 0.01$ , * $p < 0.05$	45

<b>Figure 23:</b> Caspase 3/7 activity in (A) HepG2 and (B) SH-SY5Y after exposure to the IC <sub>25</sub> , IC <sub>50</sub> and IC <sub>75</sub> of Cd for 24 h. Comparison to the negative control. ** $p < 0.01$ , * $p < 0.05$	46
<b>Figure 24:</b> Dose-dependent reduction of cell density in (A) HepG2 and (B) SH-SY5Y cells after exposure to Hg for 24 h. Comparison to the negative control. *** $p < 0.001$ , ** $p < 0.01$	49
<b>Figure 25:</b> Cell density in (A) HepG2 and (B) SH-SY5Y cells after exposure to the IC <sub>25</sub> , IC <sub>50</sub> and IC <sub>75</sub> of Hg for 24 h. Comparison to the negative control. *** $p < 0.001$	49
<b>Figure 26:</b> Mitochondrial membrane potential in (A) HepG2 and (B) SH-SY5Y cells after 24 h exposure the IC <sub>25</sub> , IC <sub>50</sub> and IC <sub>75</sub> of Hg. Comparison to the negative control. ** $p < 0.01$ , * $p < 0.05$	50
<b>Figure 27:</b> Intracellular ATP levels in (A) HepG2 and (B) SH-SY5Y cells after 24 h exposure the IC <sub>25</sub> , IC <sub>50</sub> and IC <sub>75</sub> of Hg. Comparison to the negative control. *** $p < 0.001$ , ** $p < 0.01$ , * $p < 0.05$	51
<b>Figure 28:</b> Reactive oxygen species levels in (A) HepG2 and (B) SH-SY5Y cells after 24 h exposure to the IC <sub>25</sub> , IC <sub>50</sub> and IC <sub>75</sub> of Hg. Comparison to the negative control. *** $p < 0.001$ , ** $p < 0.01$ , * $p < 0.05$	52
<b>Figure 29:</b> Glutathione concentration in (A) HepG2 and (B) SH-SY5Y cells after 24 h exposure to the IC <sub>25</sub> , IC <sub>50</sub> and IC <sub>75</sub> of Hg. Comparison to the negative control. *** $p < 0.001$ , ** $p < 0.01$	53
<b>Figure 30:</b> Caspase-3/7 activity in (A) HepG2 and (B) SH-SY5Y cells after treatment after 24 h exposure to the IC <sub>25</sub> , IC <sub>50</sub> and IC <sub>75</sub> of Hg. Comparison to the negative control. *** $p < 0.001$ , ** $p < 0.01$ , * $p < 0.05$	54
<b>Figure 31:</b> Cell density in (A) HepG2 and (B) SH-SY5Y cells after exposure to the IC <sub>25</sub> , IC <sub>50</sub> and IC <sub>75</sub> mixtures of As, Cd and Hg for 24 h. Comparison to the negative control. *** $p < 0.001$	55
<b>Figure 32:</b> Dose-dependent reduction of cell density in (A) HepG2 and (B) SH-SY5Y cells after exposure to EPA mixtures with respect to As for 24 h. Cadmium and Hg concentrations are according to the EPA ratio of As, Cd and Hg (10:5;2). Comparison to the negative control. *** $p < 0.001$ , ** $p < 0.01$ , * $p < 0.05$	56
<b>Figure 33:</b> Mitochondrial membrane potential in (A) HepG2 and (B) SH-SY5Y cells after exposure to the IC <sub>20</sub> , IC <sub>25</sub> and IC <sub>35</sub> mixtures of As, Cd and Hg for 24 h. Comparison to the negative control. *** $p < 0.001$ , ** $p < 0.01$ , * $p < 0.05$	57

**Figure 34:** Dose-dependent reduction of  $\Delta\Psi_m$  in (A) HepG2 and (B) SH-SY5Y cells after exposure to EPA mixtures with respect to As for 24 h. Cadmium and Hg concentrations are according to the EPA ratio of As, Cd and Hg (10:5:2). Comparison to the negative control. \*\*\*  $p < 0.001$ , \*\*  $p < 0.01$  58

**Figure 35:** Dose-dependent reduction of ATP levels in (A) HepG2 and (B) SH-SY5Y cells after exposure to EPA mixtures with respect to As for 24 h. Cadmium and Hg concentrations are according to the EPA ratio of As, Cd and Hg (10:5;2). Comparison to the negative control. \*\*\*  $p < 0.001$ , \*\*  $p < 0.01$ , \*  $p < 0.05$  58

**Figure 36:** Reactive oxygen species in (A) HepG2 and (B) SH-SY5Y cells after exposure to the IC<sub>20</sub>, IC<sub>25</sub> and IC<sub>35</sub> mixtures of As, Cd and Hg for 24 h. Comparison to the negative control. \*\*\*  $p < 0.001$  59

**Figure 37:** Dose-dependent reduction of ROS levels in (A) HepG2 and (B) SH-SY5Y cells after exposure to EPA mixtures with respect to As for 24 h. Cadmium and Hg concentrations are according to the EPA ratio of As, Cd and Hg (10:5;2). Comparison to the negative control. \*\*\*  $p < 0.001$ , \*  $p < 0.05$  60

**Figure 38:** Reduced glutathione levels in (A) HepG2 and (B) SH-SY5Y cells after exposure to the IC<sub>20</sub>, IC<sub>25</sub> and IC<sub>35</sub> mixtures of As, Cd and Hg for 24 h. Comparison to the negative control. \*  $p < 0.001$  60

**Figure 39:** Dose-dependent reduction of GSH levels in (A) HepG2 and (B) SH-SY5Y cells after exposure to EPA mixtures with respect to As for 24 h. Cadmium and Hg concentrations are according to the EPA ratio of As, Cd and Hg (10:5;2). Comparison to the negative control. \*\*\*  $p < 0.001$  61

**Figure 40:** Caspase-3/7 activity in (A) HepG2 and (B) SH-SY5Y cells after exposure to EPA mixtures with respect to As for 24 h. Cadmium and Hg concentrations are according to the EPA ratio of As, Cd and Hg (10:5;2). Comparison to the negative control. \*\*\*  $p < 0.001$ , \*\*  $p < 0.01$  62

## List of Tables

---

Contents	Page number
<b>Table 1:</b> Inhibitory concentrations of As determined after 24 h exposure in the HepG2 and SH-SY5Y cell lines.	28
<b>Table 2:</b> Reduction in cell density (%) after exposure to the IC <sub>25</sub> , IC <sub>50</sub> and IC <sub>75</sub> of As, Cd and Hg for 24 h in the HepG2 and SH-SY5Y cell lines.	29
<b>Table 3:</b> Inhibitory concentrations of Cd determined after 24 h exposure in the HepG2 and SH-SY5Y cell lines.	40
<b>Table 4:</b> Inhibitory concentrations of Hg determined after 24 h exposure in the HepG2 and SH-SY5Y cell lines.	49

## List of abbreviations

---

### Symbols and numerical values

%	Percentage
% w/v	Percentage weight per volume
% v/v	Percentage volume per volume
$\Delta\Psi_m$	Mitochondrial membrane potential
$\bullet\text{O}_2^-$	Superoxide anion
$\bullet\text{OH}$	Hydroxyl radicals
$^\circ\text{C}$	Degree centigrade
$\Delta$	Delta
$\alpha$	Alpha
$\beta$	Beta
$\mu\text{L}$	Microliter
$\mu\text{g}$	Microgram
$\mu\text{M}$	Micromolar
$\lambda_{\text{ex}}$	Excitation wavelength
$\lambda_{\text{em}}$	Emission wavelength

### A

AAPH	2,2'-Azobis (2-methylpropionamide) dihydrochloride
Ac-DEVD-AMC	Acetyl Asp-Glu-Val-Asp-7-amido-4-methyl-coumarin
AMC	7-Amido-4-coumarin
ADP	Adenosine diphosphate
Ag	Silver



ANOVA	Analysis of variance
ANT	Adenine nucleotide transporters
Apaf -1	Apoptotic protease activating factor-1
As	Arsenic
As <sub>2</sub> O <sub>3</sub>	Arsenic trioxide
ATCC	American Tissue Culture Collection
ATP	Adenosine triphosphate
ATSDR	Agency of Toxic Substances and Disease Registry

## B

BBB	Blood-brain barrier
-----	---------------------

## C

CaNa <sub>2</sub> EDTA	Calcium disodium ethylenediamine tetraacetic acid
CAT	Catalase
Cd	Cadmium
CdCl <sub>2</sub>	Cadmium chloride
CNS	Central nervous system
Cr	Chromium
Cu	Copper
cyt C	Cytochrome c

## D

DCF	Dichlorofluorescein
H <sub>2</sub> -DCF-DA	Dihydrodichlorofluorescein diacetate
DMEM	Dulbecco's Modified Eagle Medium
DMSO	Dimethyl sulfoxide

DMSA 2,3-Dimercaptosuccinic acid

DNA Deoxyribonucleic acid

DR Death receptor

## E

EPA Environmental Protection Agency

EMEM Eagle's Minimum Essential Medium

## F

FCS Foetal calf serum

FDA Food and Drug Administration

Fe Iron

FITC Fluorescein isothiocyanate

## G

GR Glutathione reductase

GSH Reduced glutathione

GSH-Px Glutathione peroxidase

g Gram

*g* Relative centrifugal force

## H

HBSS Hanks Buffered Salt Solution

Hg Mercury

HgCl<sub>2</sub> Mercury chloride

H<sub>2</sub>O<sub>2</sub> Hydrogen peroxide

**J**

JC-1            5,5',6,6'-Tetrachloro-1,1,3,3'- tetraethylbenzimidazolylcarbocyanine iodide

JNK            c-Jun N-terminal kinase pathway

**L**

L                Liter

LDH            Lactate Dehydrogenase

**M**

MAPK          Mitogen activated protein kinase

MCB            Monochlorobimane

MCL            Maximum contamination limits

mM            Millimolar

mL            Milliliter

MPTP          Mitochondrial permeability transition pore

MT            Metallothionein

MTT            3-(4,5-dimethylthiazol-2-yl)-2,5-diphenyltetrazolium bromide

**N**

NaAsO<sub>2</sub>        Sodium arsenite

**P**

Pb            Lead

PBS            Phosphate-buffered saline

PI            Propidium iodide

**R**

RNS            Reactive nitrogen species

ROS            Reactive oxygen species

RPMI           Roswell Park Memorial Institute

**S**

SEM            Standard error of the mean

SOD            Superoxide dismutase

SRB            Sulforhodamine B

**T**

TCA            Trichloroacetic acid

**U**

UV            Ultraviolet light

**W**

WHO           World Health Organization

**Z**

Zn            Zinc

# Chapter 1

## Literature review

---

Heavy metals are metallic elements that have a relatively high atomic density (four- to five-times greater than water) and have the potential to exert toxicity at low concentrations.<sup>1</sup> Some heavy metals such as cobalt, copper (Cu), iron (Fe), manganese, molybdenum, and zinc (Zn) are required by humans at very low concentrations as cofactors for enzymes and to mediate redox reactions.<sup>1</sup> However, even these are toxic at higher concentrations.<sup>2</sup> Some heavy metal oxides, such as arsenic trioxide ( $\text{As}_2\text{O}_3$ ), present with minimal toxicity at low concentrations.<sup>3</sup> Examples of heavy metals which are toxic and are not known to have beneficial properties include arsenic (As), cadmium (Cd), chromium (Cr), lead (Pb), mercury (Hg), silver (Ag), the platinum (Pt)-group elements, and Zn.

Environmental contamination with heavy metals occurs through the air, soil and water. Heavy metals are generally non-biodegradable and their persistent contamination has been linked to severe health detriments.<sup>4</sup> The major route of metal exposure is via food and water, which may occur simultaneously or sequentially. Heavy metal exposure has been linked to numerous diseases, such as cancer, hepatotoxicity, nephrotoxicity and neurotoxicity.<sup>5</sup> The Agency of Toxic Substances and Disease Registry (ATSDR) has listed As, Cd and Hg among the top eight hazardous contaminants in site frequency count in their exposure pathway report.<sup>6</sup>

### 1.1. Arsenic

#### 1.1.1. Background and exposure sources

Arsenic is a p-block element that is placed in group 15 of the periodic table. In its natural form, it is mainly found as arsenates (~60%), but may also occur as sulphides, arsenites, arsenides, oxides, silicates (~20%) and elemental arsenic (~20%).<sup>7</sup> The main source of human exposure is through food, air and water. Arsenic may enter the food chain through seafood, fish, algae and cereals. Polluted air near coal-power generation sites, mining, smelting and water of industrial areas are also common sources of As-exposure.<sup>8</sup> Arsenic is colourless, odourless and tasteless, which generally makes it undetectable.<sup>9</sup> Global estimates suggest that 160 million people live in areas where there are increased levels of As in drinking water due to enriched geological formations.<sup>10</sup> Although As-toxicity

has been extensively described, humans are still exposed as a result of the agriculture and pesticide industry use thereof. An example is where fifteen million pounds of As-based pesticides leached into the soil in New Jersey between 1980 and 1990, which resulted in environmental contamination.<sup>11, 12</sup> Extensive use of As in pesticides has further increased the risk of exposure to humans. The United States Environmental Protection Agency (EPA) has set maximum contaminant levels (MCL) of As to 10 µg/L in drinking water.<sup>13</sup> These limits are not adhered to as As measurements in Argentina, Bangladesh, Chile, China, India, Mexico and USA have been reported to exceed EPA thresholds.<sup>14-17</sup>

### 1.1.2. Toxicokinetics and toxicodynamics

After oral administration, about 80–90% of a single dose of arsenite or arsenate is absorbed from the gastrointestinal tract, while airborne As (mostly trivalent arsenic oxide) is deposited in the lungs.<sup>18</sup> Distribution from the lungs is dependent on particle size and chemical form.<sup>18</sup> After absorption, As accumulates mainly in the liver, but also in the kidney, heart, neural tissue and lungs.<sup>18</sup> The elimination half-life is approximately three to five days, and a small amount of inorganic As is excreted in urine.<sup>19</sup> Arsenic metabolism involves more than five metabolites, and starts with the methylation of inorganic As compounds (Figure 1).

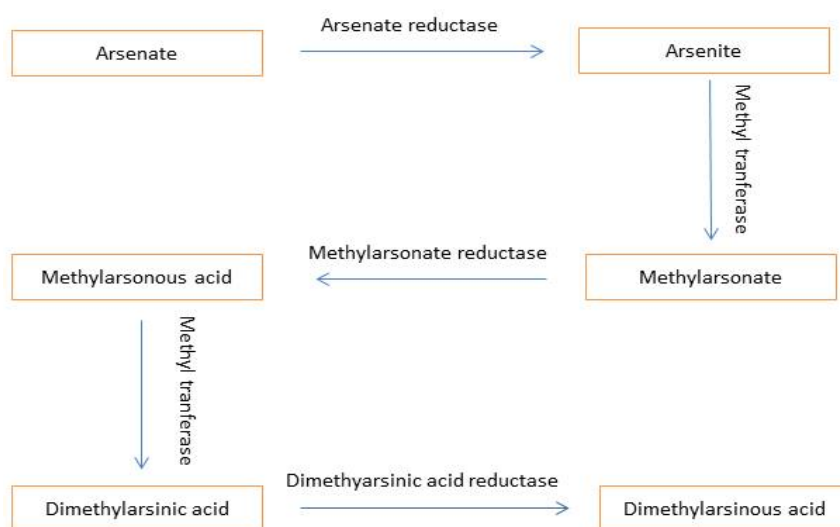


**Figure 1:** Biotransformation of inorganic arsenic in mammalian systems.

Arsenic can cross the blood-brain barrier (BBB), and thus it can enter the central nervous system (CNS). Arsenic accumulates in the CNS, and undergoes bio-methylation in the brain.<sup>20</sup> In the body,

inorganic pentavalent arsenate is converted into trivalent arsenite in the testis, followed by the kidney, liver, and lungs. Trivalent arsenite generates reactive oxygen species (ROS), and induces carcinogenesis.<sup>21</sup> Arsenic-toxicity may also result in many non-cancerous diseases as a result of depletion of reduced glutathione (GSH) and binding to sulfhydryl groups of proteins.<sup>22, 23</sup> Arsenic-induced oxidative stress results in the depletion of endogenous antioxidants, such as superoxide dismutase (SOD), catalase (CAT), glutathione peroxidase (GSH-Px), and heme oxygenase-1. Removal of antioxidants in turn may result in deoxyribonucleic acid (DNA) damage and lipid peroxidation during oxidative stress.<sup>20</sup> Mechanisms of carcinogenicity include inhibition of enzymes implicated in DNA repair [poly-(Adenosine diphosphate-ribose) polymerase], alteration of DNA-methylation, oxidative stress, uncontrolled cell proliferation, tumour promotion, and co-carcinogenesis.<sup>24, 25</sup>

### **1.1.3. Health risks and treatment options**

Long-term exposure to As has been linked to several prominent diseases in humans. Arsenic has been ranked as the top most hazardous contaminant in site frequency count by the ATSDR.<sup>6</sup> Epidemiological studies have shown that arsenite is three times more toxic than arsenate due its high cellular uptake and accumulation in cells.<sup>26</sup> Acute and chronic toxicity of As may result in hypertension, altered haem metabolism, skin rashes, neuropathy, bone marrow depression, ischaemia, encephalopathy, hepatomegaly, cirrhosis, proximal tubule degeneration, severe arteriosclerosis and many types of cancers.<sup>27-29</sup> Gastrointestinal disturbances including nausea, vomiting, pain and watery diarrhea and may lead to endothelial damage and hypovolemic shock. Torsade de pointes ventricular arrhythmias, distal symmetric peripheral neuropathy and CNS encephalopathy may also occur.<sup>20</sup> Arsenic has been classified as a class I human carcinogen by the International Agency of Research on Cancer (IARC)<sup>30</sup> and is linked to lung, skin, liver, and bladder cancers.<sup>31</sup> Among As-induced neoplasms, skin cancer is the most frequent, while lung cancer presents with the highest mortality.<sup>32, 33</sup> A longitudinal study in Bangladesh indicated that exposure to As in well water from 10.1–50 µg/L to 100.1–200 µg/L increased the incidence of dose-dependent skin lesions from 15.5% to 23.8%.<sup>34</sup> Long-term exposure to lower concentrations (<100 µg/L) caused skin reactions.<sup>34</sup> Elevated As-exposure (>100 µg/L) has been associated with increased risk of cardiovascular disease (CVD), especially ischaemic heart disease.<sup>35, 36</sup> Chronic exposure to As appears to be associated with type 2 diabetes mellitus.<sup>37</sup> Arsenic-contaminated ground water in Bangladesh

led to one of the largest mass poisonings reported in history<sup>38</sup> resulting in arsenicosis.<sup>39</sup> This disease presents as a serious public health problem, especially in developing countries. Pregnant females chronically exposed to As through drinking water have been found to give birth to infants with a higher risk of congenital heart anomalies.<sup>36</sup> Furthermore, these mothers had an increased risk of spontaneous abortion, stillbirth and reduced body weight.<sup>40</sup> Arsenic exposure through drinking water has also been associated with a higher risk of cognitive impairment and black foot disease, leading to gangrene of the extremities.<sup>41, 42</sup> Acute toxicity may result in pancytopenia and anemia within 96 h of exposure.<sup>43</sup>

An indicator of As poisoning is a prolonged QT interval on electrocardiograms. Urinary As excretion can be monitored for 24 h to diagnose arsenic poisoning.<sup>44</sup> Treatment is dependent on removal of the contaminant, reduction of further exposure and supportive measures.<sup>45</sup> Chelation is used to manage toxicity, for example, through the use of succimer (2,3-dimercaptosuccinic acid) and dimercaprol.<sup>45</sup> In patients with kidney failure, haemodialysis is used to improve outcome. Vitamin B12 and folic acid administration has been shown to decrease oxidative stress-induced damage of the heart.<sup>46</sup>

## **1.2. Cadmium**

### **1.2.1. Background and exposure sources**

Cadmium is a transition metal and belongs to group 12 (IIB) in the periodic table. Fossil fuel, run-off from agricultural land and mining sites which contain Cd results in contamination of the environment.<sup>47</sup> Human exposure to Cd mainly occurs through inhalation of cigarette smoke, ingestion of contaminated food (organ meat, seafood, grains, root crops and leafy vegetables), and water intake.<sup>48, 49</sup> Cadmium also contaminates the environment through smelting, nickel-Cd batteries, mining and use of fertilizers.<sup>50</sup> As Cd is highly water-soluble, it can enter the food-chain through edible plants which have been irrigated with Cd-contaminated water. The EPA has set the MCL for Cd to 5 µg/L in drinking water.<sup>13</sup>



### **1.2.2. Toxicokinetics and toxicodynamics**

Following absorption, Cd binds to albumin and is transported to the liver, where it promotes the synthesis of metallothionein, a heavy metal-binding protein. Complexes of Cd and metallothionein are reabsorbed from the proximal tubules of the nephron, where it accumulates in the cortex of the kidney and has a half-life of >10 years.<sup>51</sup> A strong correlation has been found between Cd-induced kidney toxicity and urine concentrations.<sup>52, 53</sup> The half-life of Cd is biphasic, with an initial decrease in blood levels due to re-distribution. The half-life thus lengthens as elimination takes longer. The fast-component is 75 to 128 days, while the slow-component may take between 7.4 and 16.0 years.<sup>54</sup>

Cadmium exerts its toxicity through oxidative stress, which involves GSH depletion and protein-bound sulfhydryl groups, resulting in enhanced ROS production, superoxide anion ( $\bullet\text{O}_2^-$ ), hydrogen peroxide ( $\text{H}_2\text{O}_2$ ) and hydroxyl radicals ( $\bullet\text{OH}$ ). Cadmium-induced ROS generation leads to lipid peroxidation and DNA damage.<sup>55</sup> Cadmium chloride ( $\text{CdCl}_2$ ) causes DNA damage and apoptosis through generation of ROS in human liver carcinoma (HepG2) cells.<sup>56</sup> Other mechanisms for chronic toxicity include alteration to serotonergic and gabaminergic pathways.<sup>56</sup>

### **1.2.3. Health risks and treatment options**

Cadmium is ranked seventh on the Priority List of Hazardous Substances by the ATSDR.<sup>6</sup> Acute toxicity of Cd can be fatal after ingestion or inhalation, and results in pulmonary oedema, fulminating hepatitis, hemorrhage and testicular injury. Chronic intoxication may lead to disturbance of metabolism, osteomalacia, pulmonary disease, obstruction of kidney function, blood pressure fluctuations, deformations of bones and immune deficiencies.<sup>48, 57-59</sup> Cadmium is known to have toxic effects on the renal, cardiovascular and respiratory systems. As one of the key substances involved in cigarette smoke, it is known to be a major reason for bronchitis. Cadmium affects cell proliferation, differentiation, and apoptosis. These activities interact with DNA repair mechanism, the generation of ROS and the induction of apoptosis. Cadmium binds to the mitochondria and can inhibit both cellular respiration and oxidative phosphorylation at low concentrations. Cadmium exposure may result in decreased glomerular filtration rate and proteinuria, consisting mainly of albumin.<sup>60</sup> Chronic exposure may cause sleep disorders, headaches and memory loss. Dryness of the throat, choking, coughing, restlessness, chest pain, nausea and vomiting are common indications of toxicity.<sup>61</sup> Severe

complications start with glycosuria and proteinuria, leading to renal and hepatic failure.<sup>60</sup> Increased proteinuria in different populations after exposure to Cd has been indicated.<sup>60, 62, 63</sup> Cardiovascular and lung damage may also occur.<sup>20</sup> Exposure to Cd also results in headaches, vertigo, olfactory dysfunction, slowing of vasomotor functioning, peripheral neuropathy, decreased equilibrium and learning disabilities.<sup>64, 65</sup>

It has been demonstrated that Cd is a possible etiological factor of neurodegenerative diseases, such as Alzheimer's disease and Parkinson's disease.<sup>66, 67</sup> Cadmium accumulation prior to and at birth, might cause irreversible toxicity in the brain, which in turn leads to altered gene expression.<sup>68</sup> The IARC confirmed on the basis of lung cancer studies, that Cd is a class 1 human carcinogen.<sup>69</sup> Cadmium has also been linked to increased breast cancer risk.<sup>70</sup> The liver is a major target organ for Cd toxicity and hepatotoxicity is dose- and time-dependent, which includes hepatocellular degeneration at lower concentrations and multifocal necrosis at higher concentrations.<sup>71</sup>

Treatment involves limiting exposure, and supportive measures. Chelation therapy with calcium disodium ethylenediamine tetraacetic acid (CaNa<sub>2</sub>EDTA) 75 mg/kg/day for five days is recommended.<sup>72</sup> However, carbodithioates including diethyl (De)-, dimethyl (Dm)-, and diisopropyl (Di)-dithiocarbamates have been found to be more effective than CaNa<sub>2</sub>EDTA in Cd toxicity management.<sup>72</sup>

### **1.3. Mercury**

#### **1.3.1. Background and exposure sources**

Mercury is a d-block transition element placed in group 12 of the periodic table. This compound is present in three forms: organic, inorganic and elemental. Atmospheric contamination with Hg-vapours is mainly due to volcanic emissions and volatilisation from aquatic sources, degassing from geological materials and wind-blown dust.<sup>73</sup> Burning of fossil fuels, mining and extraction, and the cement industry are other sources contributing to atmospheric contamination.<sup>74</sup> Mercury is used in industry for thermostats, batteries and switches, dental amalgams, production of caustic soda, nuclear reactors, as an antifungal agent, a preservative in pharmaceutical products and a solvent for reactive metals.<sup>75</sup> Environmental pollution has resulted from dumping inorganic mercury along the

Amazon River in Brazil, pit working in gold mines in Tanzania, Philippines and Indonesia, Faroe islands, Peru, New Zealand, Ecuador, Seychelles island and Slovenia.<sup>76,77</sup>

Human exposure to Hg is through food (mainly fish and shellfish), environmental contamination, preventive medical practices, dental amalgams, industrial, occupational and agricultural activities. In 1956, 2 200 people in Japan were afflicted with Minamata disease due to Hg-contaminated fish and shellfish consumption.<sup>78</sup> The EPA has set a MCL of 2 µg/L Hg in drinking water.<sup>13</sup>

### **1.3.2. Toxicokinetics and toxicodynamics**

Vapors of organic mercury are readily absorbed in the lungs.<sup>79</sup> Approximately 95% of orally-ingested Hg is bioavailable.<sup>80</sup> It is widely distributed due to its lipophilic nature and readily crosses the BBB.<sup>80</sup> The half-life of Hg in blood is 50 days where 50% of the dose is concentrated in the liver and 10% in CNS.<sup>81</sup> Methyl mercury is de-methylated to mercuric (Hg<sup>2+</sup>) in tissue macrophages, intestinal flora, and the foetal liver.<sup>82</sup> Approximately 80% of an inhaled dose of elemental Hg is absorbed.<sup>83</sup> Once in the blood, it is oxidized to Hg<sup>2+</sup> by CAT and H<sub>2</sub>O<sub>2</sub> in tissue and blood.<sup>82</sup> Seven to fifteen percent of inorganic Hg ingested is absorbed where it accumulates in kidneys.<sup>84</sup> The half-life of inorganic Hg in blood is 19.7 to 65.6 days.<sup>84</sup> It does not readily cross the BBB but its CNS penetration is higher in children as the BBB is not fully developed.<sup>82</sup>

Inorganic divalent mercury, such as mercury chloride (HgCl<sub>2</sub>), can replace the hydrogen atom in sulphhydryl groups of enzymes to form mercaptides. The latter leads to cellular GSH depletion and inactivation of various enzymes.<sup>85</sup> This dysregulation of enzymes results in interruptions of biological functions which are regulated by sulphhydryl compounds, including metabolism, intracellular redox balances and cell signaling pathways.<sup>86, 87</sup> Other mechanisms for Hg-toxicity are oxidative stress, inhibition or disturbance of enzyme activity, disrupting intracellular calcium balance, altering the immune system, as well as DNA and protein synthesis inhibition.<sup>88</sup>

### **1.3.3. Health risks and treatment options**

Mercury is ranked third on the Priority List of Hazardous Substances by the ATSDR.<sup>6</sup> Mercury accumulates in the brain, liver and kidneys, which results in neurotoxicity, gastrointestinal toxicity

and nephrotoxicity.<sup>85</sup> In cases of acute ingestion, nausea, vomiting, gastroenteritis, colic, abdominal pain, bloody diarrhoea and renal failure may occur.<sup>85</sup> Chronic toxicity may lead to extensive salivation, tremors of lips and tongue, corrosive damage to the mouth, anorexia and tooth loss. Once absorbed, Hg concentrates in the proximal tubules of kidneys where it may induce complex nephritis due to tubular damage and proteinuria.<sup>89</sup> Acute toxicity through inhalation usually results in breathing difficulties, tightness of the chest with associated pain, acute chemical pneumonitis and bronchiolitis.<sup>90</sup> Mercury vapours can easily cross the BBB, and become oxidized to a mercuric form which accumulates in the cortex and cerebellum.<sup>91</sup> Central nervous system toxicity caused by Hg vapours includes psychotic reactions, delirium, hallucination, loss of memory and cognitive impairment.<sup>91</sup> Methyl mercury also damages the CNS, which is characterized by ataxia, constriction of the visual fields, dysarthria and loss of hearing.<sup>92</sup> Gastrointestinal irritation, abdominal cramps, and anorexia are initial symptoms of toxicity. Clinical symptoms may include CNS effects like paresthesia, a tightening sensation around the mouth and lips, numbness, ataxia, difficulty in swallowing and speaking, vision and hearing loss, fatigue, weakness, neurasthenia, tremors and spasticity which may lead to a coma.<sup>92</sup>

Monitoring of vital organs, oxygen support, or mechanical ventilation is used as first-line treatment. Thereafter, intravenous fluid is administered to prevent shock.<sup>93</sup> As corrosive injury causes upper airway obstruction and oedema, endoscopic examination should be carried out.<sup>93</sup> In the case of direct contact with Hg, the skin should be washed.<sup>94</sup> Gastric lavage is recommended after ingestion because of the corrosive action and perforation potential of inorganic mercury.<sup>94</sup> Polyethylene glycol can be used for whole bowel irrigation to remove residual mercury.<sup>95</sup> Chelating agents such as penicillamine, and its derivative D-penicillamine, increase urinary excretion of Hg and Pb. Dimercaprol and its analogues, meso 2,3-dimercaptosuccinic acid (DMSA) and 2,3-dimercapto-1-propane sulfonic acid are also used alone or in combination with other chelating agents to treat inorganic mercury toxicity.<sup>96</sup> Although the FDA has not approved any chelating agent for methyl mercury treatment, DMSA is usually used in severe cases. Plasma exchange should be carried out when the patient's life is at stake and should be initiated about 24-36 hours after diagnosis.<sup>95, 97</sup>

#### **1.4. Organ toxicity of heavy metals**

Industrial, domestic, agricultural, medical, and technological applications of heavy metals have led to their wide distribution in the environment, raising concerns over their potential effects on human health. Their toxicity depends on several factors including the dose, route of exposure, and chemical form, as well as the age, gender, genetics, and nutritional status of exposed individuals.<sup>1</sup> Heavy metals including As, Cd and Hg are considered systemic toxicants that are known to induce multiple organ damage, even at lower levels of exposure.<sup>1</sup> The liver is the main target for xenobiotics and hence it is imperative to study the effects of heavy metals on this organ when ingested orally.<sup>98</sup> Most heavy metals including As, Cd and Hg can cross the BBB and have adverse effects on the brain. The liver and brain are the main targets of heavy metals since they accumulate at these sites.<sup>98</sup> There is paucity in literature with regards to the combinational toxic effects of As, Cd and Hg in these two organs.

##### **1.4.1. Hepatotoxicity**

Arsenic leads mainly to cancers of the skin, albeit there is epidemiological evidence for liver and kidney cancers being caused by exposure to As.<sup>99</sup> It is thought that the mechanism by which these cancers originate may involve the promotion of oxidative stress by As, in which the antioxidant capacity of the living organism is overwhelmed by ROS, resulting in molecular damage to proteins, lipids and most significantly DNA.<sup>100</sup> Repeated exposure to doses of 0.01–0.1 mg As per kg per day has shown symptoms of hepatic injury after oral exposure in humans.<sup>101</sup> After clinical examinations liver damage has been noted,<sup>102</sup> which has been confirmed by blood tests by way of elevated levels of hepatic enzymes. Histological examination of the livers of individuals repeatedly exposed to As, has revealed a consistent finding of portal tract fibrosis.<sup>103</sup> Longer periods of exposure has resulted in cirrhosis, which is considered to be a secondary effect of damage to the hepatic blood vessels.<sup>101</sup>

Epidemiological and experimental studies have linked occupational exposure to Cd with liver cancers.<sup>104</sup> The hepatotoxicity has been found to be dose- and time-dependent, with hepatocellular degeneration at lower concentrations and multifocal necrosis at higher concentrations.<sup>71</sup> Initially chronic exposure to Cd results in glycosuria and proteinuria, and later renal and hepatic failure.<sup>60</sup>

As a critical organ for drug metabolism, the liver is a primary target for toxic chemicals. In chronic poisoning experiments, inorganic Hg was shown to induce severe liver injury as shown by hepatic morphological changes and apoptosis, as well as having a detrimental effect on hepatic function.<sup>105</sup>

#### **1.4.2. Neurotoxicity**

Arsenic exposure to humans has been linked with various types of cancer and neurological disorders<sup>106</sup> The most common neurological effect of long-term As toxicity is peripheral neuropathy. This is accompanied by toxic hepatitis as indicated by increased levels of liver enzymes.<sup>101</sup> A possible correlation between As in drinking water and neurobehavioral alterations in children has been reported.<sup>107</sup> Adolescents from various regions of Taiwan and China exposed to low (0.0017–0.0018 mg/kg per day) levels of As in their drinking water showed a decreased performance in the switching attention task, while children in the high exposure group (0.0034–0.0042 mg/kg per day) showed a decreased performance in both the switching attention task and in tests of pattern memory, relative to unexposed controls.<sup>107</sup> Arsenic exposure at a level of 2 mg/kg per day or more can lead to encephalopathy, with symptoms of headache, mental confusion, seizures and coma.<sup>108</sup> Prolonged exposures to lower levels of As (0.03–0.1 mg/kg per day) are typically characterized by a symmetrical peripheral neuropathy,<sup>109</sup> which in its early stages is characterized by numbness in the hands and feet, which further develops into a painful sensation of pins-and-needles. Both sensory and motor nerves are affected and muscle weakness often develops.<sup>110</sup> Studies on patients with As neuropathy have shown a reduced nerve conducting velocity in their peripheral nerves, as is a typical feature of axonal degeneration.<sup>111</sup> In a similar fashion to other neurodegenerative diseases, As-induced neurotoxicity causes changes in cytoskeletal protein composition and hyperphosphorylation. These changes may lead to disorganization of the cytoskeletal structure, which is a potential cause of As-induced neurotoxicity.<sup>112</sup>

Exposure to Cd also severely affects the function of the nervous system<sup>113, 114</sup> with symptoms including headache and vertigo, olfactory dysfunction, parkinsonian-like symptoms, slowing of vasomotor functioning, peripheral neuropathy, decreased equilibrium, decreased ability to concentrate, and learning disabilities.<sup>64, 115</sup> It has been demonstrated in several studies that Cd is a possible etiological factor of Alzheimer's disease and Parkinson's disease.<sup>66, 67</sup> Cadmium

accumulation prior to and at birth, might cause irreversible toxicity in the brain, which in turn leads to altered gene expression.<sup>68</sup>

Disruption of attention, fine motor function and verbal memory has been documented in adults who have a high fish diet and are exposed to low mercury levels.<sup>116</sup> Long periods of exposure to low levels of mercury has led to increased complaints of tiredness, memory disturbance, subclinical finger tremor, abnormal EEG by computerized analysis and impaired performance in neurobehavioral or neuropsychological tests by those affected.<sup>117</sup> Mercury can directly induce synuclein fibril formation in dopaminergic neurons of the substantia nigra leading to Parkinson's disease.<sup>116</sup> People exposed to methylmercury during its dispersion from Minamata on the coast of the Shiranui sea demonstrated hypoesthesia, ataxia, dysarthria and impairment of hearing and visual change, 10 years after the end of exposure.<sup>118</sup>

### **1.5. Metal mixtures**

Human exposure to heavy metals has increased due to their more frequent use in agricultural, industrial, technological and domestic applications.<sup>85</sup> Sources of As, Cd and Hg in the environment are agricultural, geogenic, pharmaceutical, industrial, atmospheric sources and domestic effluents.<sup>119</sup>

Single-metal exposure rarely occurs whereas co-exposure with metals is the norm.<sup>120, 121</sup> These metals contaminate the air and water as a result of extensive mining processes.<sup>122</sup> Industrial wastes, contaminated fish consumption and mining processes are other sources of co-exposure to these metals. Leaching of inorganic As compounds formerly used in pesticide sprays, from the combustion of As-containing fossil fuels and from the leaching of mine tailings and smelter runoff contribute to As-contamination of drinking water.<sup>123</sup> Cadmium occurs naturally, in association with the sulphide ores of Pb, Zn, and Cu.<sup>124</sup> Industrial sources release Cd-contaminated water which may be used for irrigation.<sup>124</sup> As plants absorb Cd, it enters the food-chain. Cadmium and Hg-toxicity in Japan has also resulted from consumption of Cd- and Hg-contaminated fish caught in rivers near industrial plants.<sup>125</sup> South Africa has coastlines approximately 3 000 km long. Seafood is a good source of nutrition and recommended as part of a balanced healthy diet. Studies have identified toxic levels of metals like

As, Cd and Hg in seafood caught in the Langebaan lagoon, Western Cape, and other parts of the South African coastline.<sup>126</sup> High levels of Cd, Hg and Zn were found in the Buffalo, Keiskamma, Tyume and Umtata Rivers and in the Sandile and Umtata Dams of South Africa.<sup>127</sup> Medicinal plant samples from the Western Cape Province in South Africa were found to contain As and Cd at levels exceeding those recommended by the WHO.<sup>128</sup>

Metal mixture exposure poses serious health risks to humans. The CNS and liver are common targets for many metals.<sup>129</sup> As the number of possible combinations is infinite, it poses a great challenge for researchers to address the role of mixed exposure in human health. Understanding how metal mixtures affect health is critical to enable treatment.<sup>130-132</sup> Many proteins involved in cell growth, apoptosis, oxidative stress, and inflammation are modulated by metals.<sup>133, 134</sup> The mixtures can induce unique protein changes or cytotoxic effects that are not observed after single metal exposures.<sup>135-138</sup> Furthermore, metals may interact synergistically or antagonistically. Arsenic neurotoxicity has been found to be increased after mixed exposure to metals.<sup>139</sup> Children who are exposed to toxic metals may develop cognitive and/or behavioral effects.<sup>140, 141</sup> There is clearly a need to investigate the effects of metal combinations on cellular pathways. The lack of research with regards to simultaneous exposure to different metals poses an enormous challenge for the scientific community. This study is designed on HepG2 (hepatic origin) and SH-SH5Y (neuronal origin) cell lines to study the effects of As, Cd and Hg singly and in combinations to understand the cellular mechanism leading to toxicity.

## **1.6. Common mechanisms leading to cytotoxicity**

### **1.6.1. Cytotoxicity**

Cytotoxicity testing is one of the major assays employed during the assessment of compounds, which focus mainly on cell death or some measure of growth/metabolic impairment. This type of testing is used to evaluate the intrinsic ability of a compound to negatively impact cells.<sup>142</sup> Three factors play a major role in the toxicology of a substance: the dosage, the duration of exposure to the compound, and the compound's mechanism of toxicity.<sup>143</sup> At a cellular level, cytotoxicity can be expressed in a number of ways including: i) reduced or no cellular adhesion, ii) major morphological changes, iii) decreased growth rates and/or iv) reduced overall viability.<sup>144</sup>



### 1.6.2. Mitochondrial membrane potential

Mitochondria are the powerhouses of cells,<sup>145</sup> and produce the highest amount of adenosine triphosphate (ATP), especially in fasting conditions.<sup>146</sup> Mitochondria are present in almost all eukaryotic cells; and their main purpose is to produce energy for proper cellular functioning. Mitochondrial toxicity results in not only depletion of energy stores but also disturbed signaling pathways.<sup>145</sup>

Mitochondria have an outer and inner bilayer separated by an intermembrane space. The inner mitochondrial membrane contains mitochondrial DNA and enzymes, and is folded to form cristae which increases the surface area.<sup>146</sup> Transfer of substances through the inner matrix is selective and protein mediated.<sup>146, 147</sup> The inner membrane contains several protein systems including electron transport chain complexes, adenine nucleotide translocator and ATP-synthase.<sup>145, 147</sup> Mitochondria can accumulate positively-charged lipophilic molecules, and certain acidic compounds, due to the alkaline matrix and negative charge of the inner membrane. This explains the selective mitochondrial toxicity of some compounds.<sup>145</sup>

In mitochondria, ATP is produced from dietary carbohydrates and lipids, which are required for proper cell function and survival.<sup>111, 148</sup> Oxidative degradation of amino acids, fatty acid and pyruvate results in production of energy as ATP. In mitochondria, fatty acids from lipolysis and pyruvate from glycolysis are converted into acetyl-coenzyme A by  $\beta$ -oxidation and pyruvate dehydrogenase, respectively, under aerobic conditions.<sup>111, 148</sup>

Mitochondria generate an electrochemical proton gradient across it's the inner membrane, also referred to as the mitochondrial membrane potential ( $\Delta\Psi_m$ ).<sup>145, 146</sup> The backflow of protons down the electrochemical gradient, through the  $F_0$  portion of ATP synthase (complex V) into the mitochondrial matrix, releases energy. The  $F_1$  portion uses this released energy for phosphorylation of adenosine diphosphate (ADP) to ATP by the enzyme, ATP synthase which provides cellular energy.<sup>146</sup> The ATP is transported across the membrane through ANT in exchange for ADP, so that it may provide energy for cellular functioning.<sup>147</sup> The  $\Delta\Psi_m$  ranges from -200 to -180 mV, and the pH gradient from  $-\Delta 0.4-0.6$  U across the inner mitochondrial membrane. Respiration is inversely linked

to changes in  $\Delta\Psi_m$ . High  $\Delta\Psi_m$  results in decreased respiration and vice versa.<sup>145</sup> Mitochondrial toxicity may result from different points, including uncoupling of electron transport chain by lipophilic and slightly acidic compounds, disruption of electron shifting to oxygen, changes in redox cycling, opening of mitochondrial permeability transition pore (MPTP) resulting in oxidative stress or calcium influx, reduced mitochondrial DNA synthesis and impaired fatty acid oxidation.<sup>149</sup>

Mitochondrial toxicity results in oxidative stress, energy depletion, steatosis, cell cycle perturbations and differentiation leading to cell death.<sup>145, 146</sup> Pro-apoptotic factors in the intermembrane space lead to cell death pathways once mitochondrial leakage occurs (Figure 2).<sup>147</sup> Opening of the MPTP results in decreased mitochondrial membrane stability. The MPTP complex is located on the outer and inner membrane of the mitochondria and forms a channel.<sup>146, 147</sup> The MPTP is primarily composed of two proteins in the outer and inner mitochondrial membrane: the voltage-dependent anion channel (VDAC) and ANT, respectively (Figure 2). The formation of the MPTP complex involves the association of the peripheral benzodiazepine receptor on the outer membrane, creatinine kinase in the intermembrane space, hexokinase II linked to VDAC on the cytosolic portion of outer membrane, cyclophilin D in the matrix, Bax and Bcl-2.<sup>146,147</sup> The reduction in  $\Delta\Psi_m$  results in depolarization of the mitochondrial membrane and opens the MPTP.<sup>147</sup> Many toxic substances inhibit  $\beta$ -oxidation or mitochondrial respiration, reducing ATP formation and increasing oxidative stress.<sup>150</sup> Inhibition of respiratory chain protein complexes and enzymes like ATPase may lead to blockade of respiration.<sup>150</sup> Moderate inhibition may result in cellular dysfunction but in severe cases, it can result in necrosis with cholestasis and fibrotic outcomes.<sup>150</sup>

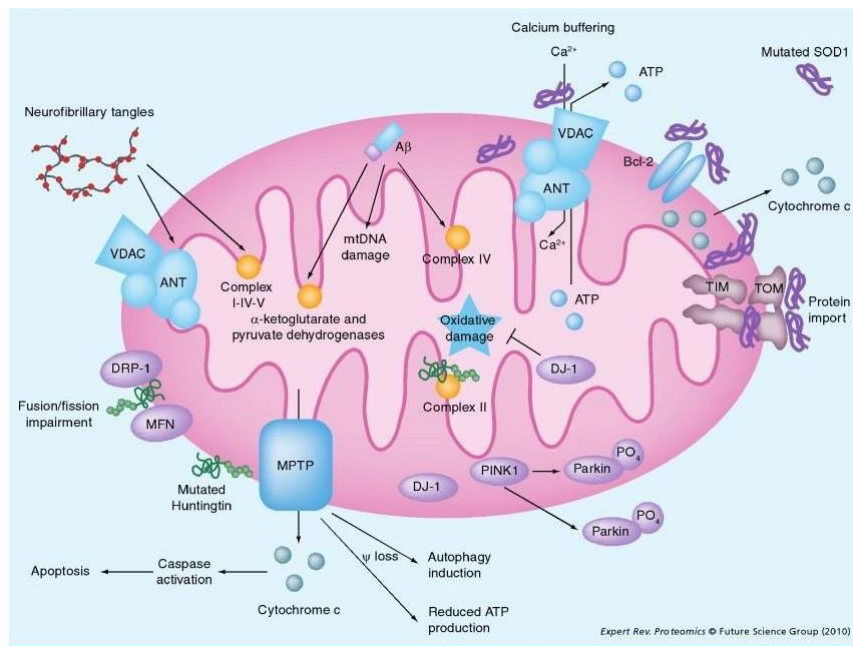


**Figure 2:** Dysfunction of Ca<sup>2+</sup> buffering, protein import, loss of mitochondrial membrane potential, mitochondrial respiration and ATP production. The final result is the loss of the mitochondrial membrane potential, causing the induction of mitophagy and/or the release of proapoptotic factors from the organelle<sup>151</sup>.

Mitochondria play a key role in the regulation of apoptosis. Mitochondrial dysfunction results in the loss of  $\Delta\Psi_m$ , permeability transition, and release of cytochrome c (cyt C) from mitochondria into the cytosol during the apoptosis induction process.

### 1.6.3. Adenine di- and triphosphate levels

Mitochondria produce ATP via the electron transport chain (ETC).<sup>152, 153</sup> By-products of the Krebs cycle, reduced nicotinamide adenine dinucleotide and reduced flavin adenine dinucleotide donate electrons to the ETC resulting in  $\Delta\Psi_m$ .<sup>154</sup> The phosphorylation of ADP is done through the action of ATP synthase.<sup>152, 154</sup> During electron transport, mitochondrial complex I and III leaks electrons to oxygen to produce  $\bullet O_2^-$  radical which is highly reactive, generating  $\bullet OH$  and  $H_2O_2$  through enzymatic conversion.<sup>152</sup> Within proliferating cells, a low ADP/ATP is expected, as more ADP is converted to ATP for cellular cycling.<sup>155</sup> As ATP formation is dependent on correct mitochondrial functioning, alterations may indicate loss of mitochondrial integrity.<sup>155</sup> Oxidation reduces ATP levels which impairs ATP dependent cytoprotective pathways and triggers cell death.<sup>154</sup>

#### 1.6.4. Reactive oxygen species

Any atom or molecule with an unpaired valence electron(s) is called a free radical. The term ROS refers to oxygen-centred free radicals.<sup>156</sup> The ROS are the most abundant free radical species in physiological systems. The increased production of ROS and/or reduced endogenous cellular antioxidant defenses may lead to oxidative stress.<sup>157</sup> Oxidative stress can result in cellular injury in various diseases including neurological disease, hepatitis, cancer, arthritis, and can accelerate the aging process.<sup>158, 159</sup>

Important ROS species include the singlet oxygen,  $\bullet\text{O}_2^-$ ,  $\text{H}_2\text{O}_2$  and  $\bullet\text{OH}$ . Reactive nitrogen species (RNS) are nitrogen-centred equivalents of ROS, and include peroxyxynitrite and nitric oxide. The  $\bullet\text{OH}$  radical is highly reactive and results in strong oxidisation, leading to DNA damage, protein residue modification, which results in lipid peroxidation.<sup>160, 161</sup> Various mechanisms may lead to ROS production, including metabolic activity of the CYP450 system and its reductases, disruption of the mitochondrial respiratory chain and intracellular oxidases.<sup>162, 163</sup> Formation of ROS is mainly due to leakage of electrons from respiratory chain complexes I and II, which reacts with oxygen to reduce it to  $\bullet\text{O}_2^-$ .<sup>146, 148, 150</sup>

Excessive or diminished production of ROS may affect cell viability and proliferation.<sup>164</sup> Increased ROS levels may inactivate or alter protein functions and/or peroxidise lipid membranes resulting in increased permeability, and induce DNA strand breakage or damage.<sup>148</sup> At low concentrations, ROS act as secondary messengers or signaling molecules, activating or inhibiting pathways by altering cellular redox state or redox-sensitive proteins.<sup>165</sup> For example, ROS has been found to activate mitogen activated protein kinase (MAPK), which in turn promotes cell proliferation, differentiation, apoptosis and survival.<sup>165</sup> The concentration of ROS is critical in determining the cellular effect that is produced.<sup>165</sup> Cell damage can vary from slight modifications to severe functional and structural loss. Oxidation of lipids and membranes form reactive intermediates, referred to as lipid peroxides, which is a major cause of drug-induced liver injury.<sup>162</sup>

### **1.6.5. Reduced glutathione levels**

Cells have hemostasis mechanisms against the adverse effects of ROS, which include complex antioxidant compounds and enzymes, such as GSH, SOD, CAT, glutathione reductase (GR) and GSH-Px.<sup>166</sup> Reduced glutathione is the most abundant and efficient antioxidant non-protein thiol in cells.<sup>167</sup> It can neutralize a state of oxidative stress by i) directly scavenging a free radical by donating a hydrogen cation and rendering the free radical harmless,<sup>168</sup> ii) eliminating H<sub>2</sub>O<sub>2</sub> by acting as a substrate for GSH-Px,<sup>167</sup> and replenishing the activity of other oxidised antioxidant molecules such as vitamins E and C.<sup>160</sup>

Cellular GSH regulates several signaling pathways, including the c-Jun N-terminal kinase pathway (JNK), which requires a tightly controlled redox status.<sup>169, 170</sup> The c-Jun N-terminal kinase pathway is activated by exposure of cells to cytokines or environmental stress, indicating that this signaling pathway may contribute to inflammatory responses. Depletion of the cellular GSH pool causes hyper induction of JNK activity.<sup>171</sup> Many xenobiotics generate reactive metabolites in the liver which are removed either by detoxification or conjugation to GSH. Reduced glutathione depletion is well known as a sign of cytotoxicity. Reactive metabolites that are not conjugated to GSH may result in degradation of hepatic macromolecules and ultimately lead to inflammatory responses.<sup>149, 150, 172</sup> Cells become more vulnerable to increasing concentrations of ROS, oxidative by products, disturbances in metabolism, survival and proliferation pathways after GSH depletion.<sup>169</sup>

### **1.6.6. Cell death and caspase activity**

Cell death is a tightly regulated process and may occur via various pathways, including apoptosis, necrosis, oncosis and autophagy.<sup>148, 173</sup> Although these cell death mechanisms are structurally and functionally different, they have overlapping mediators. There is thus a possibility that the cytotoxicity of a compound can switch to different mechanisms depending upon which conditions are met.<sup>173</sup> Cell death occurs in various stages involving the initiation, the commitment, and finally cellular decay.<sup>173</sup> A mixture of apoptotic and necrotic processes may frequently appear as the cause of hepatic cell death.<sup>174</sup> Selective mitochondrial permeability is a common feature in cell death pathways.<sup>174</sup> During this phenomenon, cells accumulate mediators needed for permeabilisation, resulting in decreased mitochondrial membrane integrity and release of catabolic metabolites

required for cell death.<sup>161</sup> Depending on the type of cell death pathway stimulated, necrosis follows large and sudden permeabilisation of the mitochondria, while apoptosis follows a more gradual, subtle permeabilisation.<sup>147</sup> Mode of cell death thus depends on the extent of mitochondrial toxicity and number of mitochondria presenting with open MPTP.<sup>146</sup>

Apoptosis, also called programmed cell death, is a controlled process that systemically removes damaged or decayed cells under physiological conditions without serious repercussions, such as inflammation.<sup>175</sup> Damaged cells are replaced by newer cells when mitogenesis continues at a constant rate. Various pathologies are linked to deficient or excessive apoptotic events, therefore well-regulated apoptotic systems are important.<sup>175</sup>

Autophagy and apoptosis play important roles in determining cellular fate, and are involved in numerous cellular processes such as development, homeostasis, physiological and pathological mechanisms. Both autophagy and apoptosis are driven by different regulatory and executioner molecules. Activated caspases remove organelles and other cellular structures by packaging them into apoptotic bodies.<sup>176, 177</sup> Dying cells that undergo apoptosis have several morphological and biochemical features. The morphological changes include cell shrinkage, nuclear condensation and fragmentation, dynamic membrane blebbing and loss of adhesion to neighbors or to the extracellular matrix.<sup>178</sup> The biochemical changes include chromosomal DNA cleavage into internucleosomal fragments, phosphatidylserine externalization and a number of intracellular substrate cleavages by specific proteolysis<sup>179, 180</sup>.

The apoptotic-signaling cascade is divided into two major pathways: the extrinsic/death receptor (DR) pathway and intrinsic/mitochondrial pathway.<sup>181</sup> Mitochondria play an important role in the intrinsic pathway. The Bcl-2 family of pro-apoptotic proteins facilitates permeabilisation of the mitochondrial membrane with subsequent release of mitochondrial proteins such as cyt C and apoptotic protease activating factor-1 (Apaf-1) forming a new complex, together with pro-caspase-9 (apoptosome), which contains an active form of caspase-9.<sup>181</sup> This complex recruits effector caspases like pro-caspase-3 which is cleaved to caspase-3. The activation of caspase-3 is considered a final step of executor protein formation in the apoptotic cell death sequence, leading to rapid cleavage of

several structural and functional proteins including signal transduction molecules, cytoskeletal components and DNA repair enzymes.<sup>182</sup>

The DR are cell-surface receptors that bind specific ligands, such as soluble molecules of the tumour necrosis factor (TNF) family, which are secreted as homotrimers and bind to members of the TNF-receptor (TNF-R) family, including TNFR-1, Fas/CD95, and TRAIL receptors DR-4 and DR-5. Ligand binding causes receptor trimerization and subsequent activation.<sup>183, 184</sup> The TNF-Rs possess a death domain (DD), which recruits other DD-containing proteins, such as TNF-R type 1-associated death domain protein (TRADD) and Fas-associated protein with death domain (FADD). These proteins then bind to initiator caspases-8 and -10, thus enabling homodimerization and subsequent activation of death-inducing signaling complex (DISC).<sup>185-187</sup> Following the activation of caspases-8 and -10, the effector caspases-3, -6, and -7 are cleaved, leading to cellular degradation in the final stage of apoptosis.<sup>188</sup>

Both extrinsic and intrinsic pathways converge at the level of caspase-3 activation and also there is the possibility of mitochondrial involvement during the course of execution of the extrinsic pathway.<sup>189</sup> Although caspases are the most important in programmed cell death there is the possibility of apoptotic cell death without activation of caspases. Morphological characteristics of apoptosis in the absence of caspase activation resembles necrotic cell death more closely than the classical cascade of apoptosis.<sup>190</sup>

### **1.7. Aim of the study**

The aim of the study was to assess the effect of As, Cd and Hg individually and in combination on the HepG2 hepatocarcinoma and SH-SY5Y neuroblastoma cell lines as a measure of hepatotoxicity and neurotoxicity, respectively.

## 1.8. Objectives of the study

The objectives of the study were to:

- Determine the effects of As, Cd and Hg individually and in combination on the HepG2 and SH-SY5Y cell lines by assessing:
  - Cell density using the sulforhodamine B (SRB) assay.
  - Mitochondrial membrane potential using the 5,5',6,6'-tetrachloro-1,1,3,3'-tetraethylbenzimidazolylcarbocyanine iodide (JC-1) ratiometric assay.
  - Intracellular ATP levels using chemiluminescence signaling.
  - Intracellular ROS generation using the dihydrodichlorofluorescein diacetate (H<sub>2</sub>-DCF-DA) cleavage assay.
  - Intracellular GSH concentrations using the monochlorobimane (MCB) adduct formation assay.
  - Caspase-3/7 activity using a Acetyl Asp-Glu-Val-Asp-7-amido-4-methyl-coumarin (ac-devd-amc) fluorometric cleavage assay.

## 1.9. Project overview

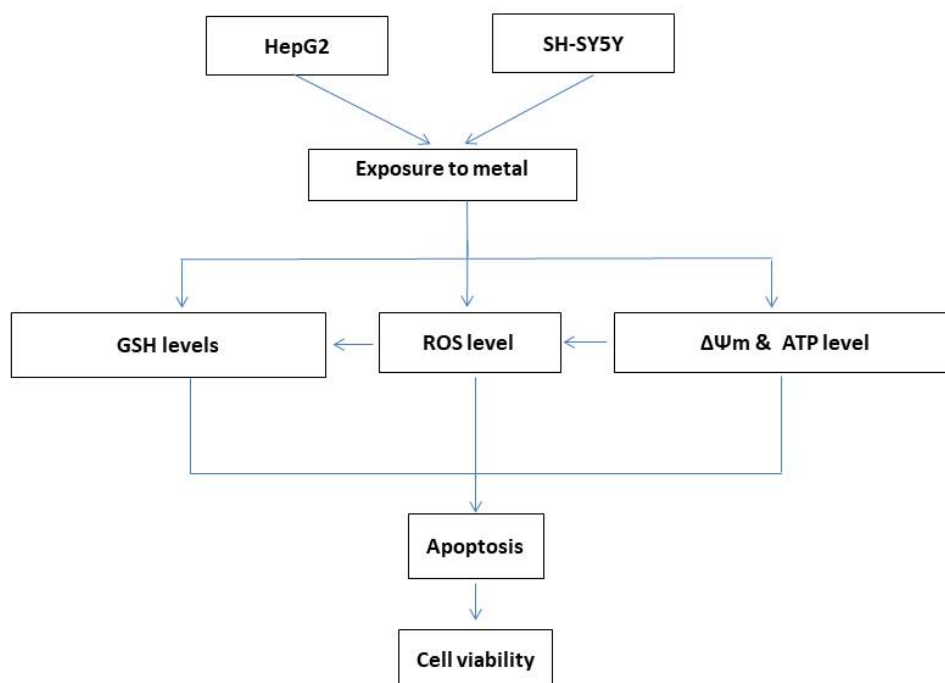


**Figure 3:** Flow diagrammatic representation of the project.



## Chapter 2

### Materials and methods

---

Ethical approval was obtained from the Faculty of Health Sciences Research Ethics Committee (REC) Ethics Reference No: 463/2016 (Appendix I). All instruments needed for the project were made available by the Department of Pharmacology at the University of Pretoria. Reagents and their preparation are provided in Appendix II.

#### 2.1. Heavy metals

Sodium arsenite (Merck, Germany) was used for As-toxicity determination as it is highly soluble in water. Sodium arsenate is also the most abundant form of As in nature, and is converted into arsenite in the body, which is then readily absorbed by cells.<sup>191-194</sup> Cadmium chloride (Sigma-Aldrich, USA) was used to induce Cd-toxicity as it is highly soluble in water, and is the most abundant form present in industrial water sources.<sup>195</sup> Mercury chloride (BDH, UK) was used to measure Hg-toxicity due to its solubility in water, and its frequent appearance in underground water near mining and industrial areas.<sup>196</sup>

#### 2.2. Cell culture and maintenance

HepG2 (HB-8065) and SH-SY5Y (CRL-2266) cells were originally purchased from the American Tissue Culture Collection (ATCC). HepG2 and SH-SY5Y cells were cultured in 75 cm<sup>2</sup> tissue culture flasks in Dulbecco's Modified Eagle's Medium (DMEM) and Eagle's Minimum Essential Medium (EMEM)/Ham's F12 medium, respectively. Medium was supplemented with 10% (v/v) foetal calf serum (FCS) and 1% (w/v) penicillin/streptomycin. The cells were cultured at 37°C in a humidified atmosphere of 5% CO<sub>2</sub>. Medium was changed as required, until cells were 80% confluent. Cells were washed with phosphate-buffered saline (PBS), and harvested using chemical detachment with Trypsin/Versene solution. Harvested cells were pelleted by centrifugation at 200 *g* for 5 min. Cells were counted using the trypan blue exclusion assay (0.1% w/v), and diluted in 10% FCS-supplemented medium to 2 x 10<sup>5</sup> cells/mL and 1 x 10<sup>5</sup> cells/mL for HepG2 and SH-SY5Y cells, respectively.

### 2.3. Seeding and exposure of cell lines

An aliquot (100  $\mu$ L) of HepG2 or SH-SY5Y cells were pipetted into clear (for spectrophotometric assays) or white (for fluorometric assays) 96-well plates to achieve  $2 \times 10^4$  cells/well and  $1 \times 10^4$  cells/well, respectively. Cells were allowed to attach overnight at 37°C in a humidified incubator. Cells were exposed to 100  $\mu$ L medium (negative control), positive control (refer to Sections 2.4 – 2.9), deionized water/medium mixture (1:4) (vehicle control) or heavy metal solutions (individually or in combination [inhibitory concentration (IC) and EPA mixtures]) prepared in FCS-free medium for 24 h. The IC<sub>20</sub>, IC<sub>25</sub> and IC<sub>35</sub> metal mixtures were prepared by mixing two fold respective concentrations of As, Cd and Hg (as calculated in Section 2.4). Blanks (200  $\mu$ L) consisted of 5% FCS-supplemented medium to account for sterility and background noise.

### 2.4. Cytotoxicity

The effect of the selected heavy metals on cell density was determined using the SRB staining assay as described by Vichai and Kirtikara.<sup>197</sup> The SRB assay is based on the measurement of fixed protein elements, which correlates to the amount of cells present.<sup>197</sup> Saponin (1%) was used as positive control.

Treated cells were fixed with 50  $\mu$ L trichloroacetic acid (TCA, 50%) overnight at 4°C. After fixation, plates were washed thrice with tap water, dried and stained with 100  $\mu$ L SRB solution (0.057% w/v in 1% v/v acetic acid) for 30 min. Excess dye was removed by rinsing plates three times with 100  $\mu$ L acetic acid (1% v/v). Bound dye was solubilised in 200  $\mu$ L Tris-base solution (10 mM, pH 10.5), followed by 30 min incubation on a shaker at room temperature. Plates were read spectrophotometrically using a Biotek ELx 800 microplate reader (Biotek Inc, Winooski, USA) at 510 nm (reference wavelength 630 nm). Values were blank-excluded and cell density determined using the following equation:

*Cell density (% relative to negative control) = (absorbance of sample/average absorbance of negative control) x 100*

Non-linear regression was used to determine the IC<sub>20</sub>, IC<sub>25</sub> and IC<sub>35</sub>. All further experimentation was conducted at these concentrations.

## 2.5. Mitochondrial membrane potential

Mitochondrial membrane potential was monitored using the JC-1 dye. The JC-1 dye is a lipophilic cationic dye that enters the mitochondria to form aggregates (emits red light) in cells with normal mitochondrial function,<sup>198</sup> whereas in cells with mitochondrial dysfunction, the dye forms monomers (emits green light).<sup>198</sup> The ratio of the red-to-green light can be measured and correlated with a loss of  $\Delta\Psi_m$ , which translates to mitochondrial depolarisation.<sup>198</sup> Rotenone (200 nM in-reaction) was used as positive control.

After treatment, 20  $\mu$ L JC-1 dye (200  $\mu$ M, prepared in PBS) was added to cells, which were incubated for a further 2 h at 37°C. Medium was aspirated and replaced with 100  $\mu$ L Hanks Buffered Salt Solution (HBSS). Fluorescence was measured using the H2 Synergy microplate reader (Biotek Inc, Winooski, USA). Fluorescence was monitored at a monomer excitation wavelength ( $\lambda_{ex}$ ) and emission wavelength ( $\lambda_{em}$ ) of 485 nm and 525 nm, respectively, while the aggregate form was monitored at  $\lambda_{ex} = 545$  nm and  $\lambda_{em} = 595$  nm. The  $\Delta\Psi_m$  was determined using the following equations:

*Fluorescence ratio = fluorescence read at 485 nm/fluorescence read at 545 nm.*

*$\Delta\Psi_m$  (fold-change relative to negative control) = fluorescent ratio of sample/average fluorescent ratio of negative control.*

## 2.6. Intracellular adenosine triphosphate levels

The monitoring of the ATP levels may assist in determining bioenergetic fluctuations in cells, which can lead to inferences related to proliferation, apoptosis and necrosis.<sup>155</sup> The assay uses the bioluminescent enzyme luciferase to catalyse the formation of light in the presence of ATP and luciferin. The amount of light can be correlated with the amount of ATP.<sup>199</sup> Staurosporine (10  $\mu$ M in-reaction) and saponin (1% in-reaction) were used as apoptotic and necrotic controls, respectively.

The ATP level was monitored using the ATP Assay Kit MAK135 (Sigma-Aldrich, St Louis, USA) according to the manufacturer's protocol (Sigma-Aldrich technical bulletin for ATP Assay kit

MAK135). After treatment, medium was replaced with 90  $\mu$ L ATP reagent, and the plate incubated for 1 min. Luminescence for the ATP assay was read in a H2 Synergy microplate reader (RLU<sub>A</sub>).

*ATP levels (fold-change relative to negative control) = Normalised value of sample/average normalised value of negative control.*

## **2.7. Reactive oxygen species generation**

Intracellular ROS concentrations were measured using the H<sub>2</sub>-DCF-DA cleavage assay.<sup>200</sup> Non-fluorescent H<sub>2</sub>-DCF-DA enters the cell passively where it is cleaved by esterases to 2',7'-dichlorodihydrofluorescein. The latter is activated by ROS to release fluorescent dichlorofluorescein (DCF).<sup>200</sup> 2,2'-Azobis (2-methylpropionamide) dihydrochloride (AAPH) (1 mM in-reaction) was used as positive control.

After treatment, 20  $\mu$ L H<sub>2</sub>-DCF-DA (110  $\mu$ M, prepared in PBS) was added to cells, which were incubated for a further 30 min at 37°C. Medium was aspirated and replaced with 100  $\mu$ L HBSS. Fluorescence was measured at  $\lambda_{\text{ex}} = 485$  nm and  $\lambda_{\text{em}} = 535$  nm. The SRB assay was used to normalise fluorescent data to cell density. All values were blank-excluded and intracellular ROS concentrations determined using the following equation:

*Normalised value: Fluorescence of well/absorbance of well.*

*ROS concentration (fold-change relative to negative control) = Normalised value of sample/average normalised value of negative control.*

## **2.8. Intracellular reduced glutathione concentrations**

Intracellular GSH levels were monitored using the (MCB) adduct formation assay.<sup>201</sup> The MCB dye enters the cell passively to bind exclusively to GSH to form a fluorescent GSH-MCB adduct. The amount of fluorescence can be measured and correlated to the amount of intracellular reduced GSH.<sup>201</sup> n-Ethylmaleimide (25  $\mu$ M in-reaction) was used as positive control.

After treatment, 20  $\mu\text{L}$  MCB (176  $\mu\text{M}$ , prepared in PBS) was added to the cells, which were incubated for a further 2 h at 37 $^{\circ}\text{C}$ . Medium was aspirated and replaced with 100  $\mu\text{L}$  HBSS. Fluorescence was measured at  $\lambda_{\text{ex}} = 360$  nm and  $\lambda_{\text{em}} = 460$  nm. The SRB assay was carried out thereafter to normalize fluorescent data to cell density. All values were blank-excluded and intracellular GSH level was determined using the following equation:

*Normalised value: Fluorescence of well/absorbance of well.*

*GSH concentration (fold-change relative to negative control) = Normalised value of sample/average normalised value of negative control.*

## **2.9. Caspase-3/7 activity**

Acetyl Asp-Glu-Val-Asp-7-amido-4-methyl-coumarin (Ac-DEVD-AMC) is a synthetic peptide molecule which is cleaved to free bound fluorogenic 7-amido-4-coumarin (AMC) by activated caspase-3/7. Intracellular caspase-3/7 is released from cells by membrane lytic solutions, which are then exposed to the substrate. Caspase-3/7 is activated by pro-apoptotic pathways, and fluorescence thus indicates apoptotic cell death.<sup>202</sup> Camptothecin (40  $\mu\text{M}$  in-reaction) was used as positive control.

After treatment, medium was replaced with 25  $\mu\text{L}$  cold lysis buffer, and plates were incubated for 15 min on ice. After lysis, 100  $\mu\text{L}$  caspase-3/7 substrate buffer containing 10  $\mu\text{M}$  Ac-DEVD-AMC was added. Plates were incubated for 4 h at 37 $^{\circ}\text{C}$ . Fluorescence was measured at  $\lambda_{\text{ex}} = 355$  nm and  $\lambda_{\text{em}} = 460$  nm. The plates were further incubated for 16 h at 37 $^{\circ}\text{C}$ , and cell density determined in alternative wells by SRB assay.<sup>197</sup> The SRB data was used to normalize fluorescent data to cell density. All values were blank-excluded, and caspase-3/7 activity was determined using the following equation:

*Normalised value: Fluorescence of well/absorbance of well.*

*Caspase 3/7 activity (fold-change relative to negative control) = Normalised value of sample/average normalised value of negative control.*

## **2.10. Statistical analysis**

All experiments were carried out in triplicate on at least three separate occasions. Results were analysed in Microsoft Excel, and statistical analyses performed using GraphPad Prism 5.0. Results are

expressed as the mean  $\pm$  standard error of the mean (SEM). The IC<sub>20</sub>, IC<sub>25</sub>, IC<sub>35</sub>, IC<sub>50</sub> and IC<sub>75</sub> were determined using non-linear regression. Differences between samples were determined using the Kruskal-Wallis test, with Dunn's post-hoc assessment. The indicator of significance was  $p < 0.05$ .

## Chapter 3

### Results and discussion

---

#### 3.1. Arsenic

##### 3.1.1. Cell density

Cell density is a common way by which cytotoxicity of chemical entities is determined. Reduction in cell density in an abnormal way infers that cytotoxicity has occurred. Controls responded as expected, with vehicles controls not affecting cell density in comparison to the negative control. The positive control, saponin, decreased cell density significantly ( $p < 0.05$ ) by 87.7% and 92.8% in HepG2 (Figure 4A) and SH-SY5Y cells (Figure 4B), respectively. There was a negligible difference between the negative and vehicle controls.

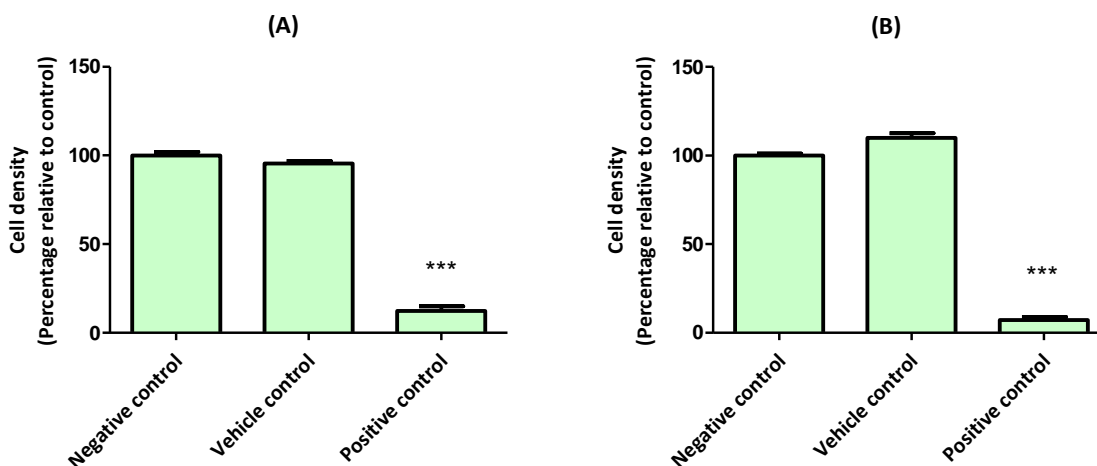


**Figure 4:** Cell density in (A) HepG2 and (B) SH-SY5Y cells after 24 h exposure to negative (untreated), vehicle (deionized water/medium mixture 1:4) and positive (saponin 1%) controls. Comparison to the negative control. \*\*\*  $p < 0.001$ .

Arsenic displayed gradual, dose-dependent cytotoxicity in both cell lines. In the HepG2 cell line, As decreased cell density ( $p < 0.05$ ) at  $\geq 6$  mg/L, with a maximum decrease of 86% at 12 mg/L. The  $IC_{50}$  of As was 6.71 mg/L (Table 1). In the SH-SY5Y cell line, As reduced the cell density significantly ( $p < 0.05$ ) at  $\geq 1.5$  mg/L (Figure 5B), suggesting a higher cytotoxicity in cells of a neural origin. Maximum reduction in cell density (84%) was seen at a dose of 4 mg/L, with an  $IC_{50}$  of 1.19 mg/L (Table 1).

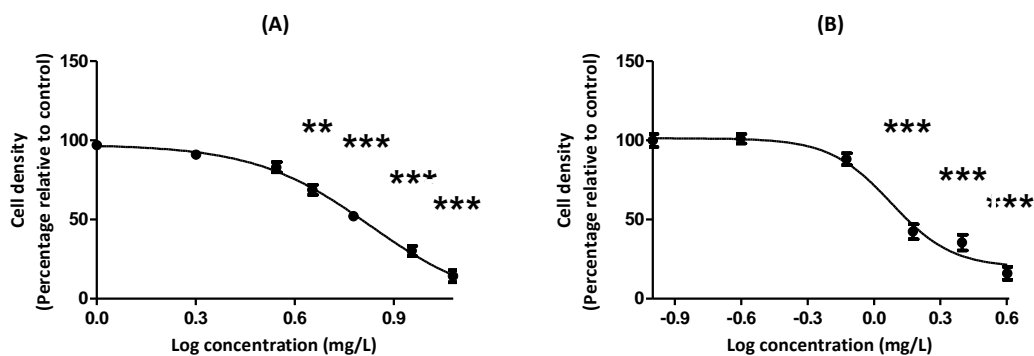


**Figure 5:** Dose-dependent reduction of cell density in (A) HepG2 and (B) SH-SY5Y cells after exposure to As for 24 h. Comparison to the negative control. \*\*\*  $p < 0.001$ , \*\*  $p < 0.01$ .

**Table 1:** Inhibitory concentrations of As determined after 24 h exposure in the HepG2 and SH-SY5Y cell lines.

Inhibitory concentration	HepG2 $\pm$ SEM	SH-SY5Y $\pm$ SEM
IC <sub>25</sub> (mg/L)	4.01 $\pm$ 1.24	0.94 $\pm$ 1.13
IC <sub>50</sub> (mg/L)	6.71 $\pm$ 1.14	1.19 $\pm$ 1.09
IC <sub>75</sub> (mg/L)	9.61 $\pm$ 1.08	2.78 $\pm$ 1.11

The effects of As on the HepG2 and SH-SY5Y cell lines were verified by exposing both cell lines to the IC<sub>25</sub>, IC<sub>50</sub> and IC<sub>75</sub> of As. Both cell lines displayed acceptable reduction of cell density as the statistical calculations would suggest (Figure 6; Table 2).

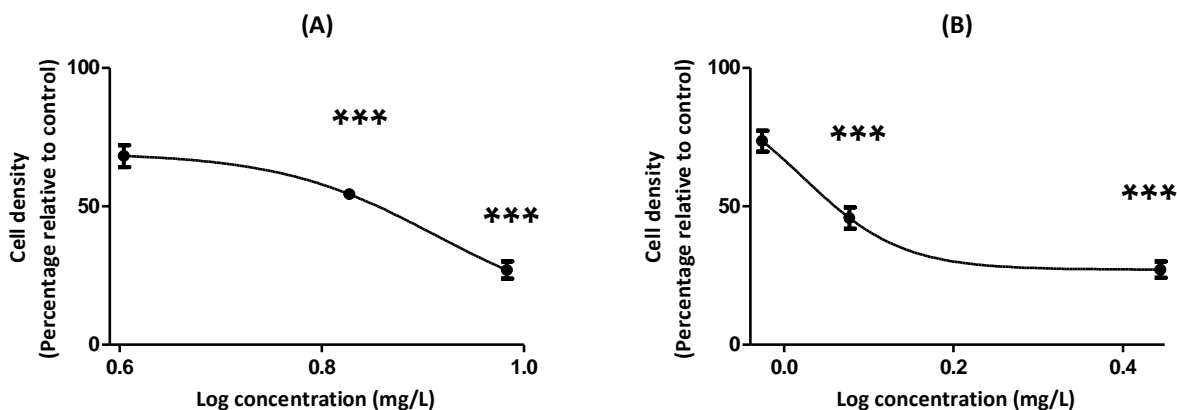


**Figure 6:** Cell density in (A) HepG2 and (B) SH-SY5Y cells after exposure to the IC<sub>25</sub>, IC<sub>50</sub> and IC<sub>75</sub> of As for 24 h. Comparison to the negative control. \*\*\*  $p < 0.001$ .



**Table 2:** Reduction in cell density (%) after exposure to the IC<sub>25</sub>, IC<sub>50</sub> and IC<sub>75</sub> of As, Cd and Hg for 24 h in the HepG2 and SH-SY5Y cell lines.

	As		Cd		Hg	
	HepG2	SH-SY5Y	HepG2	SH-SY5Y	HepG2	SH-SY5Y
<b>IC<sub>25</sub> ± SEM</b>	32 ± 3.95	26 ± 3.79	27 ± 2.29	29 ± 4.92	30 ± 1.62	26 ± 4.69
<b>IC<sub>50</sub> ± SEM</b>	46 ± 1.69	54 ± 3.86	43 ± 1.68	52 ± 4.14	63 ± 2.50	49 ± 4.65
<b>IC<sub>75</sub> ± SEM</b>	73 ± 3.15	73 ± 2.98	67 ± 2.42	73 ± 3.48	74 ± 1.74	73 ± 2.48

Metals, such as As, rarely occur in free ionic form, and thus are usually present in nature as oxides, sulphates, chlorides and other forms. Arsenic toxicity varies with the state in which it occurs; while some may be beneficial,<sup>203</sup> most are cytotoxic.<sup>204</sup> Although information was available regarding cytotoxicity in hepatic cell lines, limited information was available for those in neural cells. In the present study, a 60% reduction was observed at 7.4 and 1.7 mg/L of arsenite in HepG2 and SH-SY5Y cells, respectively. Previously published data highlights such an equivalent reduction for As<sub>2</sub>O<sub>3</sub> at 20 mg/L and arsenite at 25.98 mg/L in HepG2<sup>192</sup> and Chang human hepatocytes, respectively.<sup>205</sup> When compared to the current results, the difference in type of As salts investigated as well as the cell lines used, could explain the differences in toxicity noted. However, the IC<sub>50</sub> of As<sup>3+</sup> in rat heart micro vessel endothelial (RHMVE) cells was reported as 4.6 mg/L,<sup>206</sup> which is similar to that found in the present study in HepG2 cells (IC<sub>50</sub> 6.71 mg/L). It is known that the uptake of As differs in different cell types, which may be ascribed to different proteins being targeted and are known to be differentially expressed between cell lines. These differences may also relate to the greater sensitivity in some cell lines as has been reported for the variance in arsenicals up take into CHO-9 and HepG2 cells (<4% in CHO-9 and <1% in HepG2 cells).<sup>207</sup> The different oxidation states of As can also result in different toxicity, as As<sup>3+</sup>, was found to be taken up by the endothelial cells at rates 6–7 times faster than As<sup>5+</sup>,<sup>206</sup> which may contribute to greater cytotoxicity and genotoxicity.<sup>207</sup> Thus differences in the cell line and the rate and extent of uptake of different forms of As may explain the high IC<sub>50</sub> of As<sup>5+</sup> (45.7 mg/L) in RHMVE cells<sup>10</sup> whereas As<sub>2</sub>O<sub>3</sub> at the low concentration of 0.2 mg/L was found to reduce cell viability by 35% in H9c2 myoblasts.<sup>208</sup> In an another study, As was shown to induce minimal cytotoxicity in the SH-SY5Y neuroblastoma cell line in its As<sup>3+</sup> state.<sup>209</sup>

### 3.1.2. Mitochondrial membrane potential

The mitochondrion plays a key role in cell survival. Mitochondrial dysfunction is directly associated with alterations to mitochondrial membrane potential. The vehicle control had similar effects to the negative control on  $\Delta\Psi_m$  whereas the positive control reduced  $\Delta\Psi_m$  significantly ( $p < 0.05$ ) by 43% and 36% in HepG2 and SH-SY5Y cell lines, respectively (Figure 7). Such a reduction is indicative of mitochondrial depolarization.

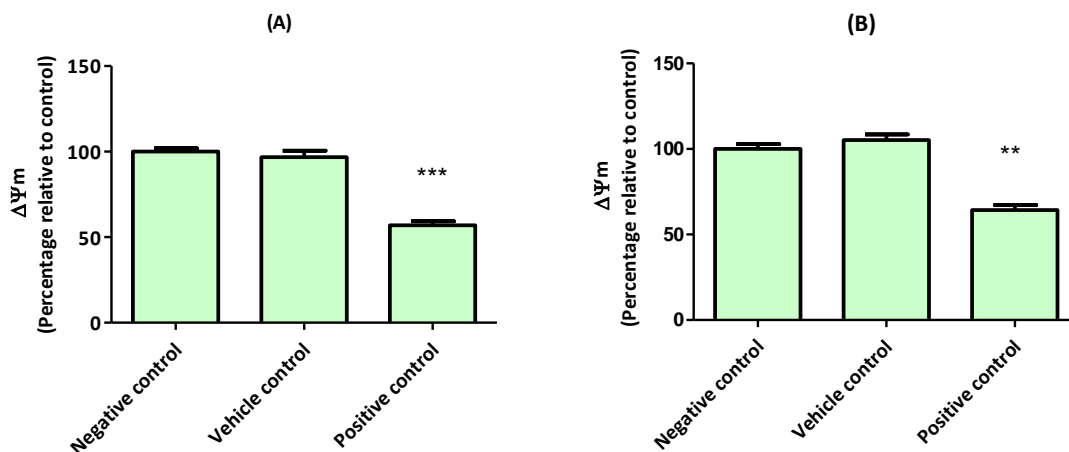


**Figure 7:** Mitochondrial membrane potential in (A) HepG2 and (B) SH-SY5Y cells after 24 h exposure to the negative (untreated), vehicle (deionized water/medium mixture 1:4) and positive (Rotenone 200 nM) controls Comparison to the negative control. \*\*\*  $p < 0.001$ , \*\*  $p < 0.01$

Arsenic had minimal effects (not significant when compared to negative control) on HepG2  $\Delta\Psi_m$  at the  $IC_{25}$  and  $IC_{50}$  (~12%), with a significant ( $p < 0.05$ ) reduction of 45% at the  $IC_{75}$  (Figure 8A). These results suggest that although mitochondrial toxicity is apparent in the HepG2 cell line, it only occurs at higher concentrations. Depolarisation may thus be of lesser consequence at lower concentrations. A gradual, tapered reduction was observed in the SH-SY5Y cell line from the  $IC_{25}$  to  $IC_{75}$  (25% to 62%) (Figure 8B). In SH-SY5Y cells, reduction in  $\Delta\Psi_m$  was not significant at  $IC_{25}$  but a significant ( $p < 0.05$ ) reduction at higher concentrations when compared to the negative control was noted. This decline parallels the reduction in cell density in the SH-SY5Y cell line, suggesting a greater relation between the two parameters. SH-SY5Y cell lines are thus more susceptible to mitochondrial toxicity induced by As. Cytochrome C leaks out prior to  $\Delta\Psi_m$  depolarization and this loss of  $\Delta\Psi_m$  is a common feature of apoptosis and necroptosis.<sup>210</sup> Mitochondrial cytochrome C, which functions as an electron carrier

in the respiratory chain, translocates to the cytosol in cells, where it induces the activation of DEVD-specific caspases and results in apoptotic cell death.<sup>211</sup>

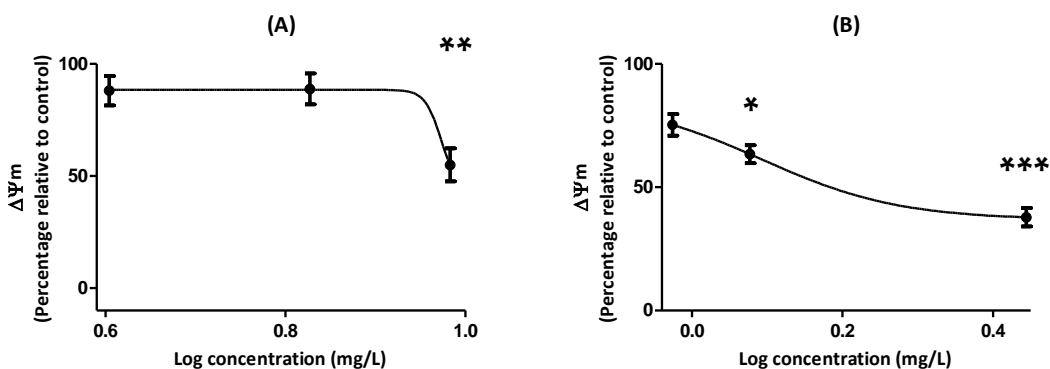


**Figure 8:** Mitochondrial membrane potential in (A) HepG2 and (B) SH-SY5Y cells after 24 h exposure the  $IC_{25}$ ,  $IC_{50}$  and  $IC_{75}$  of  $As_2O_3$ . Comparison to the negative control. \*\*\*  $p < 0.001$ , \*\*  $p < 0.01$ , \*  $p < 0.05$

From literature it is evident that differential effects of  $As_2O_3$  on cells takes place which is dependent on their origin and the oxidation state of  $As_2O_3$ . Contrary to the present study, where HepG2 cells were unaffected by low concentrations of  $As_2O_3$  after 24 h, treatment with 1 mg/L and 3 mg/L  $As_2O_3$  decreased  $\Delta\Psi_m$  by 34% and 57%, respectively. This has been found to be partially prevented by N-acetylcysteine pre-treatment, suggesting a free radical-mediated cytotoxic effect.<sup>212</sup> Arsenic (10.4 mg/L) has been reported to induce rapid and significant morphological changes in mitochondria in erythroleukaemic HEL30 cells, where disruption of internal organization occurred within 30 min.<sup>213</sup> Exposure of myeloid U937 cells to 10 mg/L  $As_2O_3$  rapidly decreased  $\Delta\Psi_m$ , possibly through opening of the MPTP, with subsequent release of cytochrome C and production of  $\bullet O_2^-$ .<sup>214</sup> In Chang human hepatocytes,  $NaAsO_2$ -induced apoptosis via dissipation of the  $\Delta\Psi_m$ , was found to release cytochrome C from the mitochondria.<sup>215</sup> In the present study, similar concentrations of  $NaAsO_2$  (1.19 mg/L) depolarized SH-SY5Y cells, however, only at high concentrations in HepG2 cells (9.61 mg/L).

### 3.1.3. Intracellular ATP levels

Adenosine triphosphate level is a measure of cellular growth and toxicity. Within proliferating cells, a high ATP is expected, as more ADP is converted to ATP for cellular cycling.<sup>155</sup> As ATP formation is dependent on healthy mitochondrial functioning, alterations may indicate loss of mitochondrial

integrity.<sup>155</sup> Oxidation reduces ATP levels and impairs ATP-dependent cytoprotective pathways thereby triggering cell death.<sup>154</sup> All controls delivered expected results. Saponin (necrosis control; 1%) abolished ATP levels in the HepG2 and SH-SY5Y cell lines (Figure 9). Camptothecin (apoptosis control; 20  $\mu$ M and 40  $\mu$ M) reduced ATP levels in the HepG2 (54% and 52%) and SH-SY5Y (89% and 87%) cell lines (Figure 9).

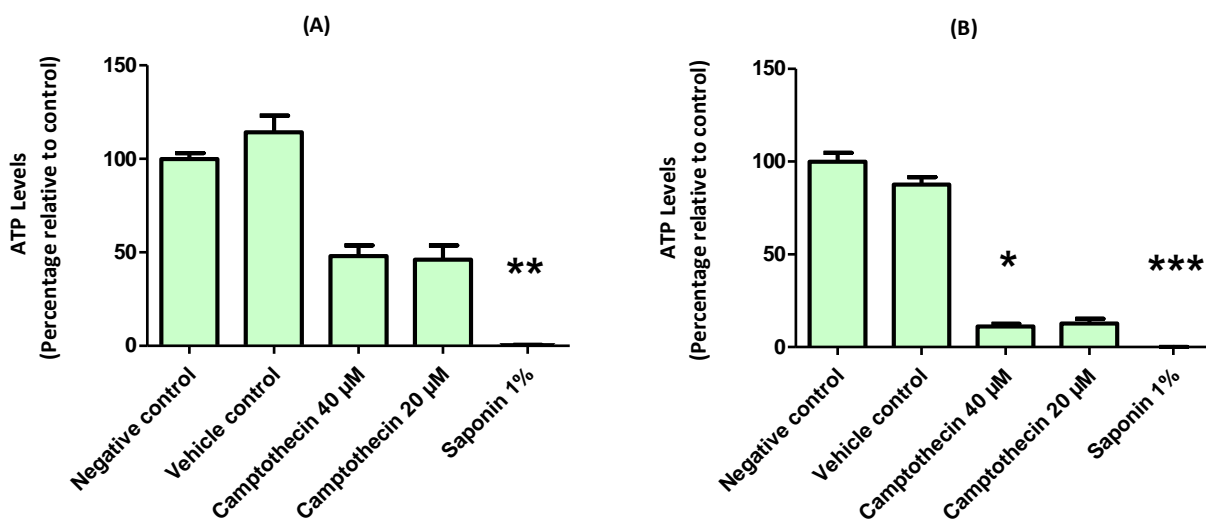


**Figure 9:** Intracellular ATP levels in (A) HepG2 and (B) SH-SY5Y cells after 24 h exposure to the negative (untreated), vehicle (deionized water/medium mixture 1:4) and positive (Camptothecin; 20  $\mu$ M and 40  $\mu$ M, Saponin 1%) controls. Comparison to the negative control. \*\*\*  $p < 0.001$ , \*\*  $p < 0.01$ , \*  $p < 0.05$

When metals were tested individually, dose dependent reduction in ATP levels was observed in HepG2 and SH-SY5Y cells. Arsenic decreased ATP at IC<sub>25</sub> by 68% and at IC<sub>50</sub>; there was a further decrease to 77%. An even further decline in ATP was noted at the highest concentration of As tested, where ATP was reduced by 87% (Figure 10A). The latter is indicative of mitochondrial toxicity in HepG2 cells. The ATP level was reduced by 98%, 97% and 98% in SH-SY5Y cells when exposed to the IC<sub>25</sub>, IC<sub>50</sub> and IC<sub>75</sub> concentrations of As (Figure 10B).

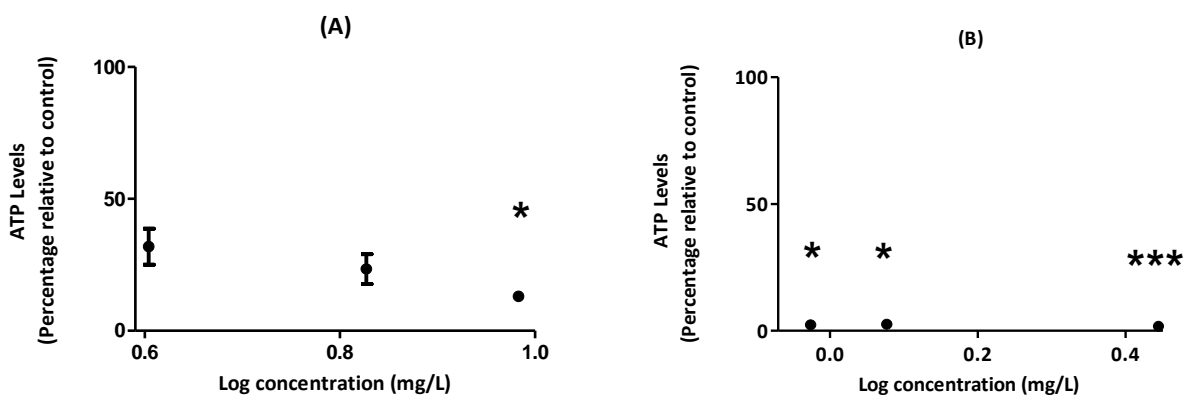


**Figure 10:** Intracellular ATP levels in (A) HepG2 and (B) SH-SY5Y cells after 24 h exposure to the  $IC_{25}$ ,  $IC_{50}$  and  $IC_{75}$  of As. Comparison to the negative control. \*\*\*  $p < 0.001$ , \*  $p < 0.05$

Excessive ATP depletion can switch the mode from apoptotic to necrotic cell death in cells exposed to oxidants and other agents.<sup>216, 217</sup> In the wild type mouse embryonic fibroblasts cells, 2 mg/L  $As_2O_3$  after 16 h exposure, decreased ATP levels by 30%.<sup>218</sup> A similar trend was found in our study and SH-SY5Y cells were more sensitive to decrease in ATP levels and 0.94 mg/L of As was able to reduce ATP levels completely by 98% when compared to HepG2 cells in which higher As levels (4.01 mg/L) reduced ATP levels by 68% (Figure 10A). In both cells, decrease in ATP levels corresponds to depolarization of mitochondrial toxicity but complete inhibition in ATP levels would suggest necrotic pathways in SH-SY5Y cells.

Incubation of isolated liver mitochondria with  $As^{+3}$  decreased ATP production, possibly due to inhibition of the mitochondrial respiratory chain and MPTP opening.<sup>219</sup> Opening of the MPTP pores leads to unlimited proton movement across the inner membrane results in uncoupling of oxidative phosphorylation and further worsening of ATP production and ROS generation. Arsenic significantly increased the outer membrane mitochondrial damage, another phenomenon which results in cytochrome c release.<sup>219</sup>

### 3.1.4. Reactive oxygen species generation

Reactive oxygen species created during oxidative stress, results in cytotoxicity and apoptosis.<sup>220</sup> All the controls produced the desired results. The vehicle control did not differ significantly from the negative control. The positive control, however, induced ROS significantly by 133% in both cell lines tested (Figure 11).

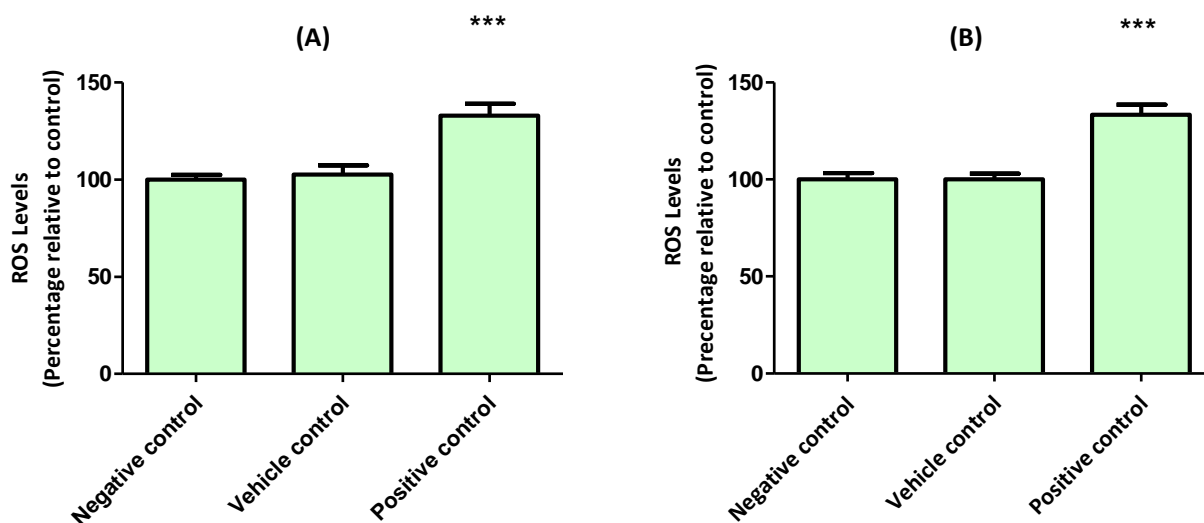


**Figure 11:** Reactive oxygen species levels in (A) HepG2 and (B) SH-SY5Y cells after 24 h exposure to the negative, vehicle (deionized water/medium mixture 1:4) and positive (AAPH, 1 mM) controls. Comparison to the negative control: \*\*\*  $p < 0.001$ .

Although mitochondrial depolarisation occurred when cells were exposed to As, ROS generation was not increased. On the contrary, As decreased ROS levels in HepG2 cells by 28%, 44% and 57%, when treated with  $IC_{25}$ ,  $IC_{50}$  and  $IC_{75}$  concentrations of As, respectively (Figure 12A). In the SH-SY5Y cell line ROS was reduced by 30%, 45% and 62%, respectively by the corresponding As concentrations (Figure 12B).

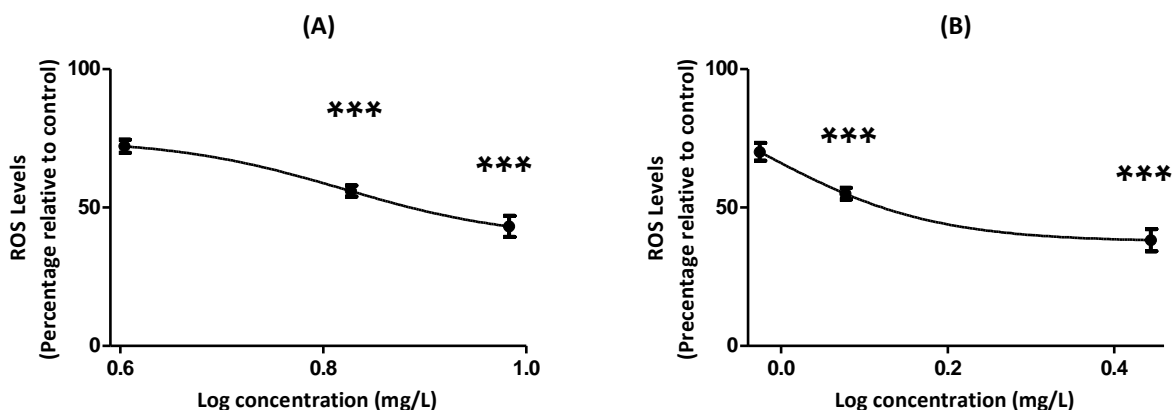


**Figure 12:** Reactive oxygen species levels in (A) HepG2 and (B) SH-SY5Y cells after 24 h exposure to the IC<sub>25</sub>, IC<sub>50</sub> and IC<sub>75</sub> of As. Comparison to the negative control. \*\*\*  $p < 0.001$ .

Contrary to the current results, As has been found to induce ROS production both *in vitro* ascites hepatoma AS-30D cells<sup>221, 222</sup> and *in vivo* Male Dunkin–Hartley guinea pigs.<sup>221, 222</sup> The reduction in ROS levels in the current study could have resulted from biphasic effect on ROS levels or possible reductive stress from GSH. Cellular oxidative stress and ROS generation have been implicated as the possible mechanism for the toxicity noted after As<sub>2</sub>O<sub>3</sub> treatment in human hepatocellular carcinoma cells.<sup>223</sup> Sodium arsenate (0.01 to 3 mg/L) was reported to increase cellular oxidative stress in murine keratinocytes in a dose-dependent manner after 15 min of treatment. This effect was checked by rotenone, indicating that As induces mitochondria to produce intracellular ROS.<sup>213</sup> However, in U937 cells, •O<sub>2</sub><sup>-</sup> production, which was increased in the early stages of apoptosis by As<sub>2</sub>O<sub>3</sub>, was arrested by pre-treatment with NAC.<sup>214</sup> Intracellular ROS generation was found to be dose-dependent in Chang human hepatocytes exposed to As.<sup>215</sup>

### 3.1.5. Reduced glutathione levels

To eliminate the detrimental effects induced by ROS, cells employ cellular mechanisms to eradicate free oxygen species. Reduced glutathione is such an antioxidant, that reduces cellular ROS, thereby preventing excessive oxidation.<sup>224</sup> All controls delivered expected results, indicating that the assay worked. Although the vehicle control did not significantly differ from the negative control, the

positive control reduced GSH significantly ( $p < 0.05$ ) by 90% and 94% in the HepG2 and SH-SY5Y cell lines, respectively (Figure 13).

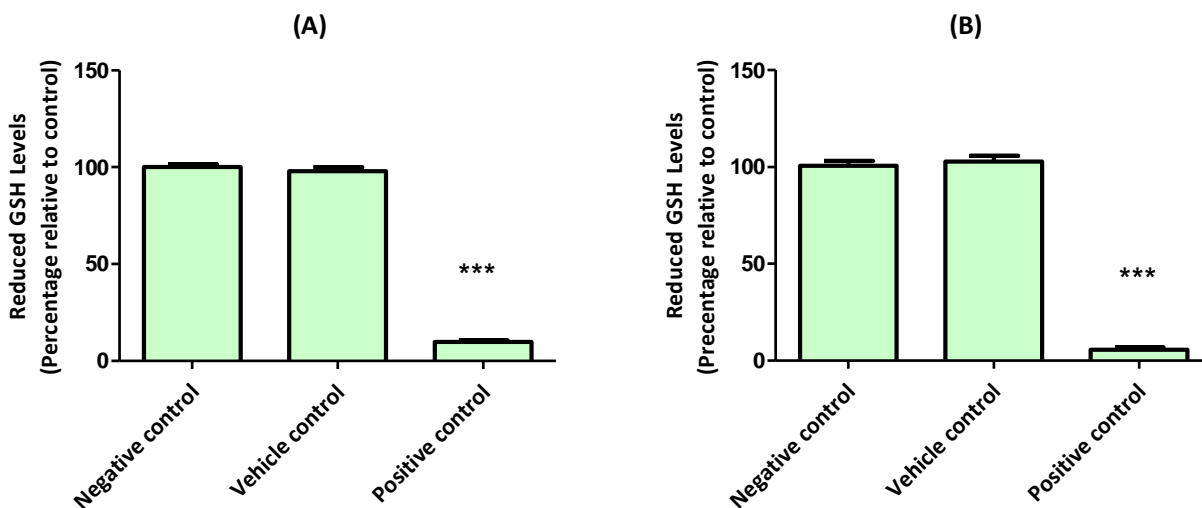


**Figure 13:** Glutathione concentration in (A) HepG2 and (B) SH-SY5Y cells after 24 h exposure to negative (medium), vehicle (deionized water/medium mixture 1:4) and positive control (n-Ethylmaleimide, 25  $\mu$ M). Comparison to the negative control: \*\*\*  $p < 0.001$ .

The GSH was reduced by 35%, 64% and 94% in HepG2 cells, when exposed to the  $IC_{25}$ ,  $IC_{50}$  and  $IC_{75}$  of As, respectively. These results paralleled those observed for cell density. No reduction in  $\Delta\Psi_m$  was noted when cells were treated with  $IC_{25}$  or  $IC_{50}$  of As. The latter may explain the mitochondrial toxicity noted at high As concentrations. Although there was an absence of mitochondrial toxicity at lower concentrations, a reduction in cell density, ATP and GSH levels was found. A 47%, 67% and 96% reduction in GSH levels was observed in SH-SY5Y cells exposed to  $IC_{25}$ ,  $IC_{50}$  and  $IC_{75}$  concentrations of As. Furthermore, there was a dose dependent reduction in GSH levels (Figure 14), which paralleled the results obtained for cell density, ATP and  $\Delta\Psi_m$ .



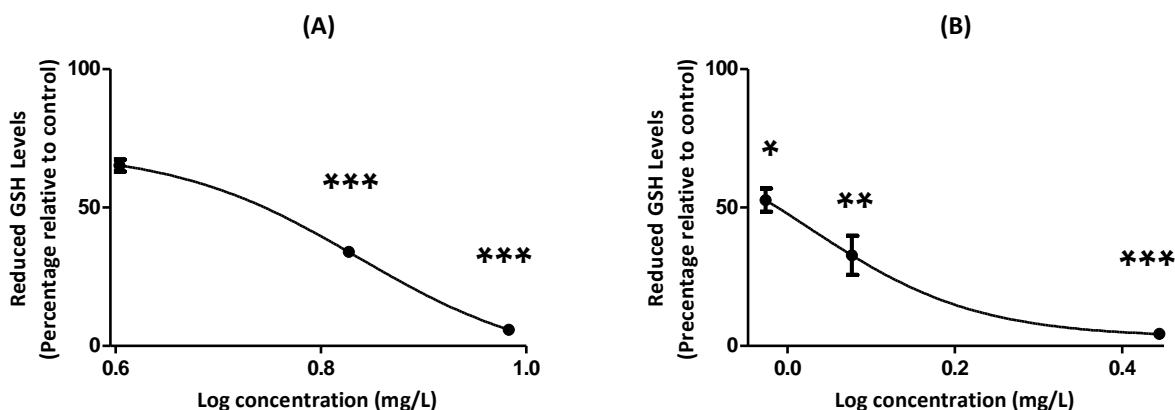


**Figure 14:** Glutathione concentration in (A) HepG2 and (B) SH-SY5Y cells after 24 h exposure to the IC<sub>25</sub>, IC<sub>50</sub> and IC<sub>75</sub> of As. Comparison to the negative control. \*\*\*  $p < 0.001$ , \*\*  $p < 0.01$ , \*  $p < 0.05$ .

Less than 50% reduction in GSH was observed after 24 h exposure to 0.5 mg/L and 10 mg/L As<sub>2</sub>O<sub>3</sub> in HepG2 cells.<sup>192</sup> In the current study, 5.6 mg/L and 1 mg/L of As reduced GSH levels to 50% in both HepG2 and SH-SY5Y cells. Time-dependent inhibition of GSH, mediated by the  $\bullet\text{O}_2^-$ , was previously demonstrated in isolated rat hepatocytes exposed to As<sub>2</sub>O<sub>3</sub>.<sup>225</sup> The level of intracellular GSH in U937 cells was found to decrease in a time-dependent manner after exposure to 9.9 mg/L As<sub>2</sub>O<sub>3</sub>.<sup>214</sup> Trivalent arsenicals form complexes with thiol-containing molecules such as GSH and cysteine *in vitro*,<sup>226</sup> which would explain the decreased levels of GSH. Inorganic arsenites to the thiol groups of enzymes and proteins, and thereby inhibit important biochemical events which results in cytotoxicity. Arsenite readily transforms from a (GSH)<sub>3</sub>-arsenic complex to the dithiol 2,3-dimercaptosuccinic acid, which has a higher affinity for dithiols than monothiols.<sup>227</sup>

### 3.1.6. Caspase 3/7 activity

The positive control increased caspase 3/7 activity by 2645% and 2369% in HepG2 and SH-SY5Y cells, respectively, whereas no effect was evident after treatment with the vehicle and negative controls (Figure 15). An increase in caspase 3/7 activity is indicative of cellular toxicity.

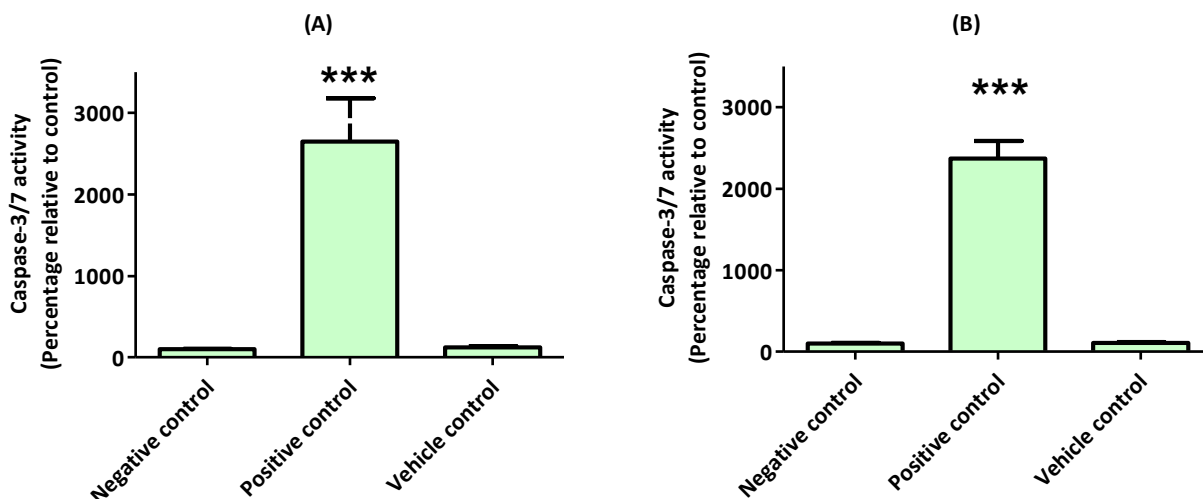


**Figure 15:** Caspase-3/7 activity in (A) HepG2 and (B) SH-SY5Y cells after treatment with negative (medium), vehicle (deionized water/medium mixture 1:4) and positive control (Camptothecin 40  $\mu$ M) for 24 h. Comparison to the negative control: \*\*\*  $p < 0.001$ .

Caspase-3/7 increased to 159% when treated with an  $IC_{25}$  concentration of As and 126% with  $IC_{50}$  concentration of As. The caspase-3/7 activity in HepG2 cells was further increased to 132% after exposure to an  $IC_{75}$  concentration of As (Figure 16A). Caspase-3/7 activity was increased by 141%, 198% and 144% in SH-SY5Y cells when exposed to  $IC_{25}$ ,  $IC_{50}$  and  $IC_{75}$  concentrations of As showing biphasic effect (Figure 16B).

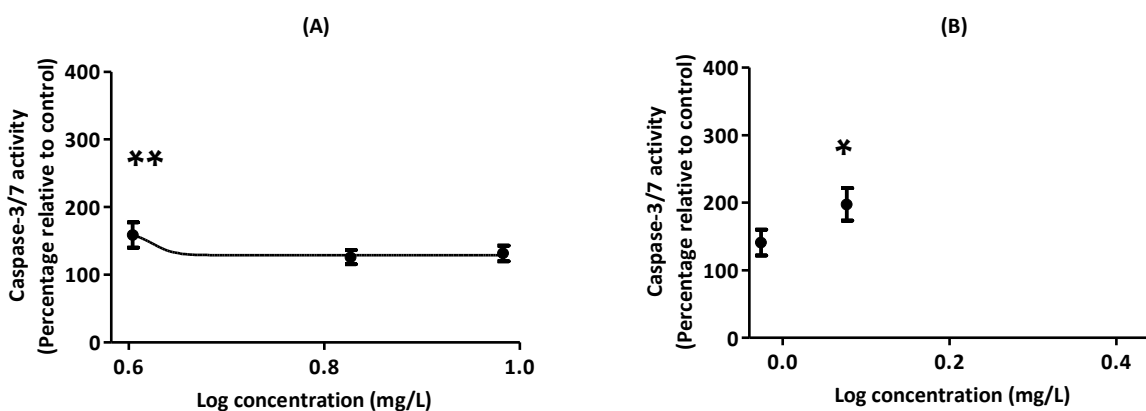


**Figure 16:** Caspase-3/7 activity in (A) HepG2 and (B) SH-SY5Y cells after treatment after 24 h exposure to the  $IC_{25}$ ,  $IC_{50}$  and  $IC_{75}$  of As. Comparison to the negative control. \*\*  $p < 0.01$ , \*  $p < 0.05$ .

In hepatocellular carcinoma cells, the activity of caspase-3/7 was evident at 0.1 mg/L concentration of As<sub>2</sub>O<sub>3</sub> after 24 h exposure.<sup>223</sup> Chromatin condensation after 24 h suggest that As<sub>2</sub>O<sub>3</sub> caused cell death via an apoptotic process.<sup>223</sup> Sodium arsenite at 3.9 mg/L, was reported to induce apoptosis in human epidermoid carcinoma A431 cells and EA.hy926 cells after 24 h exposure.<sup>228</sup> As<sub>2</sub>O<sub>3</sub>-induced apoptosis is related to ROS production in HepG2 cells, as evident from the increase in the percentage of apoptotic cells.<sup>212</sup> Apoptotic cells were already detected within 6 h of treatment with 10 mg/L As<sub>2</sub>O<sub>3</sub>, and after 12 h 86% of cells were apoptotic. Arsenic trioxide has been reported to induce apoptosis in U937 cells, by activating p38 and inactivating ERKs.<sup>215</sup>

Both early and late apoptosis, as well as necrosis was induced by NaAsO<sub>2</sub> after 24 h treatment. NaAsO<sub>2</sub> treatment induced apoptosis in a dose dependent manner.<sup>215</sup> The percentage necrotic cells was only significantly ( $p < 0.05$ ) increased in cells treated with 3.9 mg/L NaAsO<sub>2</sub>. Results obtained from Western blot analysis has indicated that NaAsO<sub>2</sub> induced the cleavage of caspase-3 (17-kDa fragments) and PARP (89-kDa fragments), which are two hallmarks of apoptosis.<sup>215</sup> In Chang human hepatocytes, a noticeable loss in  $\Delta\Psi_m$  occurred in cells exposed to NaAsO<sub>2</sub>. Moreover, a dose-dependent decrease in the mitochondrial cytochrome C level, with a concomitant increase in the corresponding cytosolic fraction, was observed when cells were incubated with NaAsO<sub>2</sub>. In addition, it was noted that NaAsO<sub>2</sub> increased cleavage of caspase-3 and PARP in a dose-dependent manner.<sup>215</sup> All these changes suggest that the mitochondrial pathway is involved in NaAsO<sub>2</sub>-induced apoptosis in Chang human hepatocytes. The elevation of ROS production and MDA levels coincided with the increase in percentage apoptotic cells, collapse of the  $\Delta\Psi_m$ , release of cytochrome C, and cleavage of caspase-3 and PARP.<sup>215</sup> Furthermore, pre-treatment with NAC effectively prevented oxidative stress as well as inhibited the apoptotic events.<sup>215</sup> Intracellular GSH elevation, instead of GSH depletion, was observed as the percentage apoptotic cells increased when treated with NaAsO<sub>2</sub>.<sup>215</sup> The extracellular addition of NAC, the known precursor of GSH and an antioxidant, increased the level of intracellular GSH. Combined, the results obtained after treating Chang human hepatocytes with NaAsO<sub>2</sub>, indicate that the arsenic-induced apoptosis is mainly dependent on the generation of intracellular ROS, and not on depletion of endogenous intracellular GSH.<sup>215</sup> Although the elevation of GSH levels was observed when NAC treatment was administrated, the decrease in apoptotic cells may mainly result from the elimination of intracellular ROS by thiol antioxidants.<sup>215</sup> Mitochondria do

not appear to be involved in arsenic-induced apoptosis in HepG2 cells<sup>214</sup> which is also evident from our study. The IC<sub>25</sub> and IC<sub>50</sub> of As did not depolarize  $\Delta\Psi_m$  in HepG2 cells but reduced cell density and GSH levels were observed at the same concentrations.

### 3.2. Cadmium

#### 3.2.1. Cell density

Greater cytotoxicity was noted in the HepG2 (IC<sub>50</sub> = 0.43 mg/L; Table 3) cell line than the SH-SY5Y cell line (IC<sub>50</sub> = 1.47 mg/L; Table 3). Cell density in the HepG2 cells decreased when treated with Cd at concentrations  $\geq 0.25$  mg/L. The decrease in cell density was dose-dependent, and was 86% when treated with 2 mg/L Cd (Figure 17A). Cadmium treatment resulted in a dose-dependent decrease in SH-SY5Y cell density when treated with concentrations  $\geq 0.5$  mg/L (Figure 17B).

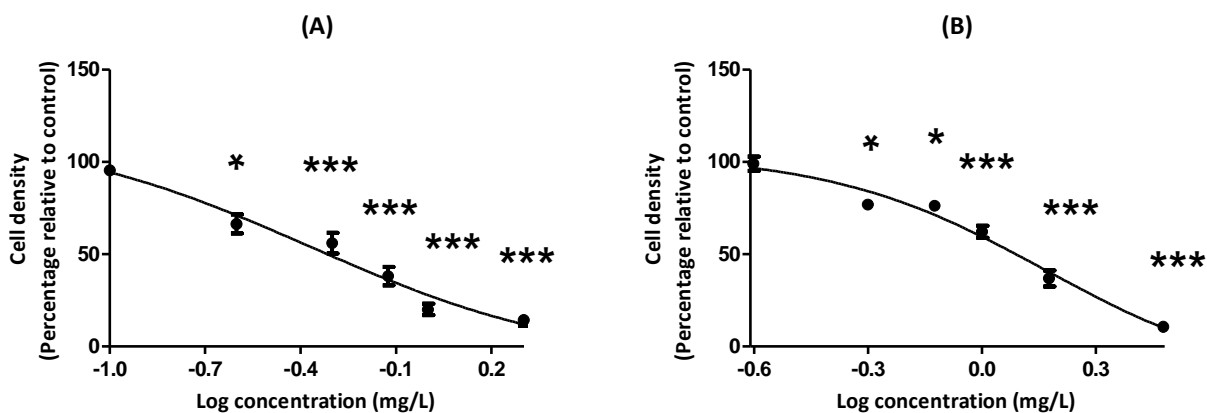


**Figure 17:** Dose-dependent reduction in cell density in (A) HepG2 and (B) SH-SY5Y cells after exposure to Cd for 24 h. Comparison to the negative control. \*\*\*  $p < 0.001$ , \*  $p < 0.05$ .

**Table 3:** Inhibitory concentrations of Cd determined after 24 h exposure in the HepG2 and SH-SY5Y cell lines.

Inhibitory concentration	HepG2 $\pm$ SEM	SH-SY5Y $\pm$ SEM
IC <sub>25</sub> (mg/L)	0.22 $\pm$ 2.00	0.68 $\pm$ 1.73
IC <sub>50</sub> (mg/L)	0.43 $\pm$ 1.40	1.47 $\pm$ 1.34
IC <sub>75</sub> (mg/L)	1.11 $\pm$ 2.33	2.08 $\pm$ 1.16

The effects of Cd on the HepG2 and SH-SY5Y cell lines were verified by exposing both cell lines to the IC<sub>25</sub>, IC<sub>50</sub> and IC<sub>75</sub> of Cd. Both cell lines displayed acceptable reduction of cell density as the statistical calculations would suggest (Figure 18; Table 3).

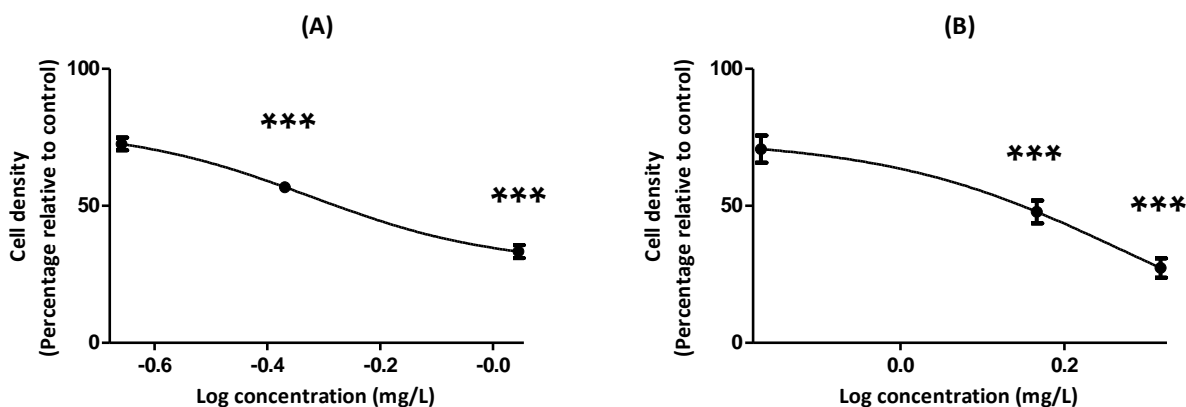


**Figure 18:** Cell density in (A) HepG2 and (B) SH-SY5Y cells after 24 h exposure to the IC<sub>25</sub>, IC<sub>50</sub> and IC<sub>75</sub> of Cd. Comparison to the negative control. \*\*\*  $p < 0.001$ .

Slightly higher IC<sub>50</sub> values have been reported by Dehn and colleagues for HepG2 cells treated with Cd (IC<sub>50</sub> 1.1 – 1.6 mg/L).<sup>229</sup> However, both this study and the study by Dehn et al. indicate the cytotoxic nature of Cd. In other studies the IC<sub>50</sub> for Cd in HepG2 cells ranged between 0.9 mg/L and 4.7 mg/L.<sup>230-232</sup> This discrepancy may be due to the use of different assays to determine cytotoxicity. Furthermore, incubation period affects results, with shorter treatment periods (3 h) resulting in less cytotoxicity (IC<sub>50</sub> of 92 mg/L).<sup>230-232</sup> The latter confirms the time-dependent cytotoxic nature of this metal. Also, the type of cells has an effect on cytotoxicity. Hepatoma AS-30D cells have been found to be more resilient to Cd, with cytotoxicity only being apparent at concentrations  $\geq 18$  mg/L.<sup>233</sup> After 3 h exposure to Cd, cytotoxicity was observed in glioma cells with an IC<sub>50</sub> of 73 mg/L.<sup>234</sup> Cadmium has been reported to cause central and peripheral neurotoxicity. This metal induces cellular damage and lipid peroxidation in neuronal tissue as a result of the generation of free radicals.<sup>235</sup>

### 3.2.2. Mitochondrial membrane potential

A similar trend was observed for Cd in the HepG2 and SH-SY5Y cell lines. In the HepG2 cell line, a reduction of 16%, 39% and 74% in the  $\Delta\Psi_m$  was observed when exposed to the IC<sub>25</sub>, IC<sub>50</sub> and IC<sub>75</sub> of Cd, respectively (Figure 19A). A similar reduction in the  $\Delta\Psi_m$  was noted when SH-SY5Y cells were

treated with the same Cd concentrations (Figure 19B). The decrease in  $\Delta\Psi_m$  noted would suggest that there is a direct correlation to the reduction in cell density.

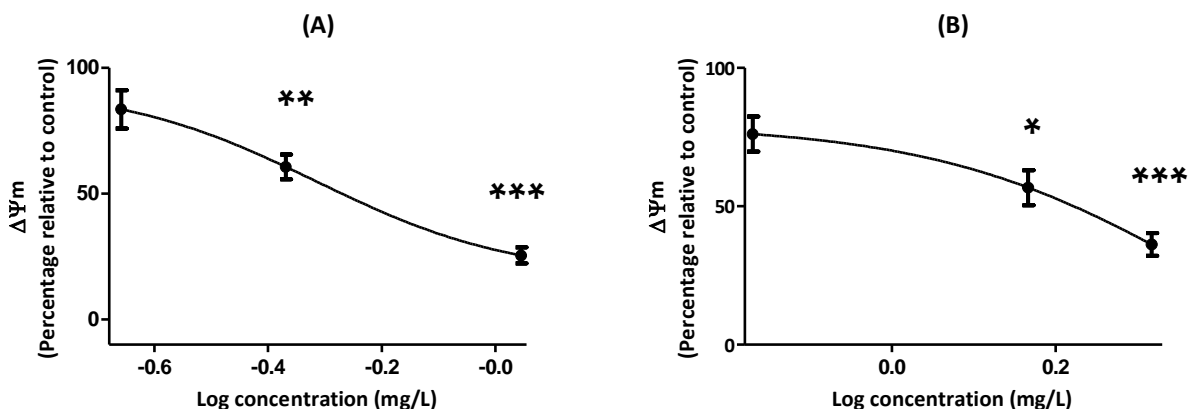


**Figure 19:** Mitochondrial membrane potential in (A) HepG2 and (B) SH-SY5Y cells after 24 h exposure the  $IC_{25}$ ,  $IC_{50}$  and  $IC_{75}$  of Cd. Comparison to the negative control. \*\*\*  $p < 0.001$ , \*\*  $p < 0.01$ , \*  $p < 0.05$ .

The oxidation state of Cd allows for variable mitochondrial toxicity. Cadmium has previously been reported to decrease  $\Delta\Psi_m$  in both cancerous and non-cancerous hepatic cells.<sup>236,237</sup> Cadmium chloride was found to dissipate  $\Delta\Psi_m$  at concentrations of 18.3 mg/L (which is higher than the concentrations tested in the present study) in normal human hepatocytes (NHH) as well as SV40-immortalized human hepatocytes (IHH).<sup>236</sup>

There was a decrease in the percentage of MRC-5 fibroblasts cells to 67% with low  $\Delta\Psi_m$  in Cd-treated cells within 8 h when compared to control.<sup>238</sup> Cadmium induced reduction in  $\Delta\Psi_m$  was only partially attenuated by inhibiting of mitochondrial ETC and MPTP. It would appear as if mitochondrial depolarisation is the initial step in the induction of apoptosis by Cd.<sup>238</sup> Cadmium initially binds to the thiol groups of proteins in the mitochondrial membrane. The interaction has been found to produce the conformational changes required for activation of cation uptake, and alter  $\Delta\Psi_m$  with subsequent ROS production.<sup>233,238,239</sup>

### 3.2.3. Intracellular ATP levels

When the cell lines were exposed to Cd for 24 h, the trend was similar to that detected for As, albeit being less toxic. Cadmium decreased ATP when exposed to the IC<sub>25</sub> by 39% and by 62% at IC<sub>50</sub>. There was an even further decline in ATP at the highest concentration of Cd tested, with a reduction of 88% (Figure 20A). Mitochondrial toxicity was thus initiated by As in HepG2 cells. The reduction in ATP levels in SH-SY5Y cells was very high and amounted to 93%, 96% and 96% when exposed to IC<sub>25</sub>, IC<sub>50</sub> and IC<sub>75</sub> concentrations of Cd, respectively (Figure 20B).

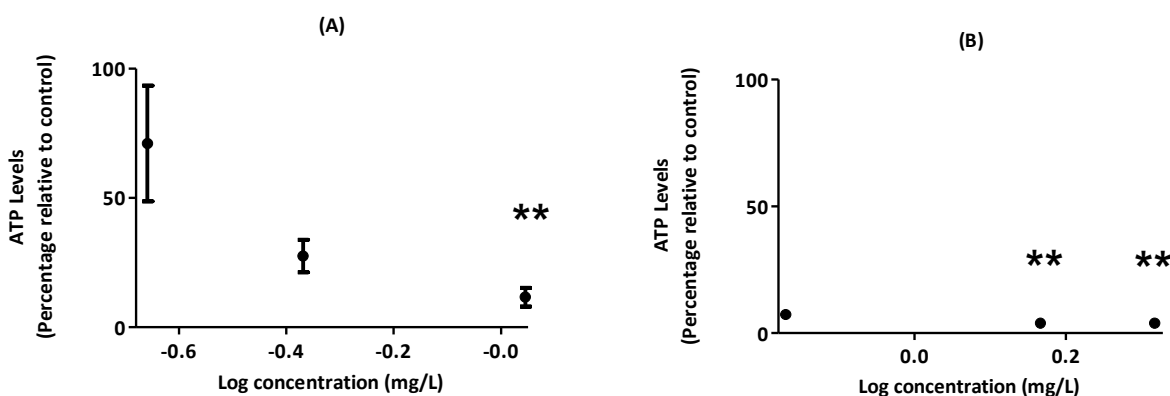


**Figure 20:** Intracellular ATP levels in (A) HepG2 and (B) SH-SY5Y cells after 24 h exposure to the IC<sub>25</sub>, IC<sub>50</sub> and IC<sub>75</sub> of Cd. Comparison to the negative control. \*\*  $p < 0.01$ .

Cadmium (1.8 to 18 mg/L) decreased the ATP levels and enhanced lipid peroxidation (LPO) in rat hepatocytes.<sup>240</sup> Incubation of isolated mitochondria with 0.001 to 0.01 mg/L Cd increased formazan production, indicating enhanced membrane permeability to succinate,<sup>240</sup> with associated diminished mitochondrial ATP. Lipid peroxidation in mitochondria strongly increased only after Cd-exposures above 0.2 mg/L Cd.<sup>240</sup> Similarly, in hepatocytes treated with Cd, decreases in ATP levels were found to correspond to increases in LPO stimulation. Even after treatment of hepatocytes with low Cd-concentrations the integrity of the mitochondrial membranes were disturbed, concomitantly impairing the hepatocellular energy supply.<sup>237</sup> Following treatment of HepG2 cells with Cd, dissipation of  $\Delta\Psi_m$  as well as, membrane permeability transition (MPT) and basal respiration stimulation was noted, which was followed by a decrease in ATP levels.<sup>237</sup>

Cadmium at 0.9 mg/L reduced ATP levels by 25, 50 and 65 % after 24 h exposure of HepG2, 1321NI and HEK293 respectively.<sup>241</sup> The different levels of inhibition of ATP levels at the same concentration of Cd could be due to difference in cell line. A similar trend was noted in our study where Cd reduced ATP level by 39% and 88% at 0.22 and 1.1 mg/L concentration after 24 h exposure in HepG2 cells (Figure 20A). Strong ATP levels inhibition was noted in SH-SY5Y cells and Cd decreased ATP levels by 93% at 0.68 (IC<sub>25</sub>) and may lead to necrotic cell death (Figure 20D). Incubation of isolated hepatocytes with 1.8–18 mg/L Cd decreased the ATP levels in a time and concentration-dependent manner.<sup>242</sup>

### 3.2.4. Reactive oxygen species

Reactive oxygen species generation was reduced by 11%, 28% and 45%, respectively in HepG2 cells treated with Cd at the IC<sub>25</sub>, IC<sub>50</sub> and IC<sub>75</sub> concentrations (Figure 21). A 30%, 49% and 42% reduction in ROS was noted in SH-SY5Y cells treated with the respective concentrations of Cd (Figure 21). A gradual decrease in ROS was noted in the HepG2 cells as the concentration of Cd increased (Figure 21A), whereas the reduction appeared to plateau in SH-SY5Y cells (Figure 21B).

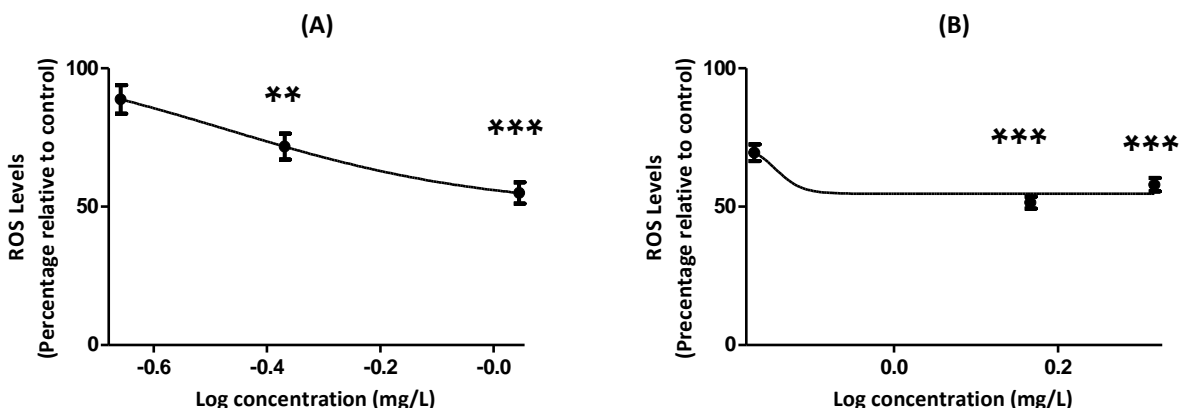


**Figure 21:** Reactive oxygen species concentrations in (A) HepG2 and (B) SH-SY5Y cells after 24 h exposure to the IC<sub>25</sub>, IC<sub>50</sub> and IC<sub>75</sub> of Cd. Comparison to the negative control. \*\*\*  $p < 0.001$ , \*\*  $p < 0.01$ .

The AIF translocation was blocked when pre-treated with 2.5 mM NAC, suggesting that ROS production plays an important role in the apoptogenic activity of Cd.<sup>238</sup> Although mitochondrial toxicity is indicative of ROS generation, this was not observed in our study. Cadmium is known to generate ROS.<sup>233,241</sup> However, the reduction in ROS concentrations has also been observed by other



investigators. Cadmium has been reported to induce a biphasic effect on ROS generation in AS-30D cells, stimulating production at 18.3 and 92 mg/L after 3 h, however, this decreased after 24h.<sup>233</sup> Although a 2.9-fold increase in ROS was observed after foetal lung fibroblasts were incubated for 3 h with Cd, levels decreased rapidly within 1 h.<sup>243</sup> After 30 min exposure to Cd<sup>2+</sup>, a significant increase in ROS levels was noted in PC12 cells, which however, began normalizing after 24 h exposure.<sup>221</sup>

### 3.2.5. Reduced glutathione levels

HepG2 cells exposed to IC<sub>25</sub>, IC<sub>50</sub> and IC<sub>75</sub> concentrations of Cd, reduced GSH levels by 40%, 60% and 93%, respectively (Figure 22A). In SH-SY5Y cells, a 40%, 56% and 93% reduction in GSH was observed (Figure 22B). The reduction in GSH levels was noted to be dose dependent in both cell lines and related to cell density as well as ΔΨ<sub>m</sub> reduction at all concentrations tested.

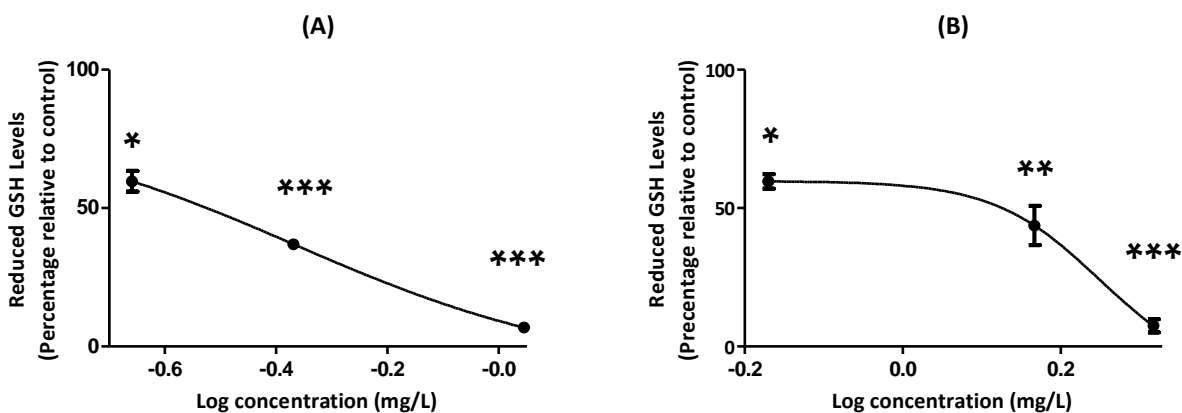


**Figure 22:** Glutathione levels in (A) HepG2 and (B) SH-SY5Y GSH after 24 h treatment with to the IC<sub>25</sub>, IC<sub>50</sub> and IC<sub>75</sub> of Cd. Comparison to the negative control. \*\*\*  $p < 0.001$ , \*\*  $p < 0.01$ , \*  $p < 0.05$ .

Cadmium-induced depletion of GSH has been found to result in disturbance of the redox balance, thereby leading to oxidative stress.<sup>244</sup> In HepG2 cells and primary rat hepatocytes, Cd decreased GSH levels and induced cell death, indicating that disruption of cellular GSH is a key element in the mechanism of Cd-induced liver damage.<sup>245</sup> At 0.5 mg/L, Cd exposure in HepG2 cells incurred a 20% GSH loss, with an IC<sub>50</sub> of 1 mg/L.<sup>245</sup> These results support the current findings that low concentrations of Cd (0.22 mg/L in HepG2 cells; 0.68 mg/L in SH-SY5Y cells) reduce GSH levels (Figure 22). In HaCaT cells, Cd (2.7, 9.2 and 18.3 mg/L) decreased the GSH/GSSG ratio, which is indicative of oxidative

stress.<sup>244</sup> Cadmium has a high affinity for thiols, including GSH.<sup>246</sup> Contrary to the above findings, it has also been reported that Cd only induces detriments to the GSH/GSSG at high concentrations (110 mg/L in HepG2 cells; 18.3 mg/L in C6 glioma cells).<sup>234</sup> Proteins containing SH-groups, such as GSH, are known to be oxidized by Cd.<sup>247</sup>

### 3.2.6. Caspase 3/7 activity

Caspase-3/7 activity in HepG2 cells was increased by 137%, 151% and 130%, respectively when exposed to IC<sub>25</sub>, IC<sub>50</sub> and IC<sub>75</sub> concentrations of Cd (Figure 23A). In SH-SY5Y cells, caspase-3/7 activity was increased by 217%, 284% and 234% when exposed to similar concentrations of Cd (Figure 23B). The increase in caspase 3/7 activity in SH-SY5Y cells was nearly double that observed in HepG2 cells at the same concentrations tested.

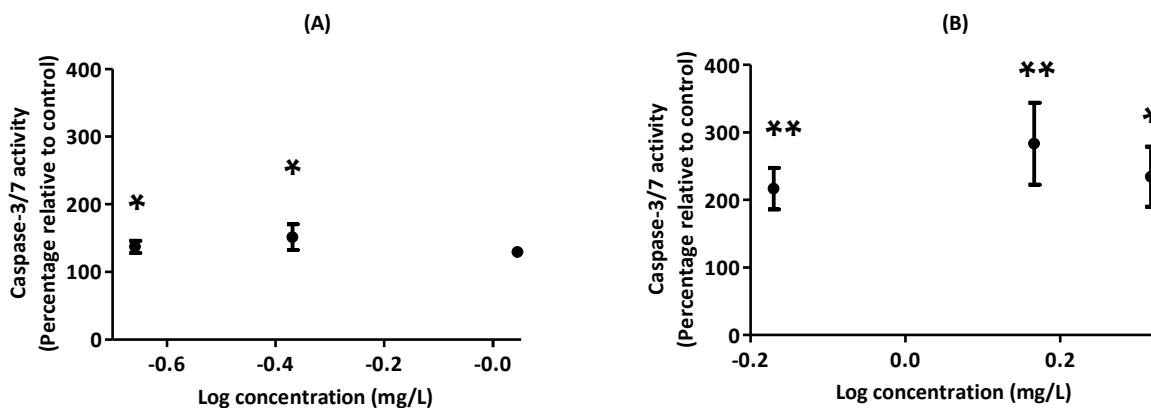


**Figure 23:** Caspase 3/7 activity in (A) HepG2 and (B) SH-SY5Y after exposure to the IC<sub>25</sub>, IC<sub>50</sub> and IC<sub>75</sub> of Cd for 24 h. Comparison to the negative control. \*\*  $p < 0.01$ , \*  $p < 0.05$ .

Cadmium has been found to induce apoptosis in leukemia and lymphoma cells,<sup>248</sup> renal epithelial cells,<sup>249</sup> proximal tubule cells,<sup>250</sup> lung epithelial cells,<sup>251</sup> as well as the liver,<sup>252</sup> testis<sup>253</sup> and prostate.<sup>112</sup> Caspase-9 is an enzyme that plays a specific role in programmed cell death. This enzyme is known to be activated after collapse of the mitochondrial membrane potential, formation of the permeability transition pore, and release of cytochrome C from mitochondria.<sup>254</sup> Caspase-9 has been reported to be activated in C6 cells after treatment with 0.9–1.8 mg/L CdCl<sub>2</sub> for 48 h.<sup>255</sup> As Cd was found to

decrease the mitochondrial membrane potential in C6 cells, it was postulated that it induces apoptosis via the mitochondrial pathway<sup>255, 256</sup> which is also confirmed by our findings.

Fluorescence microscopy of HepG2 cells treated with 3.7 mg/L CdCl<sub>2</sub> for 24 h showed the typical morphology of apoptosis (cytoplasmic shrinkage, rounding, and loss of cell-to-cell contact).<sup>232</sup> These nuclear changes were visualized using PI and Hoechst 33342 staining.<sup>232</sup> Apoptotic cells were found to contain condensed nuclear fragments and irregular aggregation of chromatin. Furthermore, some cells were found to detach from the monolayer and were observed floating in the culture medium. After 48 h of treatment, cells exhibited characteristic features of necrosis.<sup>232</sup>

Apoptosis induced by Cd is generally thought to be mediated by mitochondria and primarily by the binding of Cd to thiol groups in mitochondria resulting in mitochondria dysfunction and subsequent toxicity. The mitochondria derived protein, endonuclease G (Endo G) has been identified as the potential caspase-independent apoptotic mediator in the human hepatoma cell line, Hep3B.<sup>257</sup> The mechanism is said to involve Ca<sup>+2</sup> and ROS-related alteration of mitochondrial homeostasis with subsequent release of Endo G and AIF.<sup>257</sup>

Cadmium has been demonstrated to inhibit Ca-dependent ATPases in both the nuclei and endoplasmic reticulum, probably by binding with protein thiol groups.<sup>258</sup> A rise in Ca<sup>+2</sup>, has been suggested to cause apoptosis by inducing collapse of the  $\Delta\Psi$ M and resulting in oxidative phosphorylation uncoupling.<sup>258</sup> The Ca<sup>+2</sup> elevation in hepatocytes treated with Cd may be related to extracellular Ca entry, whereas the initial Ca<sup>+2</sup> elevation is proposed to be associated with an excessive release of Ca from intracellular stores. However, Cd-induced Ca<sup>+2</sup> elevation was shown to be attenuated in HL-7702 cells co-incubated with a Ca<sup>+2</sup> chelator.<sup>259</sup> Therefore, Cd-induced apoptosis appears to be mediated by the release of Ca<sup>+2</sup> from intracellular Ca<sup>+2</sup> storage and not from an influx of extracellular Ca<sup>+2</sup>. Cadmium has also been found to cause ER stress *in vitro* and *in vivo* and mediate induction of apoptosis in some tissues.<sup>260, 261</sup> However, no conclusive data is available regarding Cd-induced ER stress and its relation with hepatocyte apoptosis.<sup>259, 262</sup>

Other authors have demonstrated that Cd induces caspase-independent apoptosis through a mitochondria-ROS pathway in MRC-5 fibroblasts, providing evidence that mitochondrial ETC and MPTP play a role in the regulation of caspase-independent cell death triggered by Cd.<sup>243</sup> After 24 h treatment with 18.3 mg/L Cd, the apoptosis reached a plateau of ~40.0%. However, pre-treatment with broad spectrum caspase inhibitor, Z-VAD.fmk, was unable to rescue MRC-5 fibroblasts, suggesting that Cd might follow a caspase-independent apoptotic pathway.<sup>243</sup> Cadmium was found to induce caspase-independent apoptosis at concentrations between 4.6 to 27.5 mg/L, which was modulated by ROS scavengers, such as N-acetylcysteine (NAC), mannitol, and tiron. The ROS plays a crucial role in the apoptogenic activity of Cd. Furthermore, the intracellular H<sub>2</sub>O<sub>2</sub> was found to be elevated 2.9-fold after 3 h of treatment with Cd.<sup>243</sup> Intracellular H<sub>2</sub>O<sub>2</sub> levels were found to decrease within 1 h of incubation.<sup>243</sup> Inhibitors of the mitochondrial electron transport chain (ETC) (oligomycin A and rotenone for complex I and V, respectively) and mitochondrial permeability transition pore (MPTP) (cyclosporin A and aristolochic acid), were found to completely or partially abolish ROS production,  $\Delta\Psi$ M depolarization, and apoptotic content initiated by Cd exposure.<sup>243</sup>

### **3.3. Mercury**

#### **3.3.1. Cell density**

Mercury was more cytotoxic towards SH-SY5Y cells (IC<sub>50</sub> = 11.99 mg/L; Table 4) than HepG2 cells (IC<sub>50</sub> = 26.23 mg/L; Table 4). HepG2 cell density decreased after exposure to Hg concentrations  $\geq$ 20 mg/L, with a maximum reduction of 79% observed at 35 mg/L (Figure 24A). In SH-SY5Y cell lines, Hg decreased cell density significantly ( $p < 0.05$ ) at  $\geq$ 5 mg/L Hg (Figure 24B), with a maximum reduction of 93% observed at 20 mg/L (Figure 24B)

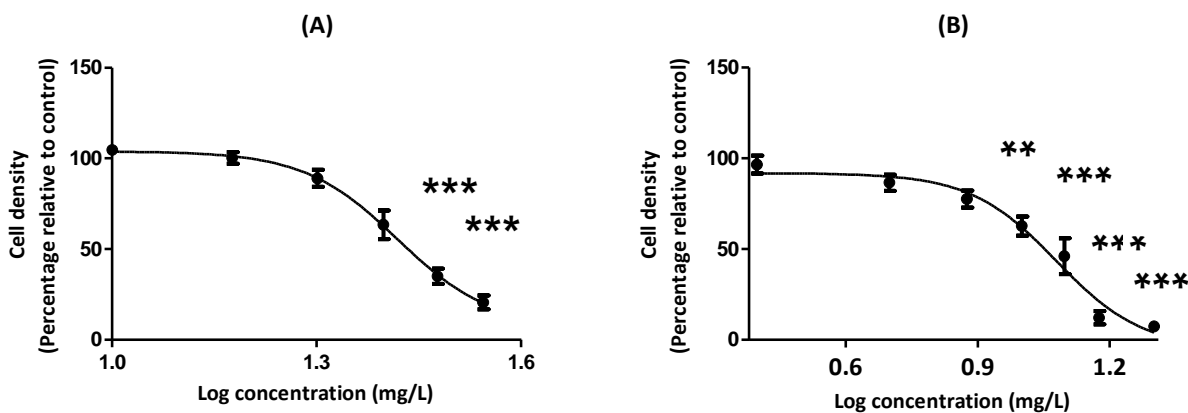


**Figure 24:** Dose-dependent reduction of cell density in (A) HepG2 and (B) SH-SY5Y cells after exposure to Hg for 24 h. Comparison to the negative control. \*\*\*  $p < 0.001$ , \*\*  $p < 0.01$ .

**Table 4:** Inhibitory concentrations of Hg determined after 24 h exposure in the HepG2 and SH-SY5Y cell lines.

Inhibitory concentration	HepG2 cells $\pm$ SEM	SH-SY5Y cells
IC <sub>25</sub> (mg/L)	22.90 $\pm$ 1.18	8.45 $\pm$ 1.14
IC <sub>50</sub> (mg/L)	26.23 $\pm$ 1.06	11.99 $\pm$ 1.08
IC <sub>75</sub> (mg/L)	33.04 $\pm$ 1.05	14.36 $\pm$ 1.07

The effects of Hg on HepG2 and SH-SY5Y cell lines were verified by exposing both cell lines to the IC<sub>25</sub>, IC<sub>50</sub> and IC<sub>75</sub> of this metal. Both cell lines displayed reduction in cell density (Figure 25; Table 4).

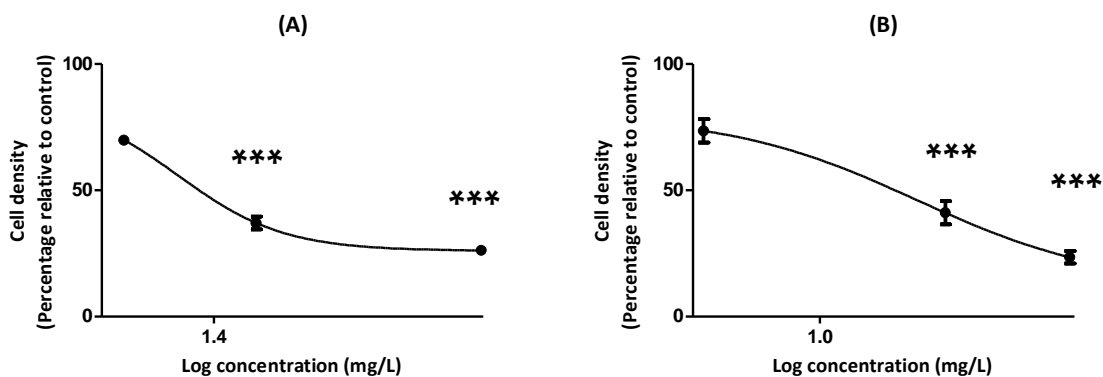


**Figure 25:** Cell density in (A) HepG2 and (B) SH-SY5Y cells after exposure to the IC<sub>25</sub>, IC<sub>50</sub> and IC<sub>75</sub> of Hg for 24 h. Comparison to the negative control. \*\*\*  $p < 0.001$ .

In PC12 adrenal pheochromocytoma cells,  $\text{HgCl}_2$  was calculated to exhibit an  $\text{IC}_{25}$  of 13.6 mg/mL after 3 h exposure,<sup>263</sup> which is higher than the  $\text{IC}_{25}$  of 8.45 mg/mL obtained in the current study for the SH-SY5Y cells after 24 h incubation. Mercury (13 mg/L) was reported to reduce the viability of AS-30D rat hepatoma cells by 90%.<sup>233</sup> The reduction in the latter study is higher than was noted in the current study (79%) and may be ascribed to the difference in cell line. The  $\text{IC}_{50}$  of Hg was 3.8 mg/L, 12.2 mg/L, 5.4 mg/L and 2.7 mg/L in the HepG2, HEK human embryonic kidney, 1321N1 astrocytoma,<sup>241</sup> and TNBC cell lines,<sup>264</sup> respectively. The differences between published and current  $\text{IC}_{50}$ 's obtained may be due to type of cells, oxidation- and/or experiment-specific effects that were different. It is well known that certain cell lines are less affected by  $\text{HgCl}_2$ , such as the PLHC-1 cell line, where an  $\text{IC}_{50}$  of 67.9 mg/L has been reported.<sup>265</sup> The organic form of Hg have been reported to induce higher cytotoxicity in HepG2 cells, with reduction in cell viability concentrations below 2 mg/L.<sup>266</sup> In comparison,  $\text{Hg}_2\text{Cl}_2$  only induced cytotoxicity at levels above 15 mg/L in the same cell line. The differences noted between organic and inorganic forms of Hg *in vitro* may explain the differences noted in the pathology of intoxicated patients.<sup>267,268</sup>

### 3.3.2. Mitochondrial membrane potential

Mercury decreased  $\Delta\Psi_m$  in HepG2 cells with a reduction of 29% and 33% for the  $\text{IC}_{25}$  and  $\text{IC}_{50}$ , followed by a more severe decrease of 60% when treated with the  $\text{IC}_{75}$  of this compound (Figure 26A). In SH-SY5Y cells the decrease was more gradual ( $\text{IC}_{25}$  = 20%,  $\text{IC}_{50}$  = 32%,  $\text{IC}_{75}$  = 44%) (Figure 26B). These decreases paralleled that of the cell density reduction observed.

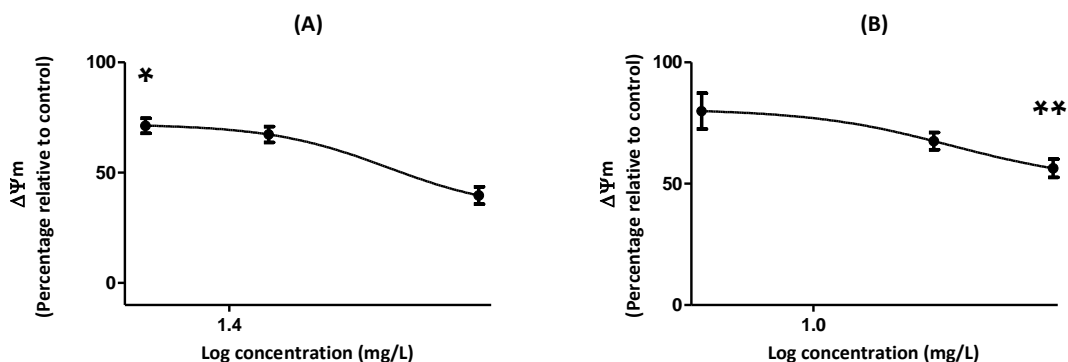


**Figure 26:** Mitochondrial membrane potential in (A) HepG2 and (B) SH-SY5Y cells after 24 h exposure to the  $\text{IC}_{25}$ ,  $\text{IC}_{50}$  and  $\text{IC}_{75}$  of Hg. Comparison to the negative control. \*\*  $p < 0.01$ , \*  $p < 0.05$ .

Methyl mercury has been shown to depolarize the mitochondrial membrane in PC12 cells<sup>263</sup> and astrocytes.<sup>269</sup> The depolarization in the latter cells was induced by lower concentrations of Hg, which may be ascribed to the organic form of Hg used. Furthermore, MeHg decreased mitochondrial metabolic function, which was measured by conversion of MTT to formazan at  $\geq 1$  mg/L after 30 mins of exposure.<sup>270</sup>

In human T-cells, MeHgCl decreased  $\Delta\psi_m$ . This was accompanied by a decrease in the dimension of the mitochondria and a loss in cristae architecture.<sup>271</sup> Furthermore, MeHgCl depleted the thiol reserves in the cell and promoted translocation of cytochrome C from the mitochondria to the cytosol. It was noted that when T cells were thiol-depleted, there was an increase in apoptosis. A temporal relationship between the decline in  $\Delta\psi_m$ , generation of ROS, and depletion of thiol reserves was also realised. The profound reduction in  $\Delta\psi_m$  and decline in GSH levels occurred within 1 h of treatment. The subsequent further decrease in thiol reserves was linked to the generation of ROS ultimately leading to activation of death-signaling pathways.<sup>271</sup>

### 3.3.3. Intracellular ATP levels

The ATP concentration was decreased drastically in HepG2 cells when treated with IC<sub>25</sub> (86%) and IC<sub>50</sub> (90%) concentrations of Hg, being totally abolished (100%) when exposed to IC<sub>75</sub> concentrations thereof (Figure 27A). Although a reduction in ATP levels was noted in SH-SY5Y cells, it was more gradual (IC<sub>25</sub> = 30%, IC<sub>50</sub> = 77%, IC<sub>75</sub> = 99%; Figure 27B).

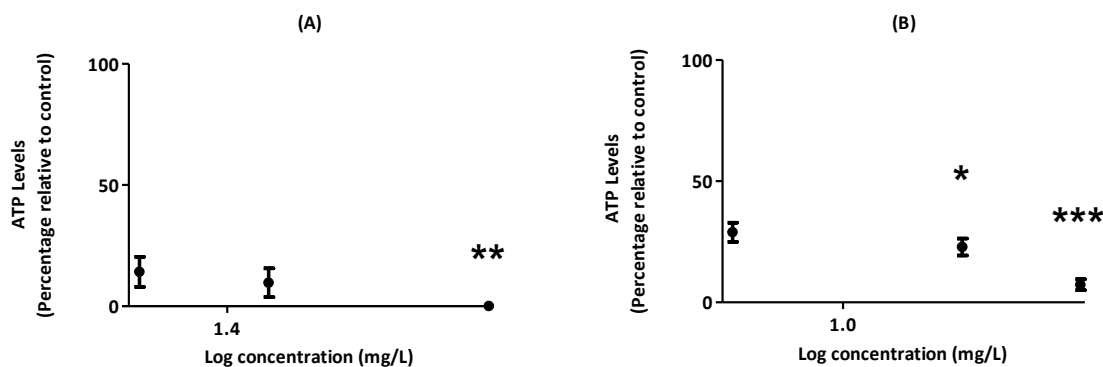


**Figure 27:** Intracellular ATP levels in (A) HepG2 and (B) SH-SY5Y cells after 24 h exposure to the IC<sub>25</sub>, IC<sub>50</sub> and IC<sub>75</sub> of Hg. Comparison to the negative control. \*\*\*  $p < 0.001$ , \*\*  $p < 0.01$ , \*  $p < 0.05$ .

Incubation of synaptosomes with methyl mercury was found to reduce ATP dose-dependently affecting synaptic neural signalling.<sup>272</sup> In another study, 2.7, 8 and 27 mg/L of Hg reduced ATP levels in a dose dependent manner and Hg was found to be more potent than Cu at the same concentrations in inhibiting ATP in the isolated perfused rat liver preparation.<sup>273</sup> A similar trend was noted in our study in both HepG2 with 86% and SH-SY5Y cells with 30% reduction in ATP levels at 22.90 and 8.45 mg/L of Hg respectively (Figure 27).

### 3.3.4. Reactive oxygen species

The ROS was reduced in a dose-dependent manner in both HepG2 and SH-SY5Y cells, when exposed to Hg (Figure 28). The highest percentage of reduction was achieved, as expected, after treatment with the IC<sub>75</sub> concentration, which accounted for 51% and 46% reduction in ROS activity in the HepG2 and SH-SY5Y cells, respectively.

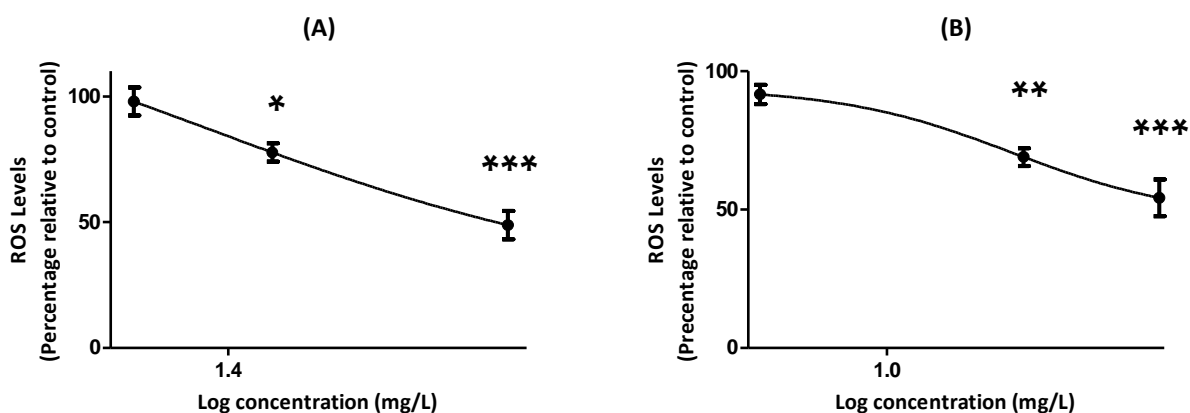


**Figure 28:** Reactive oxygen species levels in (A) HepG2 and (B) SH-SY5Y cells after 24 h exposure to the IC<sub>25</sub>, IC<sub>50</sub> and IC<sub>75</sub> of Hg. Comparison to the negative control. \*\*\*  $p < 0.001$ , \*\*  $p < 0.01$ , \*  $p < 0.05$

Reduced ROS levels have also been described in PC12 and AS-30D cells after exposure to Cd and Hg.<sup>233, 263</sup> This reduction was attributed to an almost complete blockage of cellular respiration.<sup>233, 263</sup> These results support the current findings, which suggest a biphasic response to heavy metal exposure. Short incubation periods would appear to increase ROS generation, whereas, during longer incubation periods the ROS decrease is counteracted, possibly initiating protective measures.<sup>271</sup>



### 3.3.5. Reduced glutathione levels

HepG2 cells exposed to Hg at the IC<sub>25</sub>, IC<sub>50</sub> and IC<sub>75</sub> reduced GSH by 28%, 59% and 99%, respectively (Figure 29A), while in SH-SY5Y cells, a reduction of 44%, 64% and 99% was observed (Figure 29B). The reduction in both cell lines was dose dependent, with virtually total inhibition (99%) of GSH when treated with the IC<sub>75</sub> concentration of Hg. This reduction in GSH levels correlates with the reduction in cell density as well as the loss in  $\Delta\psi_m$ .

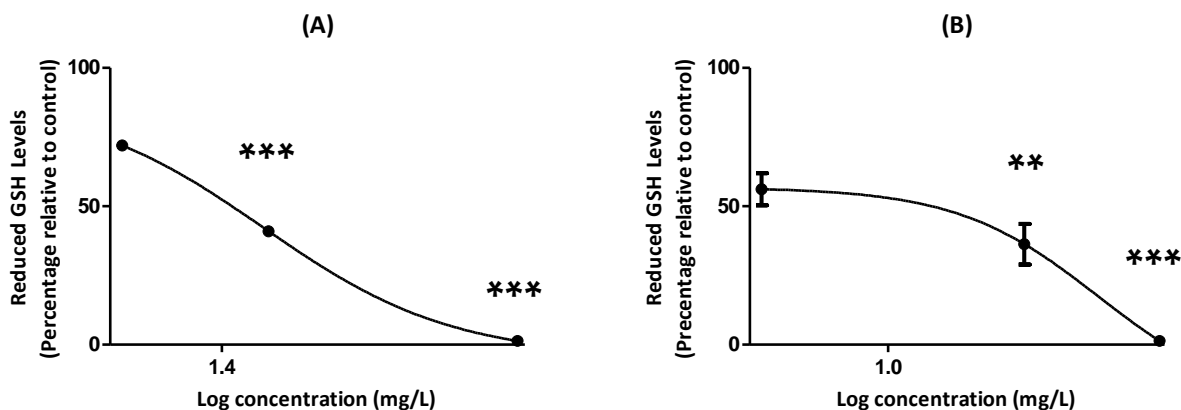


**Figure 29:** Glutathione concentration in (A) HepG2 and (B) SH-SY5Y cells after 24 h exposure to the IC<sub>25</sub>, IC<sub>50</sub> and IC<sub>75</sub> of Hg. Comparison to the negative control. \*\*\*  $p < 0.001$ , \*\*  $p < 0.01$ .

Both GSH and GSSG levels have been found to be decreased in primary rat neonatal astrocytes exposed to MeHg (>1.2 mg/L) for 6 h.<sup>274</sup> Similarly in HepG2 cells MeHg (2 mg/L) decreased GSH.<sup>266</sup> Mercury 8 mg/L reduced GSH levels by 75% in HepG2 cells after 24 h exposure<sup>275</sup> which is higher than obtained in the current study for the HepG2 cells after 24 h (59% at 26.23 mg/L). Furthermore Hg has been shown to covalently bind to two GSH molecules causing its excretion from the cells and thereby further aggravating its toxicity.<sup>276</sup> In human glioma cell line A172 cells, Hg resulted in 34% reduction in GSH content<sup>277</sup> which is in accordance to our findings in both HepG2 and SH-SY5Y cells (Figure 29). Mercury in neuroblastoma cells, [Neuro-2A (N-2A)] reduced GSH levels by 50% after 24 h exposure to 1.4 mg/L where as our findings suggested higher levels (8.45 mg/L) were able to reduce GSH levels by 44% (Figure 29B). This lower toxicity of Hg on GSH levels in our study can be explained by different cell lines used.

### 3.3.6. Caspase 3/7 activity

Mercury decreased caspase-3/7 in HepG2 cells by 85% when treated with both the IC<sub>25</sub> and IC<sub>50</sub> concentration thereof (Figure 30A). In contrast caspase-3/7 activity was increased by 320%, 181% and 327% in SH-SY5Y cells when exposed to IC<sub>25</sub>, IC<sub>50</sub> and IC<sub>75</sub> concentrations of Hg (Figure 30B).

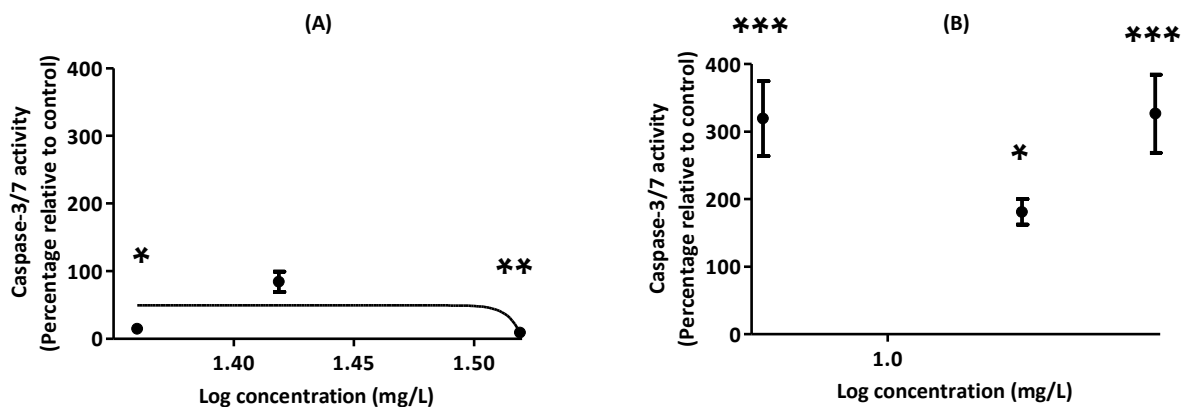


**Figure 30:** Caspase-3/7 activity in (A) HepG2 and (B) SH-SY5Y cells after treatment after 24 h exposure to the IC<sub>25</sub>, IC<sub>50</sub> and IC<sub>75</sub> of Hg. Comparison to the negative control. \*\*\*  $p < 0.001$ , \*\*  $p < 0.01$ , \*  $p < 0.05$ .

Apoptotic routes of MeHg-induced (2 mg/mL) cell death in HepG2 were investigated by determining caspase-3, -8 and -9 activities. Although no activation of caspase-8 was observed, caspase-9 activity increased after 2 h of incubation whereas caspase-3 activity increased immediately and remained enhanced over the total incubation period of 24 h.<sup>266</sup> In differentiated neuronal WHMES cells, Hg at very high concentration (81 mg/L) was able to induce caspase-3/7<sup>278</sup> whereas in our findings; relatively lower concentration (8.45 mg/L) in SH-SY5Y cells was able to increase activity to 320% which may have resulted due to difference in cell lines (Figure 30B).

### 3.4. Heavy metal combinations

#### 3.4.1. Cell density

To assess the effect of combinational cytotoxicity of the heavy metals, two different combinations were assessed: i) a mixture of the heavy metals at their respective IC<sub>20</sub>'s, IC<sub>25</sub>'s and IC<sub>35</sub>'s, and ii) a mixture at the EPA's MCL ratio for As, Cd and Hg (10:5:2) with As as the reference concentration. After exposure to the IC<sub>20</sub>, IC<sub>25</sub> and IC<sub>35</sub> mixtures, HepG2 cell density was reduced by 93%, 92% and

96%, respectively (Figure 31A), while SH-SY5Y cells were reduced by 88%, 88% and 91% (Figure 31B). The reduction in cell density was far greater than that observed for any of the single metals alone, which may imply that either additive or synergistic activity increases in cytotoxicity occurred.

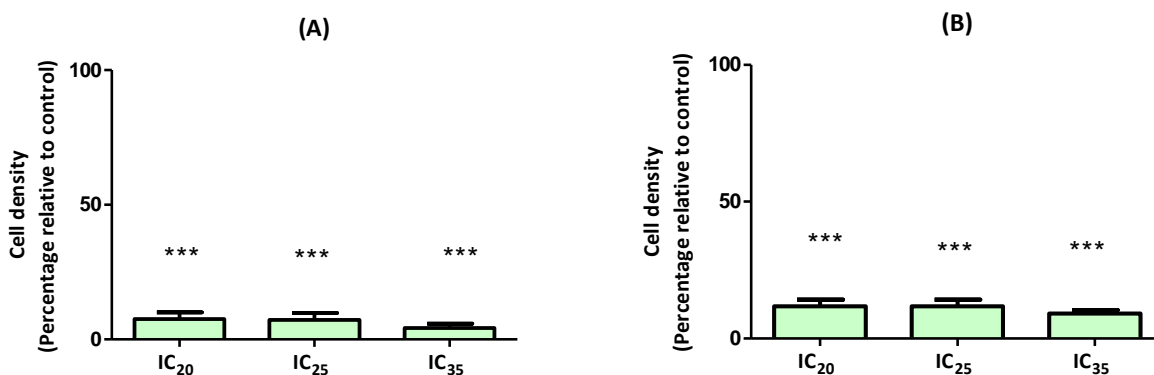


**Figure 31:** Cell density in (A) HepG2 and (B) SH-SY5Y cells after exposure to the IC<sub>25</sub>, IC<sub>50</sub> and IC<sub>75</sub> mixtures of As, Cd and Hg for 24 h. Comparison to the negative control. \*\*\*  $p < 0.001$ .

After exposure to the EPA mixture, HepG2 cell density was reduced by 45% at 0.5 mg/L reference concentration of As in HepG2 cells (Figure 32A). This is much higher than the single compounds, where only 3% or no reduction in cell density was noted after treatment with As (1 mg/L), Cd (0.25 mg/L) with 34% reduction and no reduction in cell density with Hg (10 mg/L). The EPA mixture of 4 mg/mL (with respect to As) reduced cell density by 93% (Figure 32A), whereas As alone at same concentration (4.01 mg/L) reduced cell density by 25% in the HepG2 cell line (Figure 5A). Moreover, individual Cd (2 mg/L) reduced cell density by 86% (Figure 17A) whereas Hg at 15 mg/L did not reduce cell density (Figure 24A).

After exposure to the EPA mixture, cell density was reduced by 23% at 0.5 mg/L reference concentration of As in SH-SY5Y cells (Figure 32B), whereas individual As exposure (1mg/L) reduced cell density by only 4% (Figure 5A). Cadmium as a single compound (0.25 mg/L) at 0.5 mg/L reference concentration of As, reduced cell density by 23% (Figure 17B). Mercury alone at a concentration of 2.5 mg/L led to a reduction in cell density of 3% (Figure 24B) showing similar toxicity of As, Cd and Hg when in EPA mixture and individually. The EPA mixture (4 mg/mL) with respect to reference

concentration of As, reduced cell density by 93% (Figure 32B), while As alone at the same concentration of the mixture (4 mg/L) reduced cell density by 84% in the SH-SY5Y cell line (Figure 5B). Moreover, individual Cd (2 mg/L) at 4 mg/L reference concentration of As, reduced cell density by 73% (Figure 17B) whereas Hg as a single compound, but higher concentration (2.5 mg/L) reduced cell density by 1% (Figure 24B) which implies antagonism is taking place.

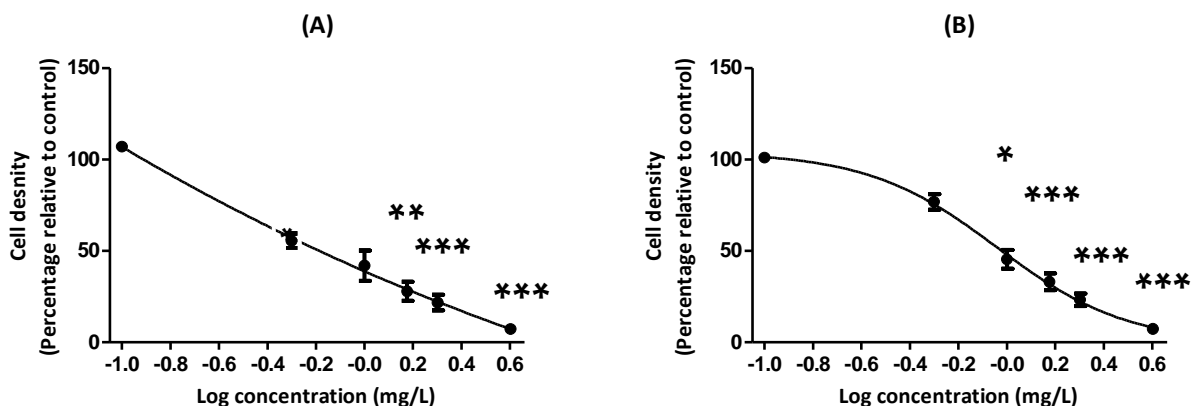


**Figure 32:** Dose-dependent reduction of cell density in (A) HepG2 and (B) SH-SY5Y cells after exposure to EPA mixtures with respect to As for 24 h. Cadmium and Hg concentrations are according to the EPA ratio of As, Cd and Hg (10:5:2). Comparison to the negative control. \*\*\*  $p < 0.001$ , \*\*  $p < 0.01$ , \*  $p < 0.05$ .

### 3.4.2. Mitochondrial membrane potential

Combinations of metal mixtures displayed greater mitochondrial toxicity than the metals alone (Figures 33-34). The effects were most prominent in the HepG2 cell line (Figure 33A). The IC<sub>20</sub>, IC<sub>25</sub> and IC<sub>35</sub> combinations reduced  $\Delta\Psi_m$  by 65%, 72% and 93%, respectively, in HepG2 cells. In SH-SY5Y cells, IC<sub>20</sub>, IC<sub>25</sub> and IC<sub>35</sub> combinations reduced  $\Delta\Psi_m$  by 29%, 41% and 64%, respectively. A gradual reduction in  $\Delta\Psi_m$  was noted in both cell lines. Given the cell density results, it appears that mitochondrial toxicity contributes to the effects seen. However, the increased depolarisation up to the IC<sub>75</sub> did not alter the level of cell density reduction observed at lower concentrations.

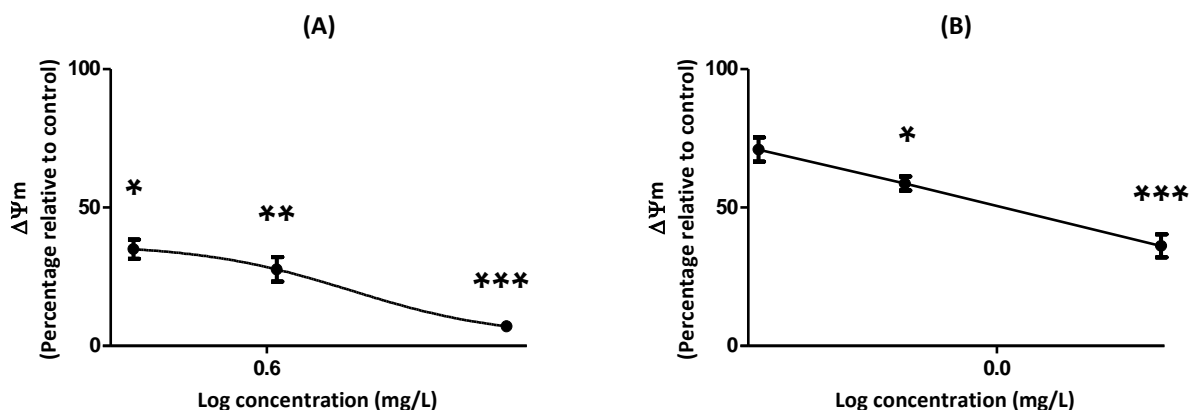


**Figure 33:** Mitochondrial membrane potential in (A) HepG2 and (B) SH-SY5Y cells after exposure to the IC<sub>20</sub>, IC<sub>25</sub> and IC<sub>35</sub> mixtures of As, Cd and Hg for 24 h. Comparison to the negative control. \*\*\*  $p < 0.001$ , \*\*  $p < 0.01$ , \*  $p < 0.05$ .

The EPA mixture induced a gradual reduction in  $\Delta\Psi_m$  which was similar in both the hepatoma and neuronal cell lines. At 4 mg/L EPA mixture (As as reference),  $\Delta\Psi_m$  was reduced by 78% in the HepG2 cell line (Figure 34A), while As alone at the same concentration (4.01 mg/L) reduced  $\Delta\Psi_m$  by only 12% (Figure 8A). The highest concentration of Cd tested alone (1.11 mg/L) was found to reduce the  $\Delta\Psi_m$  by 75% (Figure 15A) whereas Hg at a concentration of 22.90 mg/L reduced  $\Delta\Psi_m$  by 29% (Figure 26A). The EPA mixture thus produced an antagonistic effect. In SH-SY5Y cells, the EPA mixture (4 mg/L) reduced the  $\Delta\Psi_m$  by 93% (Figure 34B), whereas As alone (2.78 mg/L) reduced  $\Delta\Psi_m$  by 62% in the SH-SY5Y cell line (Figure 8B). Cadmium alone at a concentration of 2.08 mg/L reduced  $\Delta\Psi_m$  by 64% (Figure 15B) showing antagonistic effect of EPA mixture. These results are in accordance with cell density findings and depolarization of mitochondrial potential paralleled reduction in cell density.

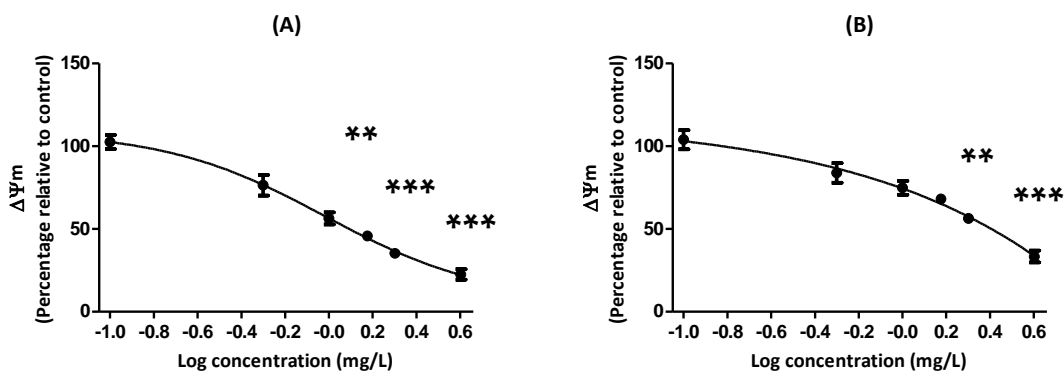


**Figure 34** Dose-dependent reduction of  $\Delta\Psi_m$  in (A) HepG2 and (B) SH-SY5Y cells after exposure to EPA mixtures with respect to As for 24 h. Cadmium and Hg concentrations are according to the EPA ratio of As, Cd and Hg (10:5:2). Comparison to the negative control. \*\*\*  $p < 0.001$ , \*\*  $p < 0.01$ .

### 3.4.3. Intracellular ATP levels

A profound decrease of 93% in the ATP concentration was noticed when HepG2 cells were exposed to the EPA mixture, containing 4 mg/L As (Figure 35A), compared to a 68% reduction when treated with 4.01 mg/L As only (Figure 10A). In SH-SY5Y cells, ATP levels were decreased by 96% by the EPA mixture (with respect to As 0.5 mg/L), whereas As alone (0.94 mg/L) reduced ATP level by 97% (Figure 10B). Both the cell lines were very sensitive to the metal mixture, almost completely inhibiting ATP levels indicating cell death from apoptotic to necrotic pathways. The mixture toxicity in both cell lines was parallel to cell density and mitochondrial damage.

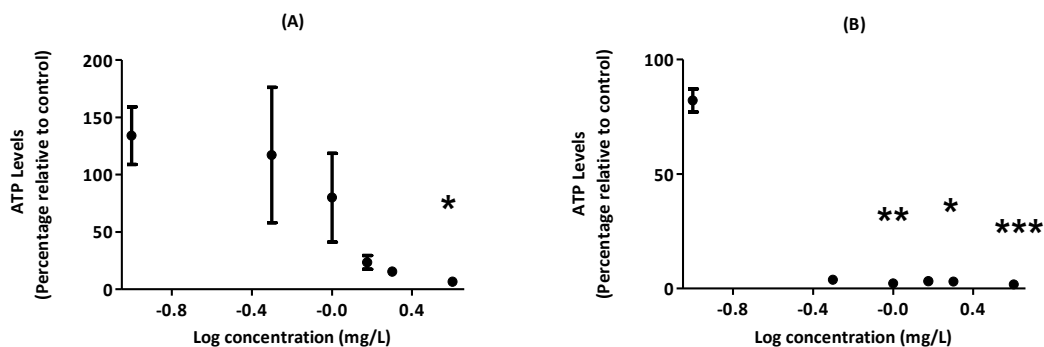


**Figure 35:** Dose-dependent reduction of ATP levels in (A) HepG2 and (B) SH-SY5Y cells after exposure to EPA mixtures with respect to As for 24 h. Cadmium and Hg concentrations are according to the EPA ratio of As, Cd and Hg (10:5:2). Comparison to the negative control. \*\*\*  $p < 0.001$ , \*\*  $p < 0.01$ , \*  $p < 0.05$ .

### 3.4.4. Reactive oxygen species

In HepG2 cells, ROS was reduced by 74%, 84% and 85% at the IC<sub>20</sub>, IC<sub>25</sub> and IC<sub>35</sub> mixture respectively (Figure 36A). In the SH-SY5Y cell line, ROS was reduced by 77%, 80% and 81%, respectively (Figure 36B).

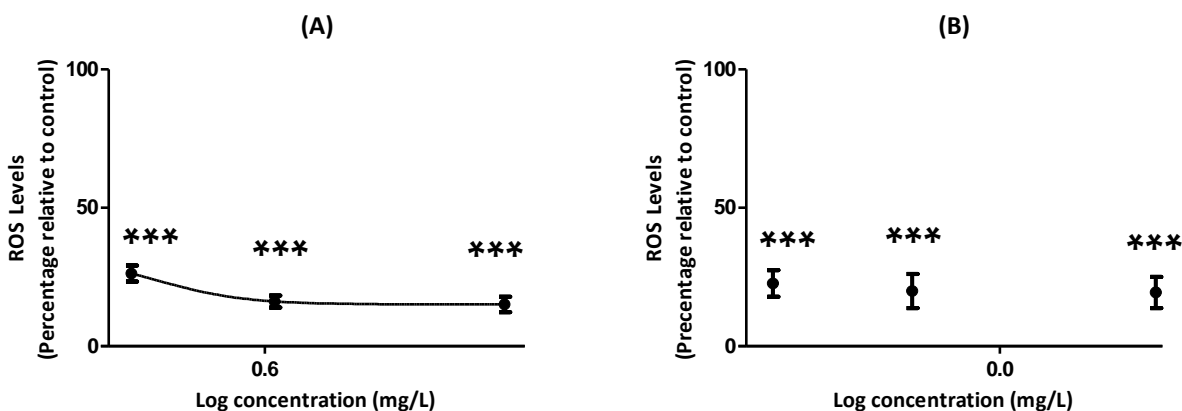


**Figure 36:** Reactive oxygen species in (A) HepG2 and (B) SH-SY5Y cells after exposure to the IC<sub>20</sub>, IC<sub>25</sub> and IC<sub>35</sub> mixtures of As, Cd and Hg for 24 h. Comparison to the negative control. \*\*\*  $p < 0.001$ .

A decrease of 85% in the ROS level was noted after exposure to the EPA mixture at 4 mg/L (As as reference), while As alone (4.01 mg/L) only reduced the ROS level by 28% in HepG2 cells (Figure 12A). The EPA combination reduced ROS levels in HepG2 cells (Figure 37A). In SH-SY5Y cells, a decrease of 62% in ROS was noticed when treated with the EPA mixture with respect to As 2 mg/L (Figure 37B), with As alone (2.78 mg/L) reducing ROS by the same amount (Figure 12B). This reduction in ROS levels after metal mixture exposure can be explained by biphasic effect of Cd and Hg on different cell lines as follows. Cadmium has been reported to induce a biphasic effect on ROS generation in AS-30D cells,<sup>233</sup> foetal lung fibroblasts<sup>243</sup> PC12 cells,<sup>221</sup> increasing ROS initially and then a profound decrease was noted in these studies after 24 h. Reduced ROS levels have also been described in PC12 and AS-30D cells when exposed to Hg after 24 h exposure.<sup>233,263</sup>

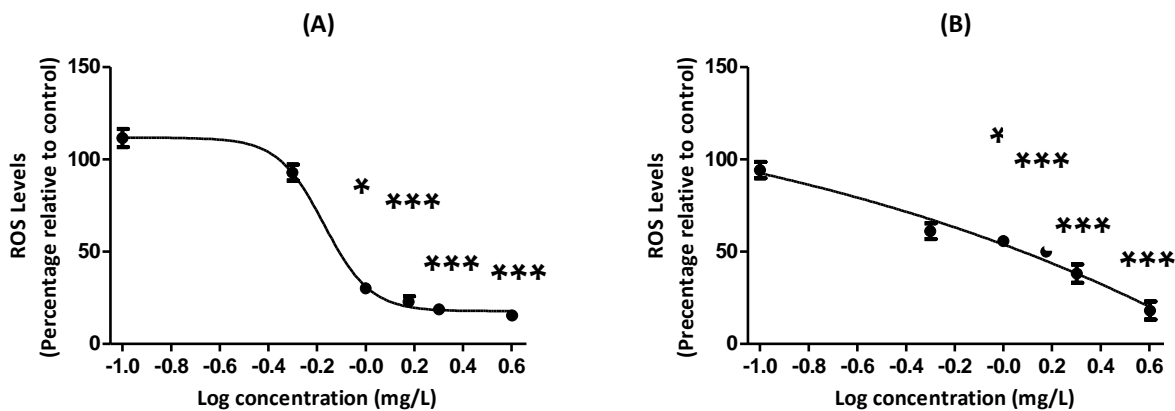


**Figure 37:** Dose-dependent reduction of ROS levels in (A) HepG2 and (B) SH-SY5Y cells after exposure to EPA mixtures with respect to As for 24 h. Cadmium and Hg concentrations are according to the EPA ratio of As, Cd and Hg (10:5;2). Comparison to the negative control. \*\*\*  $p < 0.001$ , \*  $p < 0.05$ .

### 3.4.5. Reduced glutathione levels

The IC combinations abolished GSH levels completely in hepatoma and neuronal cells (Figure 38). All the combinations reduced GSH levels when compared to reduction in GSH levels at individual  $IC_{25}$  of As, Cd and Hg.

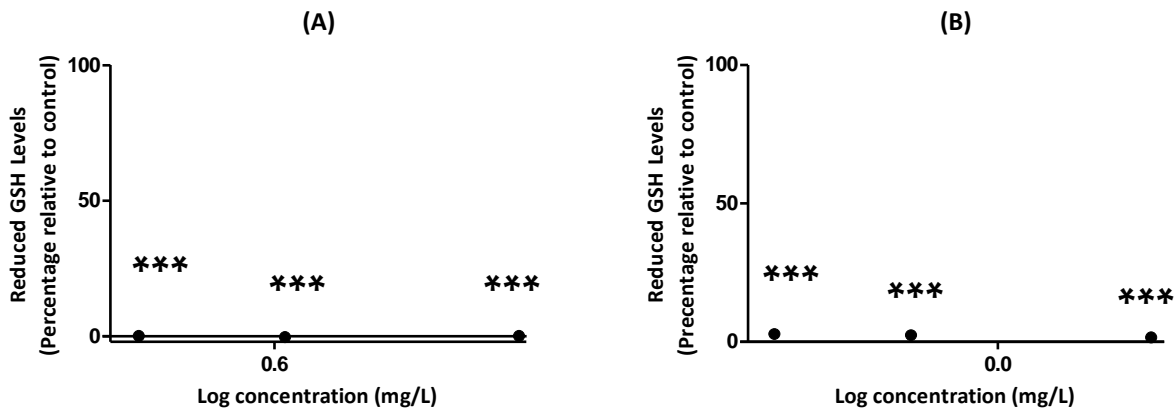


**Figure 38:** Reduced glutathione levels in (A) HepG2 and (B) SH-SY5Y cells after exposure to the  $IC_{20}$ ,  $IC_{25}$  and  $IC_{35}$  mixtures of As, Cd and Hg for 24 h. Comparison to the negative control. \*  $p < 0.001$ .



A profound decrease of 99% in GSH level was induced by the EPA mixture with respect to As 4 mg/L (Figure 39A). The As alone at a similar concentration (4.01 mg/L) reduced GSH levels by a third of that of the mixture (35%) in HepG2 cells. Cadmium alone at 1.11 mg/L completely inhibited GSH levels which shows similar effects on GSH levels of metals individually and in combination.

In SH-SY5Y cells, the GSH was decreased by 95% by the EPA mixture with respect to As 2 mg/L. The As alone, albeit at a higher concentration (2.78 mg/L) reduced ROS levels to the same degree as the mixture (96%) (Figure 39B).

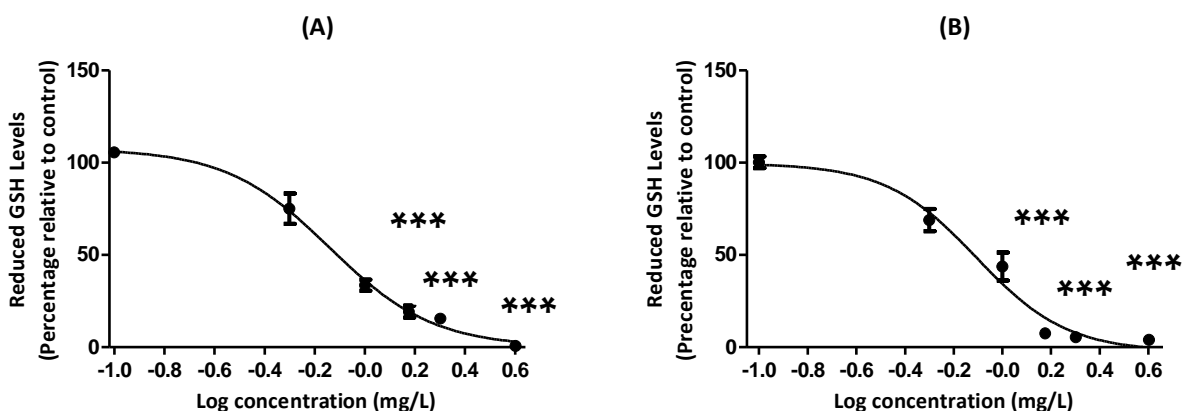


**Figure 39:** Dose-dependent reduction of GSH levels in (A) HepG2 and (B) SH-SY5Y cells after exposure to EPA mixtures with respect to As for 24 h. Cadmium and Hg concentrations are according to the EPA ratio of As, Cd and Hg (10:5:2). Comparison to the negative control. \*\*\*  $p < 0.001$ .

### 3.4.6. Caspase 3/7 activity

An increase (172%) in caspase-3/7 activity was noticed when HepG2 cells were treated with the EPA mixture with respect to As 0.5 mg/L (Figure 40A). An even higher increase in caspase 3/7 activity was noted when the cells were exposed to 4 mg/L EPA mixture concentration with respect to As (505%). The As alone at the same concentration (4.01 mg/L) increased caspase-3/7 activity to 159% in HepG2 cells while Cd at 1.11 mg/L increased caspase-3/7 activity by 130%. Mercury at even higher individual concentrations reduced caspase-3/7 activity below basal levels: all suggesting higher caspase-3/7 activity by EPA mixture combination when compared to individual metals.

In SH-SY5Y cells, a profound increase (178%) in caspase-3/7 activity was noticed after treatment with EPA mixture with respect to As 0.5 mg/L, whereas As on its own (0.94 mg/L) increased caspase-3/7 activity by 141%. Cadmium at 0.68 mg/L alone increased caspase-3/7 activity by 217% showing less increase in caspase-3/7 activity when exposed to metal mixture. At a concentration of 4mg/L EPA mixture with respect to As, caspase-3/7 activity increased by 361% (Figure 40B). While As alone at 2.78 mg/L increased caspase-3/7 activity by 144% only and Cd on its own (2.08 mg/L) increased caspase-3/7 activity by 234% showing similar caspase-3/7 activity by EPA mixture and individual metals.

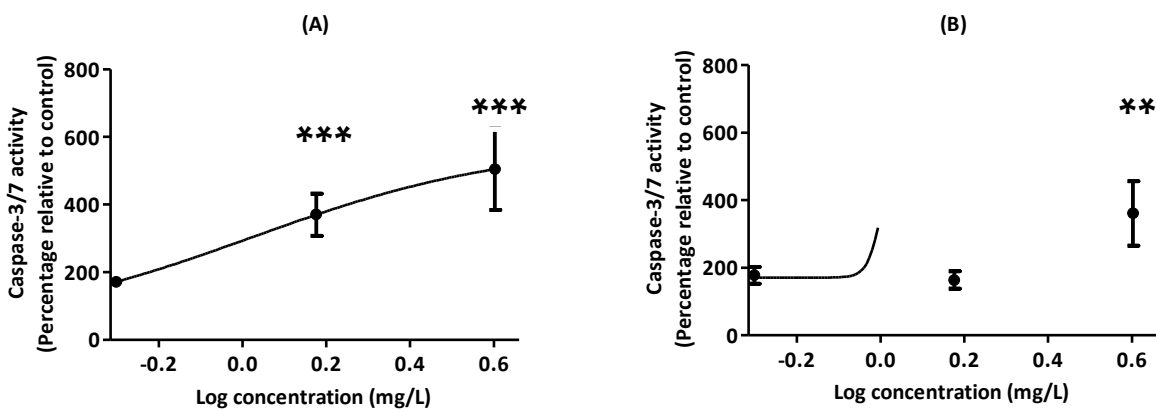


**Figure 40:** Caspase-3/7 activity in (A) HepG2 and (B) SH-SY5Y cells after exposure to EPA mixtures with respect to As for 24 h. Cadmium and Hg concentrations are according to the EPA ratio of As, Cd and Hg (10:5:2). Comparison to the negative control. \*\*\*  $p < 0.001$ , \*\*  $p < 0.01$

## Chapter 4

### General Discussion

---

The aim of the study was to assess the effect of As, Cd and Hg individually and in combination on the HepG2 and SH-SY5Y neuroblastoma cells as a measure of hepatotoxicity and neurotoxicity, respectively. The aim was achieved through investigation of individual metals and in combination on cell density, mitochondrial membrane potential, ATP levels, ROS generation, GSH and caspase-3/7 activity.

In every case of the experiments carried out, the pattern of toxicity remained assiduous, deviating only in certain conditions. Testing controls in each case gave information on the background while the heavy metal assays and their combination assays gave information on the toxicity.

Arsenic displayed gradual, dose-dependent cytotoxicity in both cell lines. In the HepG2 cells,  $IC_{50}$  of As was determined as 6.71 mg/L and in the SH-SY5Y cells,  $IC_{50}$  of 1.19 mg/L suggesting a higher cytotoxicity in cells of a neural origin. Literature suggest similar finding and the  $IC_{50}$  of  $As^{3+}$  in rat heart micro vessel endothelial (RHMVE) cells was reported as 4.6 mg/L.<sup>206</sup>

Arsenic had minimal effects on HepG2  $\Delta\Psi_m$  at the  $IC_{25}$  and  $IC_{50}$  (~12%), with a significant ( $p < 0.05$ ) reduction of 45% at the  $IC_{75}$ . Depolarisation may thus be of lesser consequence at lower concentrations in HepG2 cells. In contrary, literature showed depolarization of  $\Delta\Psi_m$  after treatment with 1 mg/L and 3 mg/L  $As_2O_3$  by 34% and 57%, respectively.<sup>212</sup> A gradual, tapered reduction was observed in the SH-SY5Y cell line from the  $IC_{25}$  to  $IC_{75}$  (25% to 62%). This decline parallels the reduction in cell density in the SH-SY5Y cell line, suggesting a greater relation between the two parameters. Thus SH-SY5Y cells are more susceptible to mitochondrial toxicity induced by As. Arsenic profoundly decreased ATP at  $IC_{25}$  by 68%,  $IC_{50}$  by 77% and by 87% at  $IC_{75}$ . The latter is indicative of mitochondrial toxicity in HepG2 cells. In the literature, a similar trend was noted in the wild type mouse embryonic fibroblasts cells where 2 mg/L  $As_2O_3$  after 16 h exposure, decreased ATP levels by 30%.<sup>218</sup> The ATP levels were almost completely reduced by 98%, 97% and 98% in SH-SY5Y cells when exposed to the  $IC_{25}$ ,  $IC_{50}$  and  $IC_{75}$  concentrations of As indicating necrotic cell death. Although

mitochondrial depolarisation occurred when cells were exposed to As, ROS generation was not increased in both cells. On the contrary, As decreased ROS levels in HepG2 cells by 28%, 44% and 57% and in the SH-SY5Y cell line ROS was reduced by 30%, 45% and 62%, respectively by the corresponding As concentrations suggesting biphasic effect as found in literature. The GSH was reduced by 35%, 64% and 94% in HepG2 cells, when exposed to the IC<sub>25</sub>, IC<sub>50</sub> and IC<sub>75</sub> of As, respectively. Similar findings were found in literature where less than 50% reduction in GSH was observed after 24 h exposure to 0.5 mg/L and 10 mg/L As<sub>2</sub>O<sub>3</sub> in HepG2 cells.<sup>192</sup> Although no reduction in  $\Delta\Psi_m$  was noted when cells were treated with IC<sub>25</sub> or IC<sub>50</sub> of As but the latter may explain the mitochondrial toxicity noted at high As concentrations. Although there was an absence of mitochondrial toxicity at lower concentrations, a reduction in cell density, ATP and GSH levels was displayed. A 47%, 67% and 96% reduction in GSH levels was observed in SH-SY5Y cells exposed to IC<sub>25</sub>, IC<sub>50</sub> and IC<sub>75</sub> concentrations of As, which paralleled the results obtained for cell density, ATP and  $\Delta\Psi_m$ . Caspase-3/7 increased to 159% , 126% and 132% after exposure to IC<sub>25</sub>, IC<sub>50</sub> and IC<sub>75</sub> concentration of As respectively. Caspase-3/7 activity was increased by 141%, 198% and 144% in SH-SY5Y cells when exposed to IC<sub>25</sub>, IC<sub>50</sub> and IC<sub>75</sub> concentrations of As showing biphasic effect in SH-SY5Y cells. Similar trend was found in literature where Sodium arsenite at 3.9 mg/L, was reported to induce apoptosis in human epidermoid carcinoma A431 cells and EA.hy926 cells after 24 h exposure.<sup>228</sup>

Greater cytotoxicity was noted in the HepG2 cells after Cd exposure (IC<sub>50</sub> = 0.43 mg/L) than the SH-SY5Y cells (IC<sub>50</sub> = 1.47 mg/L) in contrast to As which showed more toxicity towards SH-SY5Y cells. Slightly higher IC<sub>50</sub> values have been reported by Dehn and colleagues for HepG2 cells treated with Cd (IC<sub>50</sub> 1.1 – 1.6 mg/L).<sup>229</sup> However, both this study and the study by Dehn et al. indicate the cytotoxic nature of Cd. In other studies the IC<sub>50</sub> for Cd in HepG2 cells ranged between 0.9 mg/L and 4.7 mg/L.<sup>230-232</sup> Cadmium was found to be the most toxic among all three metals tested i.e., As, Cd and Hg. In the HepG2 cell line, a reduction of  $\Delta\Psi_m$  by 16%, 39% and 74% was noted and similar reduction in the  $\Delta\Psi_m$  was displayed when SH-SY5Y cells were treated with IC<sub>25</sub>, IC<sub>50</sub> and IC<sub>75</sub> concentrations of Cd. The decrease in  $\Delta\Psi_m$  noted would suggest that there is a direct correlation to the reduction in cell density. Cadmium has previously been reported to decrease  $\Delta\Psi_m$  in both cancerous and non-cancerous hepatic cells.<sup>236,237</sup> Cadmium decreased ATP when exposed to the IC<sub>25</sub> by 39%, by 62% at IC<sub>50</sub> and by 88% at IC<sub>75</sub>. The trend was similar to that detected for As, albeit being less toxic. The

reduction in ATP levels in SH-SY5Y cells was very high and amounted to 93%, 96% and 96% when exposed to IC<sub>25</sub>, IC<sub>50</sub> and IC<sub>75</sub> concentrations of Cd, respectively indicating necrotic cell death. In literature, similar findings were observed with Cd at 0.9 mg/L reduced ATP levels by 25, 50 and 65 % after 24 h exposure HepG2, 1321NI and HEK293 respectively.<sup>241</sup> The different levels of inhibition of ATP levels at same concentration of Cd could be due to difference in cell line. A gradual decrease in ROS was noted in the HepG2 cells as the concentration of Cd increased whereas the reduction appeared to plateau in SH-SY5Y cells. Cadmium has been reported to induce a biphasic effect on ROS generation in AS-30D cells, stimulating production at 18.3 and 92 mg/L after 3 h, however, this decreased after 24h.<sup>233</sup> The reduction in GSH levels was noted to be dose dependent in both cell lines and related to cell density as well as  $\Delta\Psi_m$  reduction at all Cd concentrations tested which is supported by literature findings.<sup>245</sup> Caspase-3/7 activity in HepG2 cells was increased by 137%, 151% and 130%, respectively when exposed to IC<sub>25</sub>, IC<sub>50</sub> and IC<sub>75</sub> concentrations of Cd. In SH-SY5Y cells, caspase-3/7 activity was increased by 217%, 284% and 234% when exposed to similar concentrations of Cd which is found in literature.<sup>112,252</sup> The increase in caspase 3/7 activity in SH-SY5Y cells was nearly double that observed in HepG2 cells at the same concentrations tested indicating apoptosis.

Mercury was more cytotoxic towards SH-SY5Y cells (IC<sub>50</sub> = 11.99 mg/L) than HepG2 cells (IC<sub>50</sub> = 26.23 mg/L). Mercury was found to be the least toxic among all three metals tested. Similar toxicity was found in literature when in PC12 adrenal pheochromocytoma cells, HgCl<sub>2</sub> was calculated to exhibit an IC<sub>25</sub> of 13.6 mg/mL after 3 h exposure,<sup>263</sup> which is higher than the IC<sub>25</sub> of 8.45 mg/mL obtained in the current study for the SH-SY5Y cells after 24 h incubation. Mercury decreased  $\Delta\Psi_m$  in HepG2 and SH-SY5Y cells in a dose dependent manner showing mitochondrial toxicity which may lead to apoptotic cell death. Methyl mercury has been shown to depolarize the mitochondrial membrane in PC12 cells<sup>263</sup> and astrocytes<sup>269</sup> which is similar to our study. The ATP concentration was almost completely inhibited in HepG2 cells at all Hg concentrations tested suggesting a necrotic cell death. Although a reduction in ATP levels was noted in SH-SY5Y cells, it was more gradual (IC<sub>25</sub> = 30%, IC<sub>50</sub> = 77%, IC<sub>75</sub> = 99%) which is also supported by literature.<sup>272</sup> The ROS was reduced in a dose-dependent manner in both HepG2 and SH-SY5Y cells, when exposed to Hg which might have resulted due to biphasic effect (after Initial increase in ROS, there is second phase of decline after 24 h) which is supported by literature.<sup>233,263</sup> . The GSH levels reduction in both cell lines was dose dependent, with

virtually total inhibition (99%) of GSH when treated with the IC<sub>75</sub> concentration of Hg. This reduction in GSH levels correlates with the reduction in cell density as well as the loss in  $\Delta\psi_m$ . Mercury 8 mg/L reduced GSH levels by 75% in HepG2 cells after 24 h exposure<sup>275</sup> which is similar to our findings. Mercury decreased caspase-3/7 in HepG2 cells from basal level at all concentrations tested. In contrast caspase-3/7 activity was increased by 320%, 181% and 327% in SH-SY5Y cells when exposed to IC<sub>25</sub>, IC<sub>50</sub> and IC<sub>75</sub> concentrations of Hg, supported by literature finding.<sup>278</sup>

Except for their dose dependent nature in causing toxicity, the metals also showed a comparable similarity in the amount of toxicity caused. A strong deviation is hardly observed when the toxicity of the three individual metals are independently observed and compared. However, this trend was not the same when the toxicity of the combination of metal mixtures was tested on each parameter.

After exposure to the IC<sub>20</sub>, IC<sub>25</sub> and IC<sub>35</sub> mixtures, cell density was almost completely reduced in both cell lines. The reduction in cell density was far greater than that observed for any of the single metals alone, which may imply that combinational activity increases the cytotoxicity. After exposure to the EPA mixture, cell density was reduced by 45% at 0.5 mg/L reference concentration of As in HepG2 cells. This is a much higher reduction than the single compounds when tested at similar or even higher concentrations than the EPA mixture. The EPA mixture of 4 mg/mL (with respect to As) reduced cell density by 93% which is less than individual metal reduction at similar concentrations. At 0.5 mg/L reference concentration of As in EPA mixture, reduction in cell density was similar to individual toxicity of As, Cd and Hg in SH-SY5Y cells. A similar trend was noted in SH-SY5Y cells, whereas higher concentrations of the EPA mixture than that of HepG2 cells occurred, suggesting an antagonistic effect. Combinations of metal mixtures displayed greater mitochondrial toxicity than the individual metals alone. The effects were most prominent in the HepG2 cell line. Given the cell density results, it appears that mitochondrial toxicity contributes to the effects seen. However, the increased depolarisation up to the IC<sub>75</sub> did not alter the level of cell density reduction observed at lower concentrations. Both the cell lines were very sensitive to metal mixture, almost completely inhibiting ATP levels indicating cell death from apoptotic to necrotic pathways. The toxicity of the mixture in both cell lines paralleled the cell density and mitochondrial damage noted.

In HepG2 cells, ROS was reduced by 74%, 84% and 85% at the IC<sub>20</sub>, IC<sub>25</sub> and IC<sub>35</sub>, respectively. In the SH-SY5Y cell line, ROS was reduced by 77%, 80% and 81%, respectively. This reduction in ROS levels after exposure to the metal mixtures can be explained by the biphasic effect of Cd and Hg on different cell lines; AS-30D cells,<sup>233</sup> foetal lung fibroblasts<sup>243</sup> PC12 cells,<sup>221</sup> where an increase in ROS is initially found followed by a profound decrease after 24 h. The IC combinations abolished GSH levels completely in hepatoma and neuronal cells. All the EPA combinations reduced GSH levels in dose dependent manner which is parallel to cell density,  $\Delta\psi_m$  and ATP levels. A profound increase (172%) in caspase-3/7 activity was noticed when HepG2 cells were treated with the EPA mixture with respect to As 0.5 mg/L. An even higher increase in caspase 3/7 activity was noted when the cells were exposed to 4mg/L EPA mixture concentration with respect to As (505%) suggesting some combinational effect.

The effects of two experimental metal mixtures of As, Cd and Hg (EPA mixture and IC mixture) on the different parameters (cell density, mitochondrial membrane potential, glutathione levels), were more prominent than those of any individual metal. Understanding how metal mixtures affect health is critical to determine treatment strategies. Although *in vitro* experiments shed light on the cellular pathways leading to cell death after exposure to metal mixtures, further assessment of biological pathways and their relation to the *in vivo* environment is needed.

## Chapter 5

### Conclusion

---

This study examined the toxic effects of heavy metals (As, Cd, and Hg) individually and in combination on HepG2 hepatocarcinoma and SH-SY5Y neuroblastoma cell lines. In conclusion, both single compounds and metal mixtures have potential for cytotoxicity. Single compounds like As and Hg showed greater toxicity in cells of neural origin compared to Cd that showed higher toxicity in HepG2 cells. Mitochondrial toxicity and ATP inhibition was significant when cells were exposed to As, Cd and Hg which is indicative of shifting cell death mechanism from apoptotic to necrotic cell death. Almost complete inhibition of GSH levels was observed for all three metals and their combinations, showing marked depletion of antioxidant stores of cells. Caspase-3/7 activity was increased for all the metals indicating apoptotic cell death pathways except for Hg where it decreased below basal level. Overall, Cd was found to be the most toxic among all three metals tested while Hg induced toxicity at relatively higher concentration in both cell lines.

The increased reduction in cell density in the presence of EPA mixture compared to single compounds suggest that compounds may act upon one another to increase toxic potential of individual metals. However, reduced cytotoxicity after exposure to higher concentrations of EPA mixture might be due to an antagonistic effect when compared to these individual metals. It can also be proposed that apoptotic and necrotic pathways prompted cell death due to mitochondrial damage and inhibition of ATP levels. A profound increase in caspase-3/7 activity was determined for EPA mixture indicating apoptotic pathways in both cells. The increased toxicity potential of metal mixtures warrants the use of *in vivo* models to fully elucidate toxicity mechanisms and their interactions which lead to cell death.



## Chapter 6

### Limitations of study and recommendations

---

The first and one of the major limitations is that studies and results were based on a sample of cells in laboratories. No animal or organ model were used for the experiments. Considering the complex nature of live biological systems, experiments done under artificial conditions may not give an exact idea of how the same substance (in this case, heavy metals) may react in a “true” system. Also, a biological system is associated with a lot of volatile phenomena which may exist in a particular body type and may hardly show signs in another. Pharmacogenomic properties of a particular organism also play a hard wired role in processing of foreign materials and were missing in this study.

In a human body, with such complex organ systems and tissues, experiments on only two cancerous cell lines is insufficient to deduce any important details about heavy metals effect on overall body or organ system. Although it is true that the liver and brain are main target organs of heavy metals in human; this study gives important points on hepatic and neural cells while totally ignoring the other cell lines and tissues in the organism system. Also using primary cell lines would better simulate processes in human body.

Heavy metals were tested after 24 h incubation in our project and results cannot address chronic toxicity of metals. Most of the heavy metals including As, Cd and Hg have very long half-life in human and their toxicity occurs after long term exposure.

Only three metals were tested in this study, but there is a possibility of simultaneous exposure to more heavy metals and at different ratios and concentrations which makes it very difficult to simulate environmental exposure.

Arsenic, Cd and Hg occur naturally in various organic and inorganic forms/states and their toxicity may differ from each other. Only the most common and prevalent salts were selected but other abundant forms of these metals might exert toxicity through different mechanism and to a different extent.

Another limitation was paucity of data that could be used for comparison for our combinations (IC and EPA mixtures). Only a few studies have been conducted with different combinations; mostly binary mixtures.

It is recommended that using an animal model would better help to understand the underlying toxicity mechanisms. Also, it could be advantageous if both acute and chronic studies are conducted in animal models and compared to simulate heavy metal toxicity in humans.

## References

1. Tchounwou, P. B.; Yedjou, C. G.; Patlolla, A. K.; Sutton, D. J. Heavy metal toxicity and the environment. In *Molecular, Clinical and Environmental Toxicology*, Springer: **2012**; pp 133-164.
2. Mellett, T.; Brown, M. T.; Chappell, P. D.; Duckham, C.; Fitzsimmons, J. N.; Till, C. P.; Sherrell, R. M.; Maldonado, M. T.; Buck, K. N. The biogeochemical cycling of iron, copper, nickel, cadmium, manganese, cobalt, lead, and scandium in a California Current experimental study. *Limnology and Oceanography* **2018**, 63, S425-S447.
3. Singh, R.; Gautam, N.; Mishra, A.; Gupta, R. Heavy metals and living systems: An overview. *Indian Journal of Pharmacology* **2011**, 43, 246-253.
4. Järup, L. Hazards of heavy metal contamination. *British Medical Bulletin* **2003**, 68, 167-182.
5. Tilley, S. K.; Fry, R. C. Priority Environmental Contaminants: Understanding Their Sources of Exposure, Biological Mechanisms, and Impacts on Health. In *Systems Biology in Toxicology and Environmental Health*, Fry, R. C., Ed. Elsevier: Amsterdam **2015**.
6. ATSDR Agency of Toxic Substances and Disease Registry. The ATSDR 2017 Substance Priority List. <https://www.atsdr.cdc.gov/spl/> (10 August, **2017**).
7. Jan, A. T.; Azam, M.; Siddiqui, K.; Ali, A.; Choi, I.; Haq, Q. M. R. Heavy Metals and Human Health: Mechanistic Insight into Toxicity and Counter Defense System of Antioxidants. *International Journal of Molecular Sciences* **2015**, 16, 29592-29630.
8. E. F. S. A. Scientific Opinion on Arsenic in Food. EFSA Panel on Contaminants in the Food Chain (CONTAM). *European Food Safety Authority Journal* **2009**, 7, 1351-1550.
9. Smedley, P. L.; Kinniburgh, D. G. United Nations Synthesis Report on Arsenic in Drinking-Water. *British Geological Survey* **2001**, 1-61.
10. Hirano, S.; Kobayashi, Y.; Cui, X.; Kanno, S.; Hayakawa, T.; Shraim, A. The accumulation and toxicity of methylated arsenicals in endothelial cells: important roles of thiol compounds. *Toxicology and Applied Pharmacology* **2004**, 198, 458-467.
11. Datta, R.; Sarkar, D. Consideration of soil properties in assessment of human health risk from exposure to arsenic-enriched soils. *Integrated Environmental Assessment and Management* **2005**, 1, 55-59.
12. Quazi, S.; Sarkar, D.; Datta, R. Human health risk from arsenical pesticide contaminated soils: A long-term greenhouse study. *Journal of Hazardous Materials* **2013**, 262, 1031-1038.
13. Agency, U. E. P. Maximum contaminant levels. [https://www.epa.gov/sites/production/files/2016-06/documents/npwdr\\_complete\\_table.pdf](https://www.epa.gov/sites/production/files/2016-06/documents/npwdr_complete_table.pdf) (24 June **2018**).
14. Smith, A. H.; Goycolea, M.; Haque, R.; Biggs, M. L. Marked increase in bladder and lung cancer mortality in a region of Northern Chile due to arsenic in drinking water. *American Journal of Epidemiology* **1998**, 147, 660-669.
15. Mazumder, D. N. G.; Haque, R.; Ghosh, N.; De Binay, K.; Santra, A.; Chakraborty, D.; Smith, A. H. Arsenic levels in drinking water and the prevalence of skin lesions in West Bengal, India. *International Journal of Epidemiology* **1998**, 27, 871-877.
16. Del Razo, L.; Arellano, M.; Cebrián, M. E. The oxidation states of arsenic in well-water from a chronic arsenicism area of northern Mexico. *Environmental Pollution* **1990**, 64, 143-153.
17. Rodríguez-Lado, L.; Sun, G.; Berg, M.; Zhang, Q.; Xue, H.; Zheng, Q.; Johnson, C. A. Groundwater arsenic contamination throughout China. *Science* **2013**, 341, 866-868.
18. Yager, J. W.; Greene, T.; Schoof, R. A. Arsenic relative bioavailability from diet and airborne exposures: Implications for risk assessment. *Science of the Total Environment* **2015**, 536, 368-381.
19. Zheng, Y.; Wu, J.; Ng, J. C.; Wang, G.; Lian, W. The absorption and excretion of fluoride and arsenic in humans. *Toxicology Letters* **2002**, 133, 77-82.
20. Sharma, B.; Singh, S.; Siddiqi, N. J. Biomedical implications of heavy metals induced imbalances in redox systems. *BioMed Research International* **2014**, 2014, 1-26.

21. Zhang, Z.; Pratheeshkumar, P.; Budhraj, A.; Son, Y.-O.; Kim, D.; Shi, X. Role of reactive oxygen species in arsenic-induced transformation of human lung bronchial epithelial (BEAS-2B) cells. *Biochemical and Biophysical Research Communications* **2015**, 456, 643-648.
22. Speisky, H.; Gómez, M.; Carrasco-Pozo, C.; Pastene, E.; Lopez-Alarcón, C.; Olea-Azar, C. Cu (I)–Glutathione complex: A potential source of superoxide radicals generation. *Bioorganic & Medicinal Chemistry* **2008**, 16, 6568-6574.
23. Sinicropi, M. S.; Amantea, D.; Caruso, A.; Saturnino, C. Chemical and biological properties of toxic metals and use of chelating agents for the pharmacological treatment of metal poisoning. *Archives of Toxicology* **2010**, 84, 501-520.
24. Hughes, M. Arsenic toxicity and potential mechanisms of action *Toxicology Letters* **2002**, 133, 1–16.
25. Yager, J. W.; Wiencke, J. K. Inhibition of poly (ADP-ribose) polymerase by arsenite. *Mutation Research/Reviews in Mutation Research* **1997**, 386, 345-351.
26. Bertolero, F.; Pozzi, G.; Sabbioni, E.; Saffiotti, U. Cellular uptake and metabolic reduction of pentavalent to trivalent arsenic as determinants of cytotoxicity and morphological transformation. *Carcinogenesis* **1987**, 8, 803-808.
27. Chen, C.-J.; Hsueh, Y.-M.; Lai, M.-S.; Shyu, M.-P.; Chen, S.-Y.; Wu, M.-M.; Kuo, T.-L.; Tai, T.-Y. Increased prevalence of hypertension and long-term arsenic exposure. *Hypertension* **1995**, 25, 53-60.
28. Engel, R. R.; Hopenhayn-Rich, C.; Receveur, O.; Smith, A. H. Vascular effects of chronic arsenic exposure: a review. *Epidemiologic Reviews* **1994**, 16, 184-209.
29. Tseng, W.-P. Effects and dose-response relationships of skin cancer and blackfoot disease with arsenic. *Environmental Health Perspectives* **1977**, 19, 109-119.
30. Humans, I. W. G. o. t. E. o. C. R. t. Some drinking-water disinfectants and contaminants, including arsenic. Monographs on chloramine, chloral and chloral hydrate, dichloroacetic acid, trichloroacetic acid and 3-chloro-4-(dichloromethyl)-5-hydroxy-2(5H)-furanone. *IARC Monographs on the Evaluation of Carcinogenic Risks to Humans* **2004**, 84, 269-477.
31. Martinez, V. D.; Vucic, E. A.; Becker-Santos, D. D.; Gil, L.; Lam, W. L. Arsenic exposure and the induction of human cancers. *Journal of Toxicology* **2011**, 2011, 428-440.
32. Mead, M. N. Arsenic: in search of an antidote to a global poison. *Environmental Health Perspectives* **2005**, 113, A378-86.
33. Smith, A. H.; Hopenhayn-Rich, C.; Bates, M. N.; Goeden, H. M.; Hertz-Picciotto, I.; Duggan, H. M.; Wood, R.; Kosnett, M. J.; Smith, M. T. Cancer risks from arsenic in drinking water. *Environmental Health Perspectives* **1992**, 97, 259-267.
34. Argos, M.; Kalra, T.; Pierce, B. L.; Chen, Y.; Parvez, F.; Islam, T.; Ahmed, A.; Hasan, R.; Hasan, K.; Sarwar, G. A prospective study of arsenic exposure from drinking water and incidence of skin lesions in Bangladesh. *American Journal of Epidemiology* **2011**, 174, 185-194.
35. Chen, Y.; Wu, F.; Liu, M.; Parvez, F.; Slavkovich, V.; Eunos, M.; Alauddin, A.; Argos, M.; Islam, T.; Rakibuz-Zaman, M. A prospective study of arsenic exposure, arsenic methylation capacity, and risk of cardiovascular disease in Bangladesh. *Environmental Health Perspectives* **2013**, 121, 832-838.
36. Tsuji, J. S.; Perez, V.; Garry, M. R.; Alexander, D. D. Association of low-level arsenic exposure in drinking water with cardiovascular disease: A systematic review and risk assessment. *Toxicology* **2014**, 323, 78-94.
37. Wang, W.; Xie, Z.; Lin, Y.; Zhang, D. Association of inorganic arsenic exposure with type 2 diabetes mellitus: a meta-analysis. *Journal of Epidemiology and Community Health* **2013**, 68, 176-184.
38. Smith, A. H.; Lingas, E. O.; Rahman, M. Contamination of drinking-water by arsenic in Bangladesh: a public health emergency. *Bulletin of the World Health Organization* **2000**, 78, 1093-1103.
39. Marshall, G.; Ferreccio, C.; Yuan, Y.; Bates, M. N.; Steinmaus, C.; Selvin, S.; Liaw, J.; Smith, A. H. Fifty-year study of lung and bladder cancer mortality in Chile related to arsenic in drinking water. *Journal of the National Cancer Institute* **2007**, 99, 920-928.

40. Quansah, R.; Armah, F. A.; Essumang, D. K.; Luginaah, I.; Clarke, E.; Marfoh, K.; Cobbina, S. J.; Nketiah-Amponsah, E.; Namujju, P. B.; Obiri, S. Association of arsenic with adverse pregnancy outcomes/infant mortality: A systematic review and meta-analysis. *Environmental Health Perspectives* **2015**, *123*, 412-421.
41. Hamadani, J.; Tofail, F.; Nermell, B.; Gardner, R.; Shiraji, S.; Bottai, M.; Arifeen, S.; Huda, S. N.; Vahter, M. Critical windows of exposure for arsenic-associated impairment of cognitive function in pre-school girls and boys: a population-based cohort study. *International Journal of Epidemiology* **2011**, *40*, 1593-1604.
42. Tseng, C.-H. Blackfoot disease and arsenic: a never-ending story. *Journal of Environmental Science and Health* **2005**, *23*, 55-74.
43. Ratnaike, R. N. Acute and chronic arsenic toxicity. *Postgraduate Medical Journal* **2003**, *79*, 391-396.
44. Buchet, J.-P.; Lauwerys, R.; Roels, H. Comparison of the urinary excretion of arsenic metabolites after a single oral dose of sodium arsenite, monomethylarsonate, or dimethylarsinate in man. *International Archives of Occupational and Environmental Health* **1981**, *48*, 71-79.
45. Kalia, K.; Flora, S. J. Strategies for safe and effective therapeutic measures for chronic arsenic and lead poisoning. *Journal of Occupational Health* **2005**, *47*, 1-21.
46. Bhattacharjee, S.; Sarkar, C.; Pal, S. Additive beneficial effect of folic acid and vitamin B12 co-administration on arsenic-induced oxidative damage in cardiac tissue in vivo. *Asian Journal of Pharmaceutical and Clinical Research* **2013**, *6*, 64-69.
47. Muntau, H.; Baudo, R. Sources of cadmium, its distribution and turnover in the freshwater environment. *IARC Scientific Publications* **1991**, 133-148.
48. Kasuya, M.; Teranishi, H.; Aoshima, K.; Katoh, T.; Horiguchi, H.; Morikawa, Y.; Nishijo, M.; Iwata, K. Water pollution by cadmium and the onset of Itai-itai disease. *Water Science and Technology* **1992**, *25*, 149-156.
49. Järup, L.; Åkesson, A. Current status of cadmium as an environmental health problem. *Toxicology and Applied Pharmacology* **2009**, *238*, 201-208.
50. Daud, M.; Sun, Y.; Dawood, M.; Hayat, Y.; Variath, M.; Wu, Y.-X.; Mishkat, U.; Najeeb, U.; Zhu, S. Cadmium-induced functional and ultrastructural alterations in roots of two transgenic cotton cultivars. *Journal of Hazardous Materials* **2009**, *161*, 463-473.
51. Liu, X.; Jin, T.; Nordberg, G.; Rännar, S.; Sjöström, M.; Zhou, Y. A multivariate study of protective effects of Zn and Cu against nephrotoxicity induced by cadmium metallothionein in rats. *Toxicology and Applied Pharmacology* **1992**, *114*, 239-245.
52. Nordberg, G.; Fowler, B.; Nordberg, M.; Friberg, L. *Handbook on the toxicology of metals, 3rd edn. Academic, Boston*; ISBN 978-0-12-369413-3: 2007.
53. Akerstrom, M.; Barregard, L.; Lundh, T.; Sallsten, G. The relationship between cadmium in kidney and cadmium in urine and blood in an environmentally exposed population. *Toxicology and Applied Pharmacology* **2013**, *268*, 286-293.
54. Järup, L.; Rogenfelt, A.; Elinder, C.-G.; Nogawa, K.; Kjellström, T. Biological half-time of cadmium in the blood of workers after cessation of exposure. *Scandinavian Journal of Work, Environment & Health* **1983**, *9*, 327-331.
55. Liu, F.; Jan, K.-Y. DNA damage in arsenite- and cadmium-treated bovine aortic endothelial cells. *Free Radical Biology and Medicine* **2000**, *28*, 55-63.
56. Oh, S.-H.; Lim, S.-C. A rapid and transient ROS generation by cadmium triggers apoptosis via caspase-dependent pathway in HepG2 cells and this is inhibited through N-acetylcysteine-mediated catalase upregulation. *Toxicology and Applied Pharmacology* **2006**, *212*, 212-223.
57. Järup, L.; Berglund, M.; Elinder, C. G.; Nordberg, G.; Vanter, M. Health effects of cadmium exposure—a review of the literature and a risk estimate. *Scandinavian Journal of Work, Environment & Health* **1998**, *24*, 1-51.

58. Jin, T.; Lu, J.; Nordberg, M. Toxicokinetics and biochemistry of cadmium with special emphasis on the role of metallothionein. *Neurotoxicology* **1997**, *19*, 529-535.
59. Skipper, A.; Sims, J. N.; Yedjou, C. G.; Tchounwou, P. B. Cadmium Chloride Induces DNA Damage and Apoptosis of Human Liver Carcinoma Cells via Oxidative Stress. *International Journal of Environmental Research and Public Health* **2016**, *13*, 88-97.
60. Liang, Y.; Lei, L.; Nilsson, J.; Li, H.; Nordberg, M.; Bernard, A.; Nordberg, G. F.; Bergdahl, I. A.; Jin, T. Renal function after reduction in cadmium exposure: an 8-year follow-up of residents in cadmium-polluted areas. *Environmental Health Perspectives* **2012**, *120*, 223-228.
61. Åkesson, A.; Barregard, L.; Bergdahl, I. A.; Nordberg, G. F.; Nordberg, M.; Skerfving, S. Non-renal effects and the risk assessment of environmental cadmium exposure. *Environmental Health Perspectives* **2014**, *122*, 431-438.
62. Chen, L.; Jin, T.; Huang, B.; Nordberg, G.; Nordberg, M. Critical exposure level of cadmium for elevated urinary metallothionein—an occupational population study in China. *Toxicology and Applied Pharmacology* **2006**, *215*, 93-99.
63. Ferraro, P. M.; Costanzi, S.; Naticchia, A.; Sturniolo, A.; Gambaro, G. Low level exposure to cadmium increases the risk of chronic kidney disease: analysis of the NHANES 1999-2006. *BMC Public Health* **2010**, *10*, 304-311.
64. Kim, S. D.; Moon, C. K.; Eun, S.-Y.; Ryu, P. D.; Jo, S. A. Identification of ASK1, MKK4, JNK, c-Jun, and caspase-3 as a signaling cascade involved in cadmium-induced neuronal cell apoptosis. *Biochemical and Biophysical Research Communications* **2005**, *328*, 326-334.
65. Monroe, R. K.; Halvorsen, S. W. Cadmium blocks receptor-mediated Jak/STAT signaling in neurons by oxidative stress. *Free Radical Biology and Medicine* **2006**, *41*, 493-502.
66. Okuda, B.; Iwamoto, Y.; Tachibana, H.; Sugita, M. Parkinsonism after acute cadmium poisoning. *Clinical Neurology and Neurosurgery* **1997**, *99*, 263-265.
67. Jiang, L.-F.; Yao, T.-M.; Zhu, Z.-L.; Wang, C.; Ji, L.-N. Impacts of Cd (II) on the conformation and self-aggregation of Alzheimer's tau fragment corresponding to the third repeat of microtubule-binding domain. *Biochimica et Biophysica Acta (BBA)-Proteins and Proteomics* **2007**, *1774*, 1414-1421.
68. Ishitobi, H.; Mori, K.; Yoshida, K.; Watanabe, C. Effects of perinatal exposure to low-dose cadmium on thyroid hormone-related and sex hormone receptor gene expressions in brain of offspring. *Neurotoxicology* **2007**, *28*, 790-797.
69. IARC Monographs on the evaluation of carcinogen risks to humans. <http://monographs.iarc.fr/ENG/Monographs/vol58/index.php> (20 September **2018**).
70. Adams, S. V.; Newcomb, P. A.; Shafer, M. M.; Atkinson, C.; Bowles, E. J. A.; Newton, K. M.; Lampe, J. W. Urinary cadmium and mammographic density in premenopausal women. *Breast Cancer Research and Treatment* **2011**, *128*, 837-844.
71. Sauer, J.-M.; Waalkes, M. P.; Hooser, S. B.; Kuester, R. K.; McQueen, C. A.; Sipes, I. G. Suppression of Kupffer cell function prevents cadmium induced hepatocellular necrosis in the male Sprague-Dawley rat. *Toxicology* **1997**, *121*, 155-164.
72. Srivastava, S.; Goyal, P. Detoxification of Metals—Biochelation. In *Novel Biomaterials*, Springer: **2010**; pp 11-20.
73. Lamborg, C. H.; Fitzgerald, W. F.; O'Donnell, J.; Torgersen, T. A non-steady-state compartmental model of global-scale mercury biogeochemistry with interhemispheric atmospheric gradients. *Geochimica et Cosmochimica Acta* **2002**, *66*, 1105-1118.
74. Pacyna, E. G.; Pacyna, J.; Sundseth, K.; Munthe, J.; Kindbom, K.; Wilson, S.; Steenhuisen, F.; Maxson, P. Global emission of mercury to the atmosphere from anthropogenic sources in 2005 and projections to 2020. *Atmospheric Environment* **2010**, *44*, 2487-2499.
75. Tchounwou, P. B.; Ayensu, W. K.; Ninashvili, N.; Sutton, D. Review: Environmental exposure to mercury and its toxicopathologic implications for public health. *Environmental Toxicology* **2003**, *18*, 149-175.

76. Asano, S.; Eto, K.; Kurisaki, E.; Gunji, H.; Hiraiwa, K.; Sato, M.; Sato, H.; Hasuike, M.; Hagiwara, N.; Wakasa, H. Acute inorganic mercury vapor inhalation poisoning. *Pathology International* **2000**, *50*, 169-174.
77. Dourson, M. L.; Wullenweber, A. E.; Poirier, K. A. Uncertainties in the reference dose for methylmercury. *Neurotoxicology* **2001**, *22*, 677-689.
78. Mostafalou, S.; Abdollahi, M. Environmental pollution by mercury and related health concerns: renotice of a silent threat. *Archives of Industrial Hygiene and Toxicology* **2013**, *64*, 179-181.
79. Lim, H. E.; Shim, J. J.; Lee, S. Y.; Lee, S. H.; Kang, S. Y.; Jo, J. Y.; In, K. H.; Kim, H. G.; Yoo, S. H.; Kang, K. H. Mercury inhalation poisoning and acute lung injury. *The Korean Journal of Internal Medicine* **1998**, *13*, 127-130.
80. Risher, J. F.; Murray, H. E.; Prince, G. R. Organic mercury compounds: human exposure and its relevance to public health. *Toxicology and Industrial Health* **2002**, *18*, 109-160.
81. Pfab, R.; Mückter, H.; Roeder, G.; Zilker, T. Clinical course of severe poisoning with thiomersal. *Journal of Toxicology* **1996**, *34*, 453-460.
82. Goyer, R.; Aposhian, V.; Arab, L.; Bellinger, D.; Burbacher, T.; Burke, T.; Jacobson, J.; Knobeloch, L.; Stern, A.; Ryan, L. Toxicological effects of methylmercury. *Washington, DC: National Research Council* **2000**.
83. Park, J.-D.; Zheng, W. Human exposure and health effects of inorganic and elemental mercury. *Journal of Preventive Medicine and Public Health* **2012**, *45*, 344-352.
84. Oskarsson, A.; Schütz, A.; Skerfving, S.; Hallén, I. P.; Ohlin, B.; Lagerkvist, B. J. Total and inorganic mercury in breast milk and blood in relation to fish consumption and amalgam fillings in lactating women. *Archives of Environmental Health* **1996**, *51*, 234-241.
85. Vallee, B. L.; Ulmer, D. D. Biochemical effects of mercury, cadmium, and lead. *Annual Review of Biochemistry* **1972**, *41*, 91-128.
86. Guzzi, G.; La Porta, C. A. Molecular mechanisms triggered by mercury. *Toxicology* **2008**, *244*, 1-12.
87. Vas, J.; Monestier, M. Immunology of mercury. *Annals of the New York Academy of Sciences* **2008**, *1143*, 240-267.
88. Klaassen, C. D. *Casarett and Doull's toxicology: the basic science of poisons*. McGraw-Hill New York (NY): 2013; Vol. 1236.
89. Zalups, R. K. Molecular interactions with mercury in the kidney. *Pharmacological Reviews* **2000**, *52*, 113-144.
90. Rafati-Rahimzadeh, M.; Rafati-Rahimzadeh, M.; Kazemi, S.; Moghadamnia, A. A. Current approaches of the management of mercury poisoning: need of the hour. *DARU Journal of Pharmaceutical Sciences* **2014**, *22*, 1 - 10.
91. Vroom, F. Q.; Greer, M. Mercury vapour intoxication. *Brain* **1972**, *95*, 305-318.
92. Weiss, B.; Clarkson, T. W.; Simon, W. Silent latency periods in methylmercury poisoning and in neurodegenerative disease. *Environmental Health Perspectives* **2002**, *110*, 851.
93. Graeme, K. A.; Pollack, C. V. Heavy metal toxicity, part I: arsenic and mercury. *The Journal of Emergency Medicine* **1998**, *16*, 45-56.
94. Bernhoft, R. A. Mercury toxicity and treatment: a review of the literature. *Journal of Environmental and Public Health* **2011**, *2012*, 1-10.
95. Brent, J.; Burkhardt, K.; Dargan, P. Critical care toxicology: Diagnosis and management of the critically poisoned patient, *2nd edn*. ISBN 0815143877: **2005**, 931.
96. Flora, S. J.; Pachauri, V. Chelation in metal intoxication. *International Journal of Environmental Research and Public Health* **2010**, *7*, 2745-2788.
97. Russi, G.; Marson, P. Urgent plasma exchange: how, where and when. *Blood Transfusion* **2011**, *9*, 356-361.

98. Salisbury, C.; Chan, W.; Saschenbrecker, P. W. Multielement concentrations in liver and kidney tissues from five species of Canadian slaughter animals. *Journal-Association of Official Analytical Chemists* **1991**, *74*, 587-591.
99. Rossman, T. G. Mechanism of arsenic carcinogenesis: an integrated approach. *Mutation Research/Fundamental and Molecular Mechanisms of Mutagenesis* **2003**, *533*, 37-65.
100. Liu, J.; Chen, H.; Miller, D. S.; Saavedra, J. E.; Keefer, L. K.; Johnson, D. R.; Klaassen, C. D.; Waalkes, M. P. Overexpression of glutathione S-transferase II and multidrug resistance transport proteins is associated with acquired tolerance to inorganic arsenic. *Molecular Pharmacology* **2001**, *60*, 302-309.
101. Jomova, K.; Jenisova, Z.; Feszterova, M.; Baros, S.; Liska, J.; Hudecova, D.; Rhodes, C.; Valko, M. Arsenic: toxicity, oxidative stress and human disease. *Journal of Applied Toxicology* **2011**, *31*, 95-107.
102. Liu, J.; Liu, Y.; Powell, D. A.; Waalkes, M. P.; Klaassen, C. D. Multidrug-resistance *mdr1a/1b* double knockout mice are more sensitive than wild type mice to acute arsenic toxicity, with higher arsenic accumulation in tissues. *Toxicology* **2002**, *170*, 55-62.
103. Mazumder, D. G. Effect of chronic intake of arsenic-contaminated water on liver. *Toxicology and Applied Pharmacology* **2005**, *206*, 169-175.
104. Waalkes, M. P. Cadmium carcinogenesis in review. *Journal of Inorganic Biochemistry* **2000**, *79*, 241-244.
105. Rice, K. M.; Walker Jr, E. M.; Wu, M.; Gillette, C.; Blough, E. R. Environmental mercury and its toxic effects. *Journal of Preventive Medicine and Public Health* **2014**, *47*, 74.
106. Vahidnia, A.; Van der Voet, G.; De Wolff, F. Arsenic neurotoxicity—a review. *Human & Experimental Toxicology* **2007**, *26*, 823-832.
107. Tsai, S.-Y.; Chou, H.-Y.; Chen, C.-M.; Chen, C.-J. The effects of chronic arsenic exposure from drinking water on the neurobehavioral development in adolescence. *Neurotoxicology* **2003**, *24*, 747-753.
108. Bartolome, B.; Cordoba, S.; Nieto, S.; Fernández-Herrera, J.; García-Díez, A. Acute arsenic poisoning: clinical and histopathological features. *British Journal of Dermatology* **1999**, *141*, 1106-1109.
109. Chakraborti, D.; Mukherjee, S. C.; Pati, S.; Sengupta, M. K.; Rahman, M. M.; Chowdhury, U. K.; Lodh, D.; Chanda, C. R.; Chakraborti, A. K.; Basu, G. K. Arsenic groundwater contamination in Middle Ganga Plain, Bihar, India: a future danger? *Environmental Health Perspectives* **2003**, *111*, 1194.
110. Goebel, H. H.; Schmidt, P. F.; Bohl, J.; Tettenborn, B.; Krämer, G.; Gutmann, L. Polyneuropathy due to acute arsenic intoxication: biopsy studies. *Journal of Neuropathology and Experimental Neurology* **1990**, *49*, 137-149.
111. Bartlett, K.; Eaton, S. Mitochondrial  $\beta$ -oxidation. *European Journal of Biochemistry* **2004**, *271*, 462-469.
112. Habeebu, S. S.; Liu, J.; Klaassen, C. D. Cadmium-induced apoptosis in mouse liver. *Toxicology and Applied Pharmacology* **1998**, *149*, 203-209.
113. Lopez, E.; Figueroa, S.; Oset-Gasque, M.; Gonzalez, M. Apoptosis and necrosis: two distinct events induced by cadmium in cortical neurons in culture. *British Journal of Pharmacology* **2003**, *138*, 901-911.
114. Cao, Y.; Chen, A.; Radcliffe, J.; Dietrich, K. N.; Jones, R. L.; Caldwell, K.; Rogan, W. J. Postnatal cadmium exposure, neurodevelopment, and blood pressure in children at 2, 5, and 7 years of age. *Environmental Health Perspectives* **2009**, *117*, 1580.
115. Pihl, R.; Parkes, M. Hair element content in learning disabled children. *Science* **1977**, *198*, 204-206.
116. Zahir, F.; Rizwi, S. J.; Haq, S. K.; Khan, R. H. Low dose mercury toxicity and human health. *Environmental Toxicology and Pharmacology* **2005**, *20*, 351-360.
117. Satoh, H. Occupational and environmental toxicology of mercury and its compounds. *Industrial Health* **2000**, *38*, 153-164.
118. Ninomiya, T.; Ohmori, H.; Hashimoto, K.; Tsuruta, K.; Ekino, S. Expansion of methylmercury poisoning outside of Minamata: an epidemiological study on chronic methylmercury poisoning outside of Minamata. *Environmental Research* **1995**, *70*, 47-50.



119. He, Z. L.; Yang, X. E.; Stoffella, P. J. Trace elements in agroecosystems and impacts on the environment. *Journal of Trace Elements in Medicine and Biology* **2005**, *19*, 125-140.
120. Hu, H.; Shine, J.; Wright, R. O. The challenge posed to children's health by mixtures of toxic waste: the Tar Creek superfund site as a case-study. *Pediatric Clinics of North America* **2007**, *54*, 155-175.
121. Sexton, K.; Adgate, J. L.; Fredrickson, A. L.; Ryan, A. D.; Needham, L. L.; Ashley, D. L. Using biologic markers in blood to assess exposure to multiple environmental chemicals for inner-city children 3-6 years of age. *Environmental Health Perspectives* **2006**, *114*, 453-459.
122. Nordstrom, D. K. Worldwide occurrences of arsenic in ground water. *Science(Washington)* **2002**, *296*, 2143-2145.
123. Dudka, S.; Adriano, D. C. Environmental impacts of metal ore mining and processing: a review. *Journal of Environmental Quality* **1997**, *26*, 590-602.
124. Buchauer, M. J. Contamination of soil and vegetation near a zinc smelter by zinc, cadmium, copper, and lead. *Environmental Science & Technology* **1973**, *7*, 131-135.
125. Cope, W. G. Exposure Classes, Toxicants in Air, Water, Soil, Domestic and Occupational Settings. In *A Textbook of Modern Toxicology*, Hodgson, E., Ed. Wiley Online Library: 2004; p 33.
126. Bosch, A. C.; O'Neill, B.; Sigge, G. O.; Kerwath, S. E.; Hoffman, L. C. Heavy metal accumulation and toxicity in smoothhound (*Mustelus mustelus*) shark from Langebaan Lagoon, South Africa. *Food Chemistry* **2016**, *190*, 871-878.
127. Fatoki, O.; Awofolu, R. Levels of Cd, Hg and Zn in some surface waters from the Eastern Cape Province, South Africa. *Water SA* **2003**, *29*, 375-380.
128. Street, R.; Kulkarni, M.; Stirk, W.; Southway, C.; Van Staden, J. Variation in heavy metals and microelements in South African medicinal plants obtained from street markets. *Food Additives and Contaminants* **2008**, *25*, 953-960.
129. Woimant, F.; Trocello, J.-M. Disorders of heavy metals. In *Handbook of clinical neurology*, Elsevier: 2014; Vol. 120, pp 851-864.
130. Gennings, C.; Carrico, C.; Factor-Litvak, P.; Krigbaum, N.; Cirillo, P. M.; Cohn, B. A. A Cohort study evaluation of maternal PCB exposure related to time to pregnancy in daughters. *Environmental Health* **2013**, *12*, 66-77.
131. Bobb, J. F.; Valeri, L.; Henn, B. C.; Christiani, D. C.; Wright, R. O.; Mazumdar, M.; Godleski, J. J.; Coull, B. A. Bayesian kernel machine regression for estimating the health effects of multi-pollutant mixtures. *Biostatistics* **2015**, *16*, 493-508.
132. Carlin, D. J.; Rider, C. V.; Woychik, R.; Birnbaum, L. S. Unraveling the health effects of environmental mixtures: an NIEHS priority. *Environmental Health Perspectives* **2013**, *121*, A6-8.
133. Koedrith, P.; Seo, Y. R. Advances in carcinogenic metal toxicity and potential molecular markers. *International Journal of Molecular Sciences* **2011**, *12*, 9576-9595.
134. Lee, J.-C.; Son, Y.-O.; Pratheeshkumar, P.; Shi, X. Oxidative stress and metal carcinogenesis. *Free Radical Biology and Medicine* **2012**, *53*, 742-757.
135. Sala, G. L.; Ronzitti, G.; Sasaki, M.; Fuwa, H.; Yasumoto, T.; Bigiani, A.; Rossini, G. P. Proteomic analysis reveals multiple patterns of response in cells exposed to a toxin mixture. *Chemical Research in Toxicology* **2009**, *22*, 1077-1085.
136. Wang, W.; Lampi, M. A.; Huang, X. D.; Gerhardt, K.; Dixon, D. G.; Greenberg, B. M. Assessment of mixture toxicity of copper, cadmium, and phenanthrenequinone to the marine bacterium *Vibrio fischeri*. *Environmental Toxicology* **2009**, *24*, 166-177.
137. Boatti, L.; Robotti, E.; Marengo, E.; Viarengo, A.; Marsano, F. Effects of nickel, chlorpyrifos and their mixture on the *Dictyostelium discoideum* proteome. *International Journal of Molecular Sciences* **2012**, *13*, 15679-15705.
138. Liu, F.; Wang, W.-X. Proteome pattern in oysters as a diagnostic tool for metal pollution. *Journal of Hazardous Materials* **2012**, *239*, 241-248.

139. McDermott, S.; Wu, J.; Cai, B.; Lawson, A.; Aelion, C. M. Probability of intellectual disability is associated with soil concentrations of arsenic and lead. *Chemosphere* **2011**, *84*, 31-38.
140. Laborde, A.; Tomasina, F.; Bianchi, F.; Bruné, M.-N.; Buka, I.; Comba, P.; Corra, L.; Cori, L.; Duffert, C. M.; Harari, R. Children's health in Latin America: the influence of environmental exposures. *Environmental Health Perspectives* **2015**, *123*, 201-209.
141. Sanders, A. P.; Henn, B. C.; Wright, R. O. Perinatal and Childhood Exposure to Cadmium, Manganese, and Metal Mixtures and Effects on Cognition and Behavior: A Review of Recent Literature. *Current Environmental Health Reports* **2015**, *2*, 284-294.
142. Ferro, M.; Doyle, A. Standardisation for in vitro toxicity tests. In *Cell Culture Methods for In Vitro Toxicology*, Springer: 2001; pp 1-8.
143. Riss, T. L.; Moravec, R. A. Use of multiple assay endpoints to investigate the effects of incubation time, dose of toxin, and plating density in cell-based cytotoxicity assays. *Assay and Drug Development Technologies* **2004**, *2*, 51-62.
144. Horvath, S. Cytotoxicity of drugs and diverse chemical agents to cell cultures. *Toxicology* **1980**, *16*, 59-66.
145. Wallace, K.; Starkov, A. Mitochondrial targets of drug toxicity. *Annual Review of Pharmacology and Toxicology* **2000**, *40*, 353-388.
146. Begriche, K.; Massart, J.; Robin, M.-A.; Borgne-Sanchez, A.; Fromenty, B. Drug-induced toxicity on mitochondria and lipid metabolism: mechanistic diversity and deleterious consequences for the liver. *Journal of Hepatology* **2011**, *54*, 773-794.
147. Kroemer, G.; Reed, J. C. Mitochondrial control of cell death. *Nature Medicine* **2000**, *6*, 513 - 519.
148. Oliveira, Moreira, A.; Machado, N.; Bernardo, T.; Sardao, V. *Mitochondria as a Biosensor for Drug-induced Toxicity-Is It Really Relevant?* INTECH Open Access Publisher: 2011.
149. Xu, J. J.; Diaz, D.; O'Brien, P. J. Applications of cytotoxicity assays and pre-lethal mechanistic assays for assessment of human hepatotoxicity potential. *Chemico-Biological Interactions* **2004**, *150*, 115-128.
150. Pessayre, D.; Fromenty, B.; Berson, A.; Robin, M.-A.; Lettéron, P.; Moreau, R.; Mansouri, A. Central role of mitochondria in drug-induced liver injury. *Drug Metabolism Reviews* **2012**, *44*, 34-87.
151. Rodolfo, C.; Ciccocanti, F.; Giacomo, G. D.; Piacentini, M.; Fimia, G. M. Proteomic analysis of mitochondrial dysfunction in neurodegenerative diseases. *Expert Review of Proteomics* **2010**, *7*, 519-542.
152. H Reddy, P.; P Reddy, T. Mitochondria as a therapeutic target for aging and neurodegenerative diseases. *Current Alzheimer Research* **2011**, *8*, 393-409.
153. Bhat, A. H.; Dar, K. B.; Anees, S.; Zargar, M. A.; Masood, A.; Sofi, M. A.; Ganie, S. A. Oxidative stress, mitochondrial dysfunction and neurodegenerative diseases; a mechanistic insight. *Biomedicine & Pharmacotherapy* **2015**, *74*, 101 - 110.
154. Tsang, A. H.; Chung, K. K. Oxidative and nitrosative stress in Parkinson's disease. *Biochimica et Biophysica Acta (BBA)-Molecular Basis of Disease* **2009**, *1792*, 643-650.
155. Lemasters, J. J.; Nieminen, A. L.; Qian, T.; Trost, L. C.; Elmore, S. P.; Nishimura, Y.; Crowe, R. A.; Cascio, W. E.; Bradham, C. A.; Brenner, D. A.; Herman, B. The mitochondrial permeability transition in cell death: a common mechanism in necrosis, apoptosis and autophagy. *Biochim Biophys Acta* **1998**, *1366*, 177-96.
156. Halliwell, B.; Gutteridge, J. M. *Free radicals in biology and medicine*. Oxford University Press, USA: 2015.
157. Cederbaum, A. I.; Lu, Y.; Wu, D. Role of oxidative stress in alcohol-induced liver injury. *Archives of Toxicology* **2009**, *83*, 519-548.
158. Dröge, W. Free radicals in the physiological control of cell function. *Physiological Reviews* **2002**, *82*, 47-95.
159. Wang, T.; Weinman, S. A. Causes and consequences of mitochondrial reactive oxygen species generation in hepatitis C. *Journal of Gastroenterology and Hepatology* **2006**, *21*, S34-S37.

160. Powers, S. K.; Jackson, M. J. Exercise-induced oxidative stress: cellular mechanisms and impact on muscle force production. *Physiological Reviews* **2008**, *88*, 1243-1276.
161. Zhang, R.; Kang, K. A.; Piao, M. J.; Kim, K. C.; Kim, A. D.; Chae, S.; Park, J. S.; Youn, U. J.; Hyun, J. W. Cytoprotective effect of the fruits of *Lycium chinense* Miller against oxidative stress-induced hepatotoxicity. *Journal of Ethnopharmacology* **2010**, *130*, 299-306.
162. Jaeschke, H.; McGill, M. R.; Ramachandran, A. Oxidant stress, mitochondria, and cell death mechanisms in drug-induced liver injury: lessons learned from acetaminophen hepatotoxicity. *Drug Metabolism Reviews* **2012**, *44*, 88-106.
163. Brenner, C.; Galluzzi, L.; Kepp, O.; Kroemer, G. Decoding cell death signals in liver inflammation. *Journal of Hepatology* **2013**, *59*, 583-594.
164. Finkel, T.; Holbrook, N. J. Oxidants, oxidative stress and the biology of ageing. *Nature* **2000**, *408*, 239-247.
165. Son, Y.; Cheong, Y.-K.; Kim, N.-H.; Chung, H.-T.; Kang, D. G.; Pae, H.-O. Mitogen-activated protein kinases and reactive oxygen species: how can ROS activate MAPK pathways? *Journal of Signal Transduction* **2011**, 2011, 1 - 6.
166. Polaniak, R.; Bułdak, R. J.; Karoń, M.; Birkner, K.; Kukla, M.; Żwirska-Korczala, K.; Birkner, E. Influence of an extremely low frequency magnetic field (ELF-EMF) on antioxidative vitamin E properties in AT478 murine squamous cell carcinoma culture in vitro. *International Journal of Toxicology* **2010**, *29*, 221-230.
167. Meister, A.; Anderson, M. E. Glutathione. *Annual review of biochemistry* **1983**, *52*, 711-760.
168. Yu, B. P. Cellular defenses against damage from reactive oxygen species. *Physiological Reviews* **1994**, *74*, 139-163.
169. Yuan, L.; Kaplowitz, N. Glutathione in liver diseases and hepatotoxicity. *Molecular Aspects of Medicine* **2009**, *30*, 29-41.
170. Dalleau, S.; Baradat, M.; Guéraud, F.; Huc, L. Cell death and diseases related to oxidative stress: 4-hydroxynonenal (HNE) in the balance. *Cell Death & Differentiation* **2013**, *20*, 1615-1630.
171. Wilhelm, D.; Bender, K.; Knebel, A.; Angel, P. The level of intracellular glutathione is a key regulator for the induction of stress-activated signal transduction pathways including Jun N-terminal protein kinases and p38 kinase by alkylating agents. *Molecular and Cellular Biology* **1997**, *17*, 4792-4800.
172. Vivancos, P. D.; Wolff, T.; Markovic, J.; Pallardó, F. V.; Foyer, C. H. A nuclear glutathione cycle within the cell cycle. *Biochemical Journal* **2010**, *431*, 169-178.
173. Kroemer, G.; Dallaporta, B.; Resche-Rigon, M. The mitochondrial death/life regulator in apoptosis and necrosis. *Annual Review of Physiology* **1998**, *60*, 619-642.
174. Wang, K. Molecular mechanisms of liver injury: apoptosis or necrosis. *Experimental and Toxicologic Pathology* **2014**, *66*, 351-356.
175. Bissell, D. M.; Gores, G. J.; Laskin, D. L.; Hoofnagle, J. H. Drug-induced liver injury: Mechanisms and test systems. *Hepatology* **2001**, *33*, 1009-1013.
176. Lockshin, R. A.; Zakeri, Z. Apoptosis, autophagy, and more. *Int J Biochem Cell Biol* **2004**, *36*, 2405-19.
177. Young, M. M.; Kester, M.; Wang, H. G. Sphingolipids: regulators of crosstalk between apoptosis and autophagy. *The Journal of Lipid Research* **2013**, *54*, 5-19.
178. Nishida, K.; Yamaguchi, O.; Otsu, K. Crosstalk between autophagy and apoptosis in heart disease. *Circulation Research* **2008**, *103*, 343-51.
179. Cohen, G. M.; Sun, X. M.; Fearnhead, H.; MacFarlane, M.; Brown, D. G.; Snowden, R. T.; Dinsdale, D. Formation of large molecular weight fragments of DNA is a key committed step of apoptosis in thymocytes. *The Journal of Immunology* **1994**, *153*, 507-16.
180. Martin, S. J.; Green, D. R. Protease activation during apoptosis: death by a thousand cuts? *Cell* **1995**, *82*, 349-52.
181. Mukhopadhyay, S.; Panda, P. K.; Sinha, N.; Das, D. N.; Bhutia, S. K. Autophagy and apoptosis: where do they meet? *Apoptosis* **2014**, *19*, 555-66.

182. Carambula, S. F.; Matikainen, T.; Lynch, M. P.; Flavell, R. A.; Dias Gonçalves, P. B.; Tilly, J. L.; Rueda, B. R. Caspase-3 is a pivotal mediator of apoptosis during regression of the ovarian corpus luteum. *Endocrinology* **2002**, *143*, 1495-1501.
183. Bazzoni, F.; Beutler, B. The tumor necrosis factor ligand and receptor families. *The New England Journal of Medicine* **1996**, *334*, 1717-25.
184. Mathew, S. J.; Haubert, D.; Kronke, M.; Leptin, M. Looking beyond death: a morphogenetic role for the TNF signalling pathway. *Journal Cell Science* **2009**, *122*, 1939-46.
185. Lee, E. W.; Seo, J.; Jeong, M.; Lee, S.; Song, J. The roles of FADD in extrinsic apoptosis and necroptosis. *BMB Reports* **2012**, *45*, 496-508.
186. Pennarun, B.; Meijer, A.; de Vries, E. G.; Kleibeuker, J. H.; Kruyt, F.; de Jong, S. Playing the DISC: turning on TRAIL death receptor-mediated apoptosis in cancer. *Biochim Biophys Acta* **2010**, *1805*, 123-40.
187. Pobezinskaya, Y. L.; Liu, Z. The role of TRADD in death receptor signaling. *Cell Cycle* **2012**, *11*, 871-876.
188. Chowdhury, I.; Tharakan, B.; Bhat, G. K. Caspases - an update. *Comparative Biochemistry and Physiology Part B: Biochemistry and Molecular Biology* **2008**, *151*, 10-27.
189. Danial, N. N.; Korsmeyer, S. J. Cell death: critical control points. *Cell* **2004**, *116*, 205-219.
190. Hengartner, M. O. The biochemistry of apoptosis. *Nature* **2000**, *407*, 770.
191. Mandal, B. K.; Suzuki, K. T. Arsenic round the world: a review. *Talanta* **2002**, *58*, 201-235.
192. Pongratz, R. Arsenic speciation in environmental samples of contaminated soil. *Science of the Total Environment* **1998**, *224*, 133-141.
193. Orloff, K.; Mistry, K.; Metcalf, S. Biomonitoring for environmental exposures to arsenic. *Journal of Toxicology and Environmental Health, Part B* **2009**, *12*, 509-524.
194. Cohen, S. M.; Arnold, L. L.; Eldan, M.; Lewis, A. S.; Beck, B. D. Methylated arsenicals: the implications of metabolism and carcinogenicity studies in rodents to human risk assessment. *Critical Reviews in Toxicology* **2006**, *36*, 99-133.
195. Förstner, U.; Wittmann, G. T. *Metal pollution in the aquatic environment*. Springer Science & Business Media: 2012.
196. Chemicals, U.; Chemicals, I.-O. P. f. t. S. M. o. *Global Mercury Assessment*. UNEP Chemicals: 2002.
197. Vichai, V.; Kirtikara, K. Sulforhodamine B colorimetric assay for cytotoxicity screening. *Nature Protocols* **2006**, *1*, 1112-1116.
198. Gravance, C. G.; Garner, D. L.; Baumber, J.; Ball, B. A. Assessment of equine sperm mitochondrial function using JC-1. *Theriogenology* **2000**, *53*, 1691-703.
199. Leach, F. R. ATP determination with firefly luciferase. *Journal of Applied Biochemistry* **1981**, *6*, 473-517.
200. Kalyanaraman, B.; Darley-Usmar, V.; Davies, K. J.; Dennery, P. A.; Forman, H. J.; Grisham, M. B.; Mann, G. E.; Moore, K.; Roberts, L. J.; Ischiropoulos, H. Measuring reactive oxygen and nitrogen species with fluorescent probes: challenges and limitations. *Free Radical Biology and Medicine* **2012**, *52*, 1-6.
201. Kamencic, H.; Lyon, A.; Paterson, P. G.; Juurlink, B. H. Monochlorobimane fluorometric method to measure tissue glutathione. *Analytical Biochemistry* **2000**, *286*, 35-37.
202. Van Tonder, J. J. Development of an in vitro mechanistic toxicity screening model using cultured hepatocytes. Ph.D. Thesis, University of Pretoria, 2012.
203. Newman, A.; Leung, B.; Richards, A.; Campbell, T.; Wellwood, J.; Imrie, F. Two cases of differentiation syndrome with ocular manifestations in patients with acute promyelocytic leukaemia treated with all-trans retinoic acid and arsenic trioxide. *American Journal of Ophthalmology Case Reports* **2018**.
204. Bhowmick, S.; Pramanik, S.; Singh, P.; Mondal, P.; Chatterjee, D.; Nriagu, J. Arsenic in groundwater of West Bengal, India: A review of human health risks and assessment of possible intervention options. *Science of The Total Environment* **2018**, *612*, 148-169.
205. Wang, L.; Jiang, H.; Yin, Z.; Aschner, M.; Cai, J. Methylmercury toxicity and Nrf2-dependent detoxification in astrocytes. *Toxicological Sciences* **2009**, *107*, 135-143.

206. Hirano, S.; Cui, X.; Li, S.; Kanno, S.; Kobayashi, Y.; Hayakawa, T.; Shraim, A. Difference in uptake and toxicity of trivalent and pentavalent inorganic arsenic in rat heart microvessel endothelial cells. *Archives of Toxicology* **2003**, *77*, 305-312.
207. Dopp, E.; Hartmann, L.; Von Recklinghausen, U.; Florea, A.; Rabieh, S.; Zimmermann, U.; Shokouhi, B.; Yadav, S.; Hirner, A.; Rettenmeier, A. Forced uptake of trivalent and pentavalent methylated and inorganic arsenic and its cyto-/genotoxicity in fibroblasts and hepatoma cells. *Toxicological Sciences* **2005**, *87*, 46-56.
208. Vineetha, V.; Prathapan, A.; Soumya, R.; Raghu, K. Arsenic trioxide toxicity in H9c2 myoblasts—damage to cell organelles and possible amelioration with *Boerhavia diffusa*. *Cardiovascular Toxicology* **2013**, *13*, 123-137.
209. MacCormac, L. P.; Muqit, M. M.; Faulkes, D. J.; Wood, N. W.; Latchman, D. S. Reduction in endogenous parkin levels renders glial cells sensitive to both caspase-dependent and caspase-independent cell death. *European Journal of Neuroscience* **2004**, *20*, 2038-48.
210. Wlodkowic, D.; Telford, W.; Skommer, J.; Darzynkiewicz, Z. Apoptosis and beyond: cytometry in studies of programmed cell death. In *Methods in Cell Biology* **2011**, *103*, 55-98.
211. Bossy-Wetzell, E.; Newmeyer, D. D.; Green, D. R. Mitochondrial cytochrome c release in apoptosis occurs upstream of DEVD-specific caspase activation and independently of mitochondrial transmembrane depolarization. *The EMBO Journal* **1998**, *17*, 37-49.
212. Ly, J. D.; Grubb, D.; Lawen, A. The mitochondrial membrane potential ( $\Delta\psi_m$ ) in apoptosis; an update. *Apoptosis* **2003**, *8*, 115-128.
213. Tait, S. W.; Ichim, G.; Green, D. R. Die another way—non-apoptotic mechanisms of cell death. *Journal of Cell Science* **2014**, *127*, 2135-2144.
214. Gogvadze, V.; Orrenius, S.; Zhivotovsky, B. Multiple pathways of cytochrome c release from mitochondria in apoptosis. *Biochimica et Biophysica Acta (BBA)-Bioenergetics* **2006**, *1757*, 639-647.
215. Wang, Y.; Xu, Y.; Wang, H.; Xue, P.; Li, X.; Li, B.; Zheng, Q.; Sun, G. Arsenic induces mitochondria-dependent apoptosis by reactive oxygen species generation rather than glutathione depletion in Chang human hepatocytes. *Archives of Toxicology* **2009**, *83*, 899-908.
216. Leist, M.; Single, B.; Castoldi, A. F.; Kühnle, S.; Nicotera, P. Intracellular adenosine triphosphate (ATP) concentration: a switch in the decision between apoptosis and necrosis. *Journal of Experimental Medicine* **1997**, *185*, 1481-1486.
217. Eguchi, Y.; Shimizu, S.; Tsujimoto, Y. Intracellular ATP levels determine cell death fate by apoptosis or necrosis. *Cancer Research* **1997**, *57*, 1835-1840.
218. Nutt, L. K.; Gogvadze, V.; Uthaisang, W.; Mirnikjoo, B.; McConkey, D. J.; Orrenius, S. Research Paper Indirect Effects of Bax and Bak Initiate the Mitochondrial Alterations that Lead to Cytochrome c Release during Arsenic Trioxide-Induced Apoptosis. *Cancer biology & therapy* **2005**, *4*, 459-467.
219. Hosseini, M.-J.; Shaki, F.; Ghazi-Khansari, M.; Pourahmad, J. Toxicity of arsenic (III) on isolated liver mitochondria: a new mechanistic approach. *Iranian Journal of Pharmaceutical Research: IJPR* **2013**, *12*, 121.
220. Simon, H.-U.; Haj-Yehia, A.; Levi-Schaffer, F. Role of reactive oxygen species (ROS) in apoptosis induction. *Apoptosis* **2000**, *5*, 415-418.
221. Belyaeva, E. A.; Dymkowska, D.; Więckowski, M. R.; Wojtczak, L. Reactive oxygen species produced by the mitochondrial respiratory chain are involved in Cd<sup>2+</sup>-induced injury of rat ascites hepatoma AS-30D cells. *Biochimica et Biophysica Acta (BBA)-Bioenergetics* **2006**, *1757*, 1568-1574.
222. Wang, Y.; Fang, J.; Leonard, S. S.; Rao, K. M. K. Cadmium inhibits the electron transfer chain and induces reactive oxygen species. *Free Radical Biology and Medicine* **2004**, *36*, 1434-1443.
223. Alarifi, S.; Ali, D.; Alkahtani, S.; Siddiqui, M. A.; Ali, B. A. Arsenic trioxide-mediated oxidative stress and genotoxicity in human hepatocellular carcinoma cells. *OncoTargets and Therapy* **2013**, *6*, 75-84.

224. Khan, M.; Yi, F.; Rasul, A.; Li, T.; Wang, N.; Gao, H.; Gao, R.; Ma, T. Alantolactone induces apoptosis in glioblastoma cells via GSH depletion, ROS generation, and mitochondrial dysfunction. *IUBMB Life* **2012**, *64*, 783-794.
225. Keyse, S. M.; Tyrrell, R. M. Heme oxygenase is the major 32-kDa stress protein induced in human skin fibroblasts by UVA radiation, hydrogen peroxide, and sodium arsenite. *Proceedings of the National Academy of Sciences* **1989**, *86*, 99-103.
226. Del Razo, L. M.; Quintanilla-Vega, B.; Brambila-Colombres, E.; Calderón-Aranda, E. S.; Manno, M.; Albores, A. Stress proteins induced by arsenic. *Toxicology and Applied Pharmacology* **2001**, *177*, 132-148.
227. Muthusamy, S.; Peng, C.; Ng, J. C. Effects of binary mixtures of benzo [a] pyrene, arsenic, cadmium, and lead on oxidative stress and toxicity in HepG2 cells. *Chemosphere* **2016**, *165*, 41-51.
228. Lopez, E.; Arce, C.; Oset-Gasque, M.; Canadas, S.; Gonzalez, M. Cadmium induces reactive oxygen species generation and lipid peroxidation in cortical neurons in culture. *Free Radical Biology and Medicine* **2006**, *40*, 940-951.
229. Dehn, P.; White, C.; Conners, D.; Shipkey, G.; Cumbo, T. Characterization of the human hepatocellular carcinoma (hepg2) cell line as an in vitro model for cadmium toxicity studies. *In Vitro Cellular & Developmental Biology-Animal* **2004**, *40*, 172-182.
230. Urani, C.; Melchiorretto, P.; Canevali, C.; Crosta, G. Cytotoxicity and induction of protective mechanisms in HepG2 cells exposed to cadmium. *Toxicology in Vitro* **2005**, *19*, 887-892.
231. Fotakis, G.; Timbrell, J. A. In vitro cytotoxicity assays: comparison of LDH, neutral red, MTT and protein assay in hepatoma cell lines following exposure to cadmium chloride. *Toxicology Letters* **2006**, *160*, 171-177.
232. Aydin, H. H.; Celik, H. A.; Deveci, R.; Terzioglu, E.; Karacali, S.; Mete, N.; Akarca, U.; Batur, Y. Characterization of the cellular response during apoptosis induction in cadmium-treated Hep G2 human hepatoma cells. *Biological Trace Element Research* **2003**, *95*, 139-153.
233. Belyaeva, E. A.; Dymkowska, D.; Więckowski, M. R.; Wojtczak, L. Mitochondria as an important target in heavy metal toxicity in rat hepatoma AS-30D cells. *Toxicology and Applied Pharmacology* **2008**, *231*, 34-42.
234. Yang, M.; Yu, L.; Gupta, R. Analysis of changes in energy and redox states in HepG2 hepatoma and C6 glioma cells upon exposure to cadmium. *Toxicology* **2004**, *201*, 105-113.
235. Ismail, S. M.; Ismail, H. A.; Al-Sharif, G. M. Neuroprotective effect of barley plant (*Hordeum Vulgare*) against the changes in MAO induced by lead and cadmium administration in different CNS regions of male guinea pig. *Journal of Life Sciences Research* **2015**, *2*, 53-60.
236. Jiang, L.; Wang, L.; Chen, L.; Cai, G.-H.; Ren, Q.-Y.; Chen, J.-Z.; Shi, H.-J.; Xie, Y.-H. As<sub>2</sub>O<sub>3</sub> induces apoptosis in human hepatocellular carcinoma HepG2 cells through a ROS-mediated mitochondrial pathway and activation of caspases. *International Journal of Clinical and Experimental Medicine* **2015**, *8*, 2190.
237. Iwama, K.; Nakajo, S.; Aiuchi, T.; Nakaya, K. Apoptosis induced by arsenic trioxide in leukemia U937 cells is dependent on activation of p38, inactivation of ERK and the Ca<sup>2+</sup>-dependent production of superoxide. *International Journal of Cancer* **2001**, *92*, 518-526.
238. Shih, C. M.; Ko, W. C.; Wu, J. S.; Wei, Y. H.; Wang, L. F.; Chang, E. E.; Lo, T. Y.; Cheng, H. H.; Chen, C. T. Mediating of caspase-independent apoptosis by cadmium through the mitochondria-ROS pathway in MRC-5 fibroblasts. *Journal of Cellular Biochemistry* **2004**, *91*, 384-397.
239. Lasfer, M.; Vadrot, N.; Aoudjehane, L.; Conti, F.; Bringuier, A.; Feldmann, G.; Reyl-Desmars, F. Cadmium induces mitochondria-dependent apoptosis of normal human hepatocytes. *Cell Biology and Toxicology* **2008**, *24*, 55-62.
240. Muller, L. Consequences of cadmium toxicity in rat hepatocytes: mitochondrial dysfunction and lipid peroxidation. *Toxicology* **1986**, *40*, 285-95.

241. Lawal, A. O.; Ellis, E. Differential sensitivity and responsiveness of three human cell lines HepG2, 1321N1 and HEK 293 to cadmium. *The Journal of Toxicological Sciences* **2010**, *35*, 465-478.
242. Müller, L.; Ohnesorge, F. K. Cadmium-induced alteration of the energy level in isolated hepatocytes. *Toxicology* **1984**, *31*, 297-306.
243. Corsini, E.; Asti, L.; Viviani, B.; Marinovich, M.; Galli, C. L. Sodium arsenate induces overproduction of interleukin-1 $\alpha$  in murine keratinocytes: role of mitochondria. *Journal of Investigative Dermatology* **1999**, *113*, 760-765.
244. Scott, N.; Hatlelid, K. M.; MacKenzie, N. E.; Carter, D. E. Reactions of arsenic (III) and arsenic (V) species with glutathione. *Chemical research in Toxicology* **1993**, *6*, 102-106.
245. Ray, A.; Chatterjee, S.; Mukherjee, S.; Bhattacharya, S. Arsenic trioxide induced indirect and direct inhibition of glutathione reductase leads to apoptosis in rat hepatocytes. *BioMetals* **2014**, *27*, 483-494.
246. Mendoza-Cózatl, D. G.; Butko, E.; Springer, F.; Torpey, J. W.; Komives, E. A.; Kehr, J.; Schroeder, J. I. Identification of high levels of phytochelatins, glutathione and cadmium in the phloem sap of *Brassica napus*. A role for thiol-peptides in the long-distance transport of cadmium and the effect of cadmium on iron translocation. *The Plant Journal* **2008**, *54*, 249-259.
247. Aravind, P.; Prasad, M. N. V. Modulation of cadmium-induced oxidative stress in *Ceratophyllum demersum* by zinc involves ascorbate–glutathione cycle and glutathione metabolism. *Plant Physiology and Biochemistry* **2005**, *43*, 107-116.
248. Los, M.; Mozoluk, M.; Ferrari, D.; Stepczynska, A.; Stroh, C.; Renz, A.; Herceg, Z.; Wang, Z.-Q.; Schulze-Osthoff, K. Activation and caspase-mediated inhibition of PARP: a molecular switch between fibroblast necrosis and apoptosis in death receptor signaling. *Molecular Biology of the Cell* **2002**, *13*, 978-988.
249. Chen, X.; Cheung, S. T.; So, S.; Fan, S. T.; Barry, C.; Higgins, J.; Lai, K.-M.; Ji, J.; Dudoit, S.; Ng, I. O. Gene expression patterns in human liver cancers. *Molecular Biology of the Cell* **2002**, *13*, 1929-1939.
250. Bagchi, D.; Joshi, S. S.; Bagchi, M.; Balmoori, J.; Benner, E.; Kuszynski, C.; Stohs, S. Cadmium- and chromium-induced oxidative stress, DNA damage, and apoptotic cell death in cultured human chronic myelogenous leukemic K562 cells, promyelocytic leukemic HL-60 cells, and normal human peripheral blood mononuclear cells. *Journal of Biochemical and Molecular Toxicology* **2000**, *14*, 33-41.
251. Matsuoka, M.; Call, K. M. Cadmium-induced expression of immediate early genes in LLC-PK1 cells. *Kidney International* **1995**, *48*, 383-389.
252. Hamada, T.; Tanimoto, A.; Sasaguri, Y. Apoptosis induced by cadmium. *Apoptosis* **1997**, *2*, 359-367.
253. Hart, B.; Lee, C.; Shukla, G.; Shukla, A.; Osier, M.; Eneman, J.; Chiu, J.-F. Characterization of cadmium-induced apoptosis in rat lung epithelial cells: evidence for the participation of oxidant stress. *Toxicology* **1999**, *133*, 43-58.
254. Narita, M.; Shimizu, S.; Ito, T.; Chittenden, T.; Lutz, R. J.; Matsuda, H.; Tsujimoto, Y. Bax interacts with the permeability transition pore to induce permeability transition and cytochrome c release in isolated mitochondria. *Proceedings of the National Academy of Sciences* **1998**, *95*, 14681-14686.
255. Xu, C.; Johnson, J. E.; Singh, P. K.; Jones, M. M.; Yan, H.; Carter, C. E. In vivo studies of cadmium-induced apoptosis in testicular tissue of the rat and its modulation by a chelating agent. *Toxicology* **1996**, *107*, 1-8.
256. Wätjen, W.; Haase, H.; Biagioli, M.; Beyersmann, D. Induction of apoptosis in mammalian cells by cadmium and zinc. *Environmental Health Perspectives* **2002**, *110*, 865.
257. Zhou, T.; Zhou, G.; Song, W.; Eguchi, N.; Lu, W.; Lundin, E.; Jin, T.; Nordberg, G. Cadmium-induced apoptosis and changes in expression of p53, c-jun and MT-I genes in testes and ventral prostate of rats. *Toxicology* **1999**, *142*, 1-13.
258. Arroyo, V.; Flores, K.; Ortiz, L.; Gómez-Quiroz, L.; Gutiérrez-Ruiz, M. Liver and cadmium toxicity. *Journal of Drug Metabolism and Toxicology* **2012**, *S5*, 1-7.

259. Xie, Z.; Zhang, Y.; Li, A.; Li, P.; Ji, W.; Huang, D. Cd-induced apoptosis was mediated by the release of Ca<sup>2+</sup> from intracellular Ca storage. *Toxicology Letters* **2010**, *192*, 115-118.
260. Lemarié, A.; Lagadic-Gossman, D.; Morzadec, C.; Allain, N.; Fardel, O.; Vernhet, L. Cadmium induces caspase-independent apoptosis in liver Hep3B cells: role for calcium in signaling oxidative stress-related impairment of mitochondria and relocation of endonuclease G and apoptosis-inducing factor. *Free Radical Biology and Medicine* **2004**, *36*, 1517-1531.
261. Wang, S.; Chen, L.; Xia, S. Cadmium is Acutely Toxic for Murine Hepatocytes: Effects on Intracellular Free Ca<sup>+</sup> Homeostasis. *Physiological Research* **2007**, *56*, 193.
262. Kitamura, M.; Hiramatsu, N. The oxidative stress: endoplasmic reticulum stress axis in cadmium toxicity. *Biometals* **2010**, *23*, 941-950.
263. Belyaeva, E. A.; Sokolova, T. V.; Emelyanova, L. V.; Zakharova, I. O. Mitochondrial electron transport chain in heavy metal-induced neurotoxicity: effects of cadmium, mercury, and copper. *The Scientific World Journal* **2012**, 2012.
264. Mehari, T. F.; Rorie, C. J.; Godfrey, S. S.; Minor, R. C.; Fakayode, S. O. Influence of Arsenic (III), Cadmium (II), Chromium (VI), Mercury (II), and Lead (II) Ions on Human Triple Negative Breast Cancer (HCC1806) Cell Cytotoxicity and Cell Viability. *Journal of Chemical Health Risks* **2017**, *7*, 1-17.
265. Kim, J. K.; Cha, M.; Ryu, T. H.; Han, M.; Nili, M. Combined Effects of Radiation and Mercury on PLHC-1 Cells. *Chemosphere* **2011**, *85*, 1635-1638.
266. Cuello, S.; Goya, L.; Madrid, Y.; Campuzano, S.; Pedrero, M.; Bravo, L.; Cámara, C.; Ramos, S. Molecular mechanisms of methylmercury-induced cell death in human HepG2 cells. *Food and chemical toxicology* **2010**, *48*, 1405-1411.
267. Harada, M. Minamata disease: methylmercury poisoning in Japan caused by environmental pollution. *Critical Reviews in Toxicology* **1995**, *25*, 1-24.
268. Eto, K.; Takizawa, Y.; Akagi, H.; Haraguchi, K.; Asano, S.; Takahata, N.; Tokunaga, H. Differential diagnosis between organic and inorganic mercury poisoning in human cases-the pathologic point of view. *Toxicologic Pathology* **1999**, *27*, 664-671.
269. Modi, H. R.; Katyare, S. S. Effect of treatment with cadmium on structure-function relationships in rat liver mitochondria: Studies on oxidative energy metabolism and lipid/phospholipids profiles. *Journal of Membrane Biology* **2009**, *232*, 47.
270. Dreiem, A.; Seegal, R. F. Methylmercury-induced changes in mitochondrial function in striatal synaptosomes are calcium-dependent and ROS-independent. *Neurotoxicology* **2007**, *28*, 720-6.
271. Shenker, B. J.; Guo, T. L.; O, I.; Shapiro, I. M. Induction of apoptosis in human T-cells by methyl mercury: temporal relationship between mitochondrial dysfunction and loss of reductive reserve. *Toxicol Appl Pharmacol* **1999**, *157*, 23-35.
272. Yasui, M.; Verity, M. A. *Mineral and Metal Neurotoxicology*. CRC Press: 1996.
273. Strubelt, O. Comparative studies on the toxicity of mercury, cadmium, and copper toward the isolated perfused rat liver. *Journal of Toxicology and Environmental Health Part A* **1996**, *47*, 267-283.
274. Gebhardt, R. Prevention of cadmium-induced toxicity in liver-derived cells by the combination preparation Hepeel®. *Environmental Toxicology and Pharmacology* **2009**, *27*, 402-409.
275. Agarwala, S.; Mudholkar, K.; Bhuwania, R.; Satish Rao, B. Mangiferin, a dietary xanthone protects against mercury-induced toxicity in HepG2 cells. *Environmental toxicology* **2012**, *27*, 117-127.
276. Lash, L. H.; Zalups, R. K. Alterations in renal cellular glutathione metabolism after in vivo administration of a subtoxic dose of mercuric chloride. *Journal of Biochemical Toxicology* **1996**, *11*, 1-9.
277. Lee, Y. W.; Ha, M. S.; Kim, Y. K. Role of reactive oxygen species and glutathione in inorganic mercury-induced injury in human glioma cells. *Neurochemical Research* **2001**, *26*, 1187-1193.
278. Lohren, H.; Blagojevic, L.; Fitkau, R.; Ebert, F.; Schildknecht, S.; Leist, M.; Schwerdtle, T. Toxicity of organic and inorganic mercury species in differentiated human neurons and human astrocytes. *Journal of Trace Elements in Medicine and Biology* **2015**, *32*, 200-208.



# Appendix I Ethics approval letter

The Research Ethics Committee, Faculty Health Sciences, University of Pretoria complies with ICH-GCP guidelines and has US Federal wide Assurance.

- FWA 00002567, Approved dd 22 May 2002 and Expires 28 August 2018.
- IRB 0000 2235 IORG0001762 Approved dd 22/04/2014 and Expires 22/04/2017.



UNIVERSITEIT VAN PRETORIA  
UNIVERSITY OF PRETORIA  
YUNIBESITHI YA PRETORIA

Faculty of Health Sciences Research Ethics Committee

24/11/2016

**Approval Certificate**  
**New Application**

**Ethics Reference No.: 463/2016**

**Title:** The combined effects of arsenic, cadmium and mercury on hepatocarcinoma and neuroblastoma cells in vitro

Dear Muhammad Yousaf

The **New Application** as supported by documents specified in your cover letter dated 7/11/2016 for your research received on the 8/11/2016, was approved by the Faculty of Health Sciences Research Ethics Committee on its quorate meeting of 23/11/2016.

Please note the following about your ethics approval:

- Ethics Approval is valid for 2 years
- Please remember to use your protocol number (**463/2016**) on any documents or correspondence with the Research Ethics Committee regarding your research.
- Please note that the Research Ethics Committee may ask further questions, seek additional information, require further modification, or monitor the conduct of your research.

**Ethics approval is subject to the following:**

- The ethics approval is conditional on the receipt of **6 monthly written Progress Reports**, and
- The ethics approval is conditional on the research being conducted as stipulated by the details of all documents submitted to the Committee. In the event that a further need arises to change who the investigators are, the methods or any other aspect, such changes must be submitted as an Amendment for approval by the Committee.

We wish you the best with your research.

Yours sincerely

**Dr R Sommers**; MBChB; MMed (Int); MPharMed, PhD  
Deputy Chairperson of the Faculty of Health Sciences Research Ethics Committee, University of Pretoria

*The Faculty of Health Sciences Research Ethics Committee complies with the SA National Act 61 of 2003 as it pertains to health research and the United States Code of Federal Regulations Title 45 and 46. This committee abides by the ethical norms and principles for research, established by the Declaration of Helsinki, the South African Medical Research Council Guidelines as well as the Guidelines for Ethical Research: Principles Structures and Processes, Second Edition 2015 (Department of Health).*

☎ 012 356 3084    ✉ [deepeka.behari@up.ac.za](mailto:deepeka.behari@up.ac.za) / [fhsethics@up.ac.za](mailto:fhsethics@up.ac.za)    🌐 <http://www.up.ac.za/healthethics>  
✉ Private Bag X323, Arcadia, 0007 - Tswelopele Building, Level 4, Room 60, Gezina, Pretoria

## Appendix II: Reagents and preparation

### **2,2'-Azobis (2-methylpropionamide) dihydrochloride (AAPH)**

**2,2'-Azobis (2-methylpropionamide) dihydrochloride** was obtained from Sigma-Aldrich (St. Louis, USA). A 30 mM stock solution was prepared by dissolving 8 mg in 1 mL dimethyl sulfoxide (DMSO), and storing aliquots at -80°C. Prior to use, the stock solution was diluted to 2 mM with PBS by mixing 50 mL of stock solution with 750 mL PBS.

### **Adenosine diphosphate reagent**

The ADP reagent was prepared by adding 5 µL water to 1 µL ADP Enzyme (Catalog Number MAK135E).

### **Adenosine triphosphate reagent**

The ATP reagent was prepared by mixing 95 µL of the assay buffer (Catalog Number MAK135A) with 1 µL substrate A (Catalog Number MAK135B), 1 µL co-substrate (Catalog Number MAK135C) and 1 µL ATP enzyme (Catalog Number MAK135D).

### **Foetal calf serum**

Foetal calf serum was procured from PAA (Pasching, Austria) and inactivated for any host serum complements that might have been present by incubation at 56°C for 45 min. Serum was added to medium in a ratio of 1:9 to obtain a final concentration of 10% FCS.

### **Cadmium chloride stock solution (cadmium equivalent to 100 mg/L)**

Cadmium chloride was obtained from Sigma-Aldrich (St. Louis, USA) in powder form. Cadmium chloride (16.32 mg) was dissolved in 100 mL deionized water to make a stock solution equivalent to cadmium chloride 100 mg/L.

### **Ham's F12 medium**

Ham's F12 medium was obtained from Sigma-Aldrich (St. Louis, USA) in powder form, supplemented with: 1% non-essential amino acids, 1% L-glutamine. Powder was dissolved in 5 L sterile, deionised water and sterilised using 0.22 µm cellulose acetate filters. The solution was stored at 4°C in 500 mL bottles after supplementing with 1% penicillin/streptomycin.

#### **Eagle's Minimum Essential Medium (EMEM)**

Powder medium was purchased from Sigma Aldrich (St Louis, USA) and 48 g was dissolved in 5 L sterile, deionised water. The pH was adjusted to 7.4 by adding 11 g sodium bicarbonate. The solution was filter sterilized using 0.22 µm cellulose acetate filters and stored in 500 mL bottles after adding 1% Penicillin/Streptomycin at 4°C.

#### **5,5',6,6'-tetrachloro-1,1,3,3'- tetraethylbenzimidazolylcarbocyanine iodide (JC-1)**

The JC-1 powder was purchased from Sigma-Aldrich (St Louis, USA). A 1 mM stock solution was prepared in DMSO and stored at -80°C. The stock solution was diluted to 20 µM in medium to make a working solution.

#### **Mercury chloride stock solution (mercury equivalent to 100 mg/L)**

Mercury chloride was obtained from BDH (Dorset, UK) in powder form. Mercury chloride (13.53 mg) was dissolved in 100 mL of deionized water to make a stock solution equivalent to mercury chloride 100 mg/L.

#### **Metal mixture stock solution**

Stock metal mixture solutions of As, Cd and Hg were made in deionized water representing concentrations of As, Cd and Hg at 40:20:8 mg/L, respectively. Aliquots of 2 mL, 1 mL and 0.4 mL from As, Cd and Hg stock solutions were pipetted into a 10 mL volumetric flask, and the volume made up to 10 mL. The EPA mixture was made according to the EPA MCL ratio of As, Cd and Hg (10:5:2), with respect to As concentrations of 0.1, 0.5, 1.5, 2 and 4 mg/L.

#### **Monochlorobimane**

Monochlorobimane was purchased from Sigma-Aldrich (St. Louis, USA) in powder form. A 25 mM stock solution was prepared by dissolving 5 mg in 880  $\mu$ L DMSO, which was kept at  $-80^{\circ}\text{C}$  in 20  $\mu$ L aliquots. A 500  $\mu$ M working solution was prepared by diluting two aliquots in 1.96 mL PBS prior to use

### **2',7'-Dihydrodichlorofluoresce diacetate (H<sub>2</sub>-DCFDA)**

The H<sub>2</sub>-DCF-DA was purchased from Sigma-Aldrich (St. Louis, USA) in powder form. A 2 mM stock solution was prepared by dissolving 5 mg DCFDA in 5 mL DMSO. The solution was stored at  $-20^{\circ}\text{C}$ . A 20  $\mu$ M working solution was prepared by adding 40  $\mu$ L stock solution to 100  $\mu$ L of medium to obtain final concentration of 5.7  $\mu$ M in each well.

### **Phosphate buffered saline (PBS)**

BBL™ FTA hemagglutination buffer was obtained from BD (France) in powder form. A 0.9% solution was prepared by dissolving 9.23 g per 1 L distilled water. The solution was stored at  $4^{\circ}\text{C}$ .

### **Penicillin/Streptomycin**

Penicillin (10,000 IU) and streptomycin (10 mg/mL) solutions were obtained from BioWhittaker (Walkersville, USA). Media was fortified with 1% penicillin/streptomycin.

### **Saponin**

Saponin was obtained from Sigma-Aldrich (St. Louis, USA). A 2% solution was prepared by adding 2 g of saponin in 100 mL medium. The solution was stored at  $4^{\circ}\text{C}$ .

### **Sodium arsenite stock solution (arsenic equivalent to 100 mg/L)**

Sodium arsenite was obtained from Merck (Darmstadt, Germany) in powder form. Sodium arsenite (17.34 mg) was dissolved in 100 mL of deionized water to make a stock solution equivalent to 100 mg/L sodium arsenite.

### **Trichloroacetic acid**

Trichloroacetic acid was obtained from Merck Chemicals (Darmstadt, Germany). A 50% solution was prepared in distilled water and kept at room temperature.

#### **Tris-base buffer**

Tris-base (10 mM) was prepared by dissolving 2.42 g of Tris base powder in deionized water. The pH was adjusted with sodium hydroxide to 10.5.

#### **Trypan blue counting solution**

Trypan blue was obtained from Sigma-Aldrich (St. Louis, USA) in powder form. Two hundred milligrams of the powder was dissolved in 50 mL PBS to obtain a 0.4% w/v solution. The solution was filtered through 0.45  $\mu\text{m}$  syringe filters and stored at room temperature.